Inhibition of tumor growth by adenovirus-mediated expression of antiangiogenic and immunomodulatory proteins

INAUGURAL DISSERTATION
zur
Erlangung des Doktorgrades
der Mathematisch-Naturwissenschaftlichen Fakultät
der Universität zu Köln

vorgelegt von

S.G.Vijayshankar

aus Erode, Indien

2006

Referees/Berichterstatter   Prof. Dr. Stefan Kochanek
                                 Prof. Dr. Jens Brüning

Date of oral examination/   12.07.2006
Tag der mündlichen Prüfung

The present work was carried out under the supervision and the direction of PD Dr. Stefan Kochanek at the Center for Molecular Medicine, University of Cologne, Germany from December 1998 to August 2004.

Diese Arbeit wurde von Dezember 1998 bis August 2004 am Zentrum für Molekulare Medizin, Universität zu Köln, unter der Leitung und der Betreuung von Herrn PD Dr. Stefan Kochanek durchgeführt.

Acknowledgement

Abbreviations

Ad5	Human adenovirus type 5
Ang1	Angiopoietin 1
Ang2	Angiopoietin 2
APS	Ammonium Persulphate
bp	Base pairs
CD	Cluster of differentiation
CIP	Calf intestinal phosphatase
CEPs	Circulating endothelial precursor cells
DCs	Dendritic cells
DNA	Deoxyribonucleic acid
DTT	Dithiothreitol
ECM	Extracellular matrix
ELISA	Enzyme linked immunoabsorbent assay
EDTA	Ethylenediaminotetraacetic acid
FCS	Fetal calf serum
FGF	Fibroblast growth factor
HC-Ad vector	High capacity adenoviral vector
HRP	Horse radish peroxidase
HSCs	Haematopoietic stem cells
HUVECs	Human umbilical venous endothelial cells
i.u	Infectious Units
IL-12	Interleukin 12
kD	Kilo Dalton
LLC	Lewis lung carcinoma
MAb	Monoclonal antibody
Mwt	Molecular weight
moi	Multiplicity of infection
NK cells	Natural killer cells
dNTPs	Deoxribonucleotides
OD	Optical density
PAGE	Polyacrylamide gel electrophoresis
pfu	Plaque forming units
PCR	Polymerase chain reaction
sflt1	Soluble fetal liver kinase 1/VEGFR1
stie2	Soluble Tie2 receptor
SDS	Sodium dodecyl sulphate
TBS	Tris Buffered Saline
TEMED	N, N, N`, N`, -tetramethyl-ethylendiamine
TGF	Transforming growth factor
Tris	Tris-(hydroxylmethyl) aminomethane
TTRB	Transthyretin
VEGFR1	Vascular endothelial growth factor receptor 1

Index

I Introduction

Cancer is an umbrella term covering a plethora of conditions characterized by unscheduled and uncontrolled cellular proliferation [1]. More than 200 types of cancer are known. The dominant five types of cancer, which account for more than 50% of all cancers, originate from lung, colon, breast, stomach and prostate [1]. Cancer is second only to cardiovascular diseases as the leading cause of death in the developed world, with about 2.6 million new cases diagnosed each year in Europe and USA. Despite advances in screening, education, and early diagnosis, cancer is predicted to be the most common cause of death in the 21st century [2]. New treatments are therefore urgently needed to supplement conventional methods of cancer treatment such as chemotherapy, radiotherapy, and surgery [2]. Basic research in the past few decades has aided in a greater understanding of the molecular basis of cancer, thereby providing new targets for cancer therapy. The spectrum of discoveries ranges from identification of oncogenes, tumor suppressor genes, apoptosis, angiogenesis and development of novel detection techniques [3-5]. New insights in the field of signal transduction, cell cycle regulation and DNA repair mechanisms have now made it possible to appreciate the complexity of the disease [1, 3, 6]. This is reflected in the definition of new targets for drug design and development. As a result, biological therapy is considered as a viable supplement to conventional cancer therapy [7]. Biological therapy aims at the activation of the immune system to eradicate tumors. Commonly used strategies in biological therapy encompass cancer vaccines, monoclonal antibodies (MAbs), cytokines, dendritic cells or activated lymphocytes. Apart from biological therapy, blocking of tumor angiogenesis has recently attracted interest [8]. As a result, new regimens are designed to combine biological therapy and/or antiangiogenic therapy with conventional cancer treatment methods [9]. In addition, advances in virology have made it possible to develop viral vectors for introducing nucleic acids into cells. Vectors based on adenovirus can transfer large fragments of DNA, have shown long-term expression with minimal toxicity and even may allow to regulate gene expression [10-12]. Thus it is now possible to combine advances in the fields of immunology, angiogenesis and vector development to generate novel arsenals for the treatment of cancer.

I.1 Concepts in tumor growth and intervention

I.1.1 Origin and development of tumors

Malignant tumors result from uncontrolled proliferation of cells and their migration to sites distant from their origin. Tumors originate from a single cell clone, which acquires a series of growth enhancing mutations, promoting its survival [1]. Numerous agents and factors such as chemicals, radiation, and chronic infection cause mutations [2, 13]. Malignancy often takes years before diagnosis because of the multistep nature of its development. In general, proliferation of cells within tissues is controlled by the interplay of factors such as cell-cell contact, extracellular matrix, growth factors and receptors, integrins, hormones and by the cells of immune system [14]. Thus, the tumor cells have to overcome these preventive mechanisms to attain malignancy. Irrespective of the functional complexity of tumors, all tumors types must acquire traits such as self-sufficiency in growth signals, resistance to antigrowth signals, limitless replicative potential and resistance to apoptosis for survival and growth [14, 15].
Normal cells require the presence of growth factors secreted by neighboring cells for their growth and survival. Many tumors secrete growth factors, which stimulate their own growth thereby creating a positive feedback autoloop. As a result, tumor cells are no longer dependent of neighboring cells for survival. For example, many breast tumors secrete VEGF and FGF to promote their survival [16]. Similarly, certain types of sarcomas and glioblastoma secrete TGF-β and PDGFA respectively [17, 18]. Another common mechanism utilized by the tumors involves the upregulation of growth factor receptors thereby making the cells hypersusceptible to ambient

levels of growth factors. Growth factor receptors such as EGF-R are commonly upregulated in tumors. This results in cell activation even in the presence of a low amount of growth factor [14]. An alternative strategy commonly observed in tumors is the presence of ligand independent signalling, which may occur through structural alteration of receptors such as through absence of the cytoplasmic region of the EGF receptor [14]. Along with the changes in growth factor receptor expression, integrin mediated signalling is often altered. Integrins are heterodimeric molecules found on the cell surface. They transmit signals between matrix and the cell in both directions. Integrins control numerous processes including cell proliferation, apoptosis, migration, formation of extracellular matrix etc. Cells modulate the expression of integrins in accordance with the surroundings [19]. For instance, endothelial cells often up regulate $\alpha_v\beta_3$ and $\alpha_v\beta_5$ during proliferation and $\alpha_2\beta1$ to prevent apoptosis. Interestingly, cancer cells often modulate the expression of integrins by expressing those, which promote their survival [20, 21]. Alternatively, in many tumor types downstream mediators of integrins are often mutated or unregulated. For example, Ras is upregulated or mutated in 25% of all tumors.

Cancer cells often have mutations in genes, which control cell cycle and apoptosis [22]. Many tumor types often have mutations of pRB or its related molecules, which play a central role in the entry of cells into the cycle [6, 23]. Also as a preventive mechanism, terminally differentiated cells lose their capacity to divide. Cancer cells circumvent this hurdle by expression of oncogenes such as myc protein or its related members, which inhibit differentiation. Thus, the indefinite proliferation of cells is often associated with changes in levels, mutation and types of transcription factors. Nevertheless, the capacity to divide indefinitely does not entail the cells to become malignant because of balance of death by apoptosis [1, 22, 24]. Cancer cells have mutations in genes such as p53, which control apoptosis. p53 is an important sensor, which activates the apoptosis cascade in response to DNA damage, hypoxia or activation of oncogenes. p53 tumor suppressor protein or downstream molecules are mutated in 50% of tumors [4]. Another major hurdle, which a cancer cell needs to overcome, is its ability to replicate its chromosomes indefinitely. Most cells have a finite replicative potential owing to the shortening of telomeres following each replication. Cancer cells circumvent this hurdle by over-expressing telomerase enzyme, which adds hexanucleotide repeats onto the ends of telomeric DNA [25].

Cancer cells initially are often restricted in size to few mm^3 [26]. These avascular tumors, due to absence of sufficient oxygen and nutrients, are hypoxic. At this critical stage, the progression of cancer cells rests on its ability to form new blood vessels, a process called angiogenesis. Angiogenesis is an important rate-limiting step during progression to malignancy. Endothelial cells line the inner surface of blood vessels and are quiescent in adult vasculature [27]. Angiogenesis in adult life is tightly regulated and occurs as brief bursts of capillary blood vessel growth that usually lasts only days or a week [28]. This is due to a balance between anti- and proangiogenic factors in the form of cytokines, matrix, hormones, and growth factors. Tumors cleverly tilt the balance in a process called angiogenic switch towards angiogenesis by secretion of growth factors such as VEGF, b-FGF, Ang2, EGF, IGF-1 and others. Additionally, proteolytic enzymes secreted by the tumors liberate growth factors arrested in the matrix [29]. Furthermore, tumors induce the secretion of chemokines and cytokines by immune cells promoting angiogenesis [30]. Conversely, this remodeling process also releases endogenous inhibitors such as angiostatin, endostatin, tumistatin, thromospondin, which inhibit angiogenesis [31, 32]. Tumor angiogenesis is further influenced by the presence of immune cells, which can influence angiogenesis in both directions. In total, only a net increase in the proangiogenic factors activates the normally quiescent endothelial cells in the tumor microenvironment. Activated endothelial cells upregulate integrins such as $\alpha_v\beta_3$ and $\alpha_v\beta_5$ and migrate towards the tumors mass [33]. Migrating endothelial cells proliferate and form cords, which later mature, into vessels acting as a conduit for blood flow. Angiogenesis is preceded by loosening of pericytes or smooth muscle cells, which form the outer covering of blood vessels. Once the new blood vessels are formed, pericytes cover the new vasculature again and secrete matrix and growth factors, which stabilize the vasculature [34]. Thus, tumor-induced blood vessel formation provides the hypoxic tumor with much needed oxygen and nutrients resulting in an explosive increase in size. Nevertheless, tumor induced formation of blood vessels leads to

irregular and leaky vessels that do not contain typical arteriole and venule differentiation representing a potential target for therapy [35, 36].

Angiogenesis is followed by the invasion and disruption of normal tissue architecture by tumor cells, a process summarized as metastasis [37]. Metastatic tumors are often aggressive and refractory to all forms of therapy and are the major cause of cancer death [2]. Metastasis is again a complex process involving an interplay of numerous factors such as integrins, proteases, growth factors and numerous cytokines. Cancer cells display remarkable alteration in cell adhesion molecules, which are responsible for maintenance of the tissue integrity. Notably members of calcium dependent cadherin and immunoglobulin superfamily exhibit decreased expression and binding in cancer cells [20, 38]. In addition to these changes, cancer cells secrete proteases or induce their release by recruited cells such as stromal cells and cells of the immune system [37]. Proteases belonging to matrix metalloproteases or to the serine kinase family have been often shown to be upregualted in numerous tumors. The secreted proteases bring about a breakdown in the matrix in an orchestrated manner, and are guided by altered integrins on the neighboring cell types. In addition, proteases act in a redundant manner making the absence of one member being compensated by others [27, 39]. Thus, the concerted action of proteases, cytokines and modulation in surface receptor expression culminate in the invasion of tumor cells into the neighborhood and remote areas.

During transformation tumor cells constantly subvert the immune system by direct interaction with immune cells or by secretion of cytokines [40, 41]. Cells of the immune system such as macrophages, dendritic cells, and T cells have been demonstrated to influence tumor progression. Tumor associated macrophages (TAMs) at later stages of tumor progression have been shown to display a phenotype which favors tumor growth by secretion of proangiogenic molecules and remodeling enzymes [42]. Dendritic cells (DCs) present in the tumor vicinity have been demonstrated to be immature due to the presence of an immunosuppressive microenvironment and therefore cannot effectively present antigens [43, 44]. Therefore, strategies such as vaccination or ex vivo stimulation of DCs with different means are currently in clinical trials. NK cells, another important constituent of the immune system, have been shown to lack efficient trafficking to the tumor tissue due to the loss of adhesion or costimulatory molecules and probably due to an immunosuppressive tumor microenvironment [45]. T cells, the major regulators of the immune reaction, have been shown to be anergic to tumor growth due to the lack of costimulatory molecules exhibited by APCs and by the presence of certain cytokines, shifting the immune response towards the Th2 type [46]. In addition, some tumor cells express Fas ligand, which induces apoptosis in CD8 cells. Also a new subset of CD4+ CD25+ cells has been identified which amongst other functions may be responsible for suppression of immune response against the tumor [47]. Apart form direct contact, tumor cells and immune cells communicate via cytokines. Cytokines are soluble extracellular proteins or glycoproteins affecting inflammatory host defenses, cell growth, differentiation, cell death, angiogenesis, development and repair processes. Cytokines are very potent and act at concentrations of 10^{-9} to 10^{-15} M, are produced by virtually every nucleated cell type in response to injurious stimuli and act on cells expressing complementary receptors. Cytokines play an important role in tumor initiation, progression and therapy [48]. Cytokine-induced inflammation during *H.Pylori* and Hepatitis C virus infection has been shown to cause gastric and hepatic carcinoma, respectively [13]. Mice constitutively expressing IL-15 succumbed to NKT cell leukaemia [49]. The role of cytokines as protective agents against cancer formation has been shown using knockout mouse models. Mice deficient in IFNγ or IFNγ receptor are susceptible for polycyclic hydrocarbon methyl cholanthrene induced tumors [50]. In addition, cytokines have also been postulated to be responsible for immunosupression, which causes tumor anergy in cancer patients. In this regard, elevated levels of immunosuppressive cytokines like TGFß and IL-10 have been observed in the serum of cancer patients [51]. Conversely, tumor mediated immune suppression may be mediated by down-regulation of IL-2 or its receptors. Cytokines have also been used to inhibit tumor growth in clinical settings. For example, IL-2 and IFNα have been already approved by the FDA for the treatment of renal cell carcinoma (RCC) and melanoma [52]. IL-2 is a specific T cell growth factor and can increase NK cell counts. IL-2 when

given locally enhances tumor rejection through a coordinated host reaction composed of neutrophils, eosinophils, macrophages, NK cells and lymphocytes. Apart from IL-2 and IFNα, IL-12 has shown striking anticancer effects in mouse models. Thus, the growth of tumors requires concerted deregulation of multiple pathways, alteration of surface receptor expression, and secretion of proteases and recruitment of cells in the vicinity. Numerous targets, which are currently being investigated for tumor intervention is shown in Figure I.1. An in-depth understanding of these factors shall aid in the design of new adjuvant therapies for cancer treatment. The physiological function of VEGF, angiopoietins and IL-12 and strategies for their blockade, the subject of this thesis, is discussed in the next Chapter.
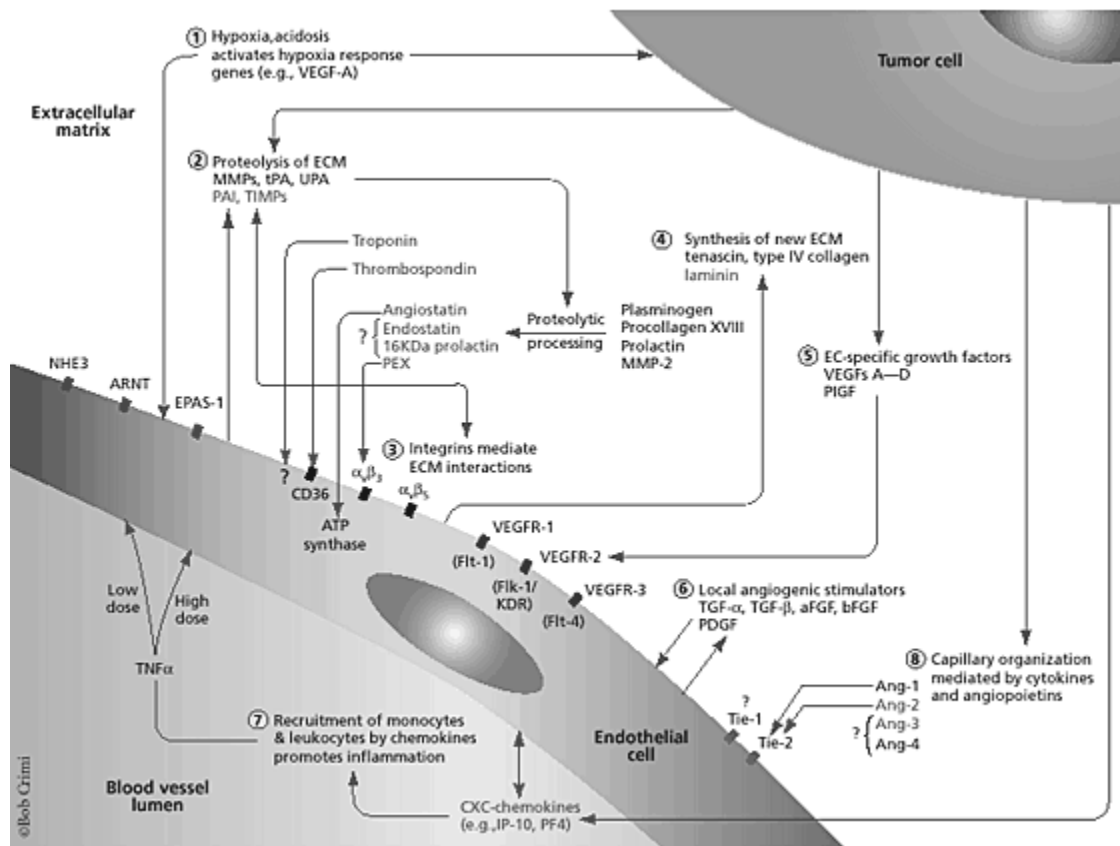
Figure I.1: Potential target molecules for antiangiogenic therapy of tumors. The picture was taken from the article "Tumor angiogenesis-new drugs on the block" published in the journal, Nature Biotechnology Vol 17 October 1999.
.

I.1.2 Physiology of angiopoietins, VEGF, and IL-12

Cancer occurs because of breakdown of several regulatory circuits as discussed earlier. Despite this complexity, cancer growth intervention can be achieved by selectively blocking growth factors or by the presence of cytokines. Among the growth factors, sequestration of members of VEGF and angiopoietins is currently being pursued in different animal models and clinical trials. Similarly, among the cytokines, IL-12 has repeatedly demonstrated tumor inhibition in different mouse models of cancer. Therefore, in this chapter the physiology of members of the VEGF and the angiopoietin growth factor families and of the cytokine IL-12 is discussed.

Proliferation of endothelial cells in adulthood occurs mainly during wound healing, muscle building and during the menstrual cycle. As discussed earlier tumor growth beyond few mm^3 requires proliferation of endothelial cells. Although numerous growth factors such as FGFs, IL-8, IFN,TNF etc [26] promote endothelial proliferation, members of the VEGF and angiopoietin growth factor and receptor families are relatively specific for endothelial cells. They have been shown to be upregulated in numerous tumor types apart from physiological angiogenesis [51, 53]. Members of the angiopoietin family of growth factors and members of their cognate receptor family namely Tie1 and Tie2 play an important role during embryonic, adult and pathological angiogenesis [54]. Unlike VEGF, which stimulates the growth of endothelial cells, angiopoietins are important for the modeling of the vasculature. On the basis of sequence homology four different angiopoietins (Ang1-4) have been discovered all binding to the tie2 receptor [54]. A ligand for the tie1 receptor has not been yet discovered. Ang1 is a 70 kD glycoprotein and binds to the tie2 receptor with a K_d of 3.7 nM. Ang1 plays an important role in the adult female reproductive system, haematopoiesis, and the maintenance of endothelial integrity in the adult vasculature [55]. Targeted inactivation of Ang1 in mice causes embryonic lethality (E12.5) as a result of defective modeling of the vascular plexus, lack of perivascular cells, a phenotype resembling tie2 knock out mice [56]. These results indicate that Ang1 recruits and sustains pericytes and is needed for the maturation of blood vessels during embryonic development. Over-expression of Ang1 results in blood vessels that are resistant to leakage induced by VEGF or inflammatory cytokines [57]. The role of Ang2 is not yet completely understood. Mice deficient in Ang2 are born relatively normal, but develop ascites and edema, have remodeling defects in the retina and die by day 14 [58]. Ang2 has been shown to be abundantly expressed in the tumor vasculature during earlier and later stages of vascular activation [54]. It has been proposed that the level of Ang1 remains constant during the vascular remodeling process but an increased ratio of Ang1/Ang2 favors vessel stabilization whereas a decreased ratio results in vessel regression [54]. All of the discovered angiopoietins mediate their action by signalling via the tie2 receptor. Tie2 knockout mice have a phenotype similar to Ang1 knockout mice [59]. High levels of tie2 expression are observed in the vasculature of endothelial cells in tumor cells as well as in healing skin wounds. Unlike Tie2, the role of the Tie1 receptor is not yet clearly understood. Mice deficient in Tie1 undergo embryonic death between E13.5 and E18.5, depending on their genetic background. It has been suggested that Tie1 might mediate its action by forming heterodimers with Tie2 [59, 60]. Absence of the identification of the Tie1 ligand has hampered an understanding of its role in angiogenesis. Recently, Ang3 and Ang4 were discovered based on sequence homology [61]. Ang3 appears to act as an antagonist, whereas Ang4 appears to function as an agonist. Further characterization of these molecules with respect to tumor development is eagerly awaited. In summary, the angiopoietins play a pivotal role in vascular remodeling and its selective inhibition might offer an opportunity to inhibit tumor growth.

VEGF A, the dominant VEGF is a specific mitogen and motogen for endothelial cells and is produced by a wide variety of cell types [62]. VEGF A has a molecular mass of 34-45 kD exhibiting multiple and diverse functions that are important under physiological and pathological situations [63]. VEGF A binds to three different receptor tyrosine kinases, VEGFR1 (Flt1) and VEGFR2 (flk1) and VEGFR3 (flt4). VEGF A displays chemotactic effects on endothelial cells and promotes their survival in adult vasculature. Over-expression of VEGF A in pathological situations

such as during tumor growth causes vasodilatation, increased expression of proteolytic enzymes from endothelial cells, upregulation of integrins, remodeling of matrix and migration of endothelial cells [64]. VEGF also inhibits the maturation of antigen presenting dendritic cells in adult mice [65]. A dramatic effect of VEGF A is observed in mice that lack one VEGF allele. VEGF +/- mice die around day 10 of embryonic development because of cardiovascular defects [66, 67]. The human gene for VEGF A on chromosome 6p21.3 is organized in eight exons. Five isoforms of hVEGF A are generated as a result of alternative splicing of the single VEGF A gene (VEGF 121, VEGF 145, VEGF 165, VEGF 189, and VEGF 206). The mouse isoforms are one amino acid shorter than the corresponding human ones. All VEGF A isoforms are secreted as covalently linked homo-dimers and they differ in their ability to bind to heparan sulphate and extracellular matrix [68]. VEGF 206 binds most strongly to heparin in contrast to VEGF 121, which is the most diffusible isoform. The abundant isoform VEGF 165 displays intermediate diffusion characteristics. It is speculated that combinatorial expression of heparin binding and soluble VEGF results in a gradient that peaks at the site of its secretion and elicits a chemotactic response for endothelial cells [69]. Many growth factors and cytokines upregulate VEGF mRNA or induce release of VEGF. These include PDGF, TNF-α. TGF-β, FGF-4, keratinocyte growth factor (KGF), epidermal growth factor (EGF), IL-1α, IL-β, IL-6 and insulin like growth factor 1 (IGF-1). VEGF A is highly upregulated by hypoxia and is believed to be the main mediator of hypoxia-induced angiogenesis in tumor growth [70, 71]. Recently, novel VEGF A related proteins were identified and characterized based on sequence homology. The identified proteins are placental growth factor (PIGF), VEGF B, C, D and E. Three isoforms of PIGF have been discovered their expression being restricted to placenta [70]. PIGF isoforms form heterodimers with VEGF, which have a weak mitogenic activity. VEGF-B has a wide distribution but is particularly abundant in the heart and skeletal muscle. Two isoforms of VEGF-B exist, which bind to VEGFR-1 and neuropilin-1 receptor. VEGF C and VEGF D proteins bind to VEGFR-3 and VEGFR-2. VEGF B and VEGF D play an important role in the development and maintenance of lymphatic vessels [72, 73]. VEGF-E is a collective term for a group of proteins encoded by strains of *orf* virus [74].

Three tyrosine kinase receptors binding to the VEGF family of growth factors namely VEGFR 1 (Flt1), VEGFR 2 (KDR), and VEGFR 3 have been identified. They are characterized by seven extracellular immunoglobulin (Ig)-like domains followed by a membrane-spanning region and a conserved intracellular tyrosine kinase domain interrupted by a kinase insert sequence [75]. In adult mice, Flt1 is expressed in endothelial cells, osteoclasts, moncytes, haematopoietic stem cells and leydig cells. Flt1 has a MW of 180 kDa and has the highest affinity for VEGF A (K_d 10-30 pM) [53]. Flt1 also binds to PIGF and VEGF-B. During embryonic development Flt1$^{-/-}$ mice die at embryonic day 8.5, but mice deficient in the intracellular domain of flt1 develop normally [76, 77]. It is speculated that the main role of VEGFR1 is to act as a decoy receptor for VEGF. A soluble form of flt1 (sflt1) is found at high concentration in the placenta and is believed to sequester excess VEGF [78]. VEGFR 2 is expressed in endothelial cells, haematopoietic stem cells, circulating endothelial precursors (CEPs) and in umbilical stroma. VEGFR2 has a molecular weight of 200-230 kDa and is bound by VEGFA (K_d = 75-125 pM) [53]. The VEGFR2 receptor also binds to VEGF C, VEGF D and VEGF E. Mice deficient in VEGFR2$^{-/-}$ undergo embryonic death due to severe vascular deformities [79]. VEGFR 2 seems to mediate almost all of the observed endothelial cell responses to VEGF A. VEGFR 3 is primarily expressed in lymphatic endothelial cells and is a high affinity receptor for VEGF C and VEGF D [80]. In summary, members of the VEGF and angiopoietin family of growth factors and receptors play an important role in the development of blood vessels during physiological and pathological angiogenesis. Sequestration of these growth factors or interfering with their receptor signalling offers a new therapeutic intervention for cancer.

Among the cytokines, IL-12 is a principal mediator of the early innate immune response to intracellular microbes and is a key inducer of cell mediated immunity [81]. IL-12 was identified as a product of Epstein-Barr Virus (EBV) transformed human B-cell lines that can activate NK cells, generate lymphokine-activated killer cells (LAKs) and induce IFNγ production and T cell proliferation [82]. In vivo IL-12 is mainly produced by dendritic cells and mononuclear phagocytes. Stimuli for the production of IL-12 are LPS and infection by intracellular bacteria or viruses. IL-12 is secreted by antigen presenting cells (APCs) in response to infection and it initiates several physiological changes such as production of IFNγ by NK cells and T lymphocytes, and the cytolytic function of activated NK cells and CD8 T lymphocytes. Since IL-12 is produced by APCs in response to infection, it links innate and adaptive immunity responses [83]. Large amounts of IL-12 are produced in response to gram-negative sepsis, which stimulate macrophages to produce TNF, the principal mediator of septic shock.

Structurally, IL-12 is a heterodimer formed by a 35 kDa light chain (known as p35 or IL-12A) and a 40-kDa heavy chain (known as p40 or IL-12B). p35 is homologous to other single chain cytokines, where as p40 is homologous to the extracellular domain of members of the haematopoietic cytokine receptor family. It has been proposed that the unusual structure of IL-12 might have evolved from a primordial cytokine of the IL-6 family and one of its receptors [81]. IL-12 p40 is produced in large excess over the IL-12 heterodimer and homodimers of p40 are observed in mice. Knock out mice lacking the p40 component of IL-12 are defective in IFN production, TH1 responses and NK cell function. The IL-12 receptor is composed of two chains IL-12 β1 and IL-12 β2 and is expressed on activated Th1 cells, NK cells and on other cell types, such as DCs and B-cell lines [84]. Human subjects with mutations in the IL-12 receptor are highly susceptible to infection with salmonella and atypical mycobacteria.

The antitumor and antimetastatic effects of IL-12 have been demonstrated in many studies using murine models of cancer [81]. The mechanism of IL-12 mediated anti-tumor action is complex and may utilize effector mechanisms of both innate resistance and adaptive immunity to mediate antitumor resistance. It has been shown that dose and route of IL-12 and the cell environment played a major role in its antitumor activity. IL-12 has been shown to directly activate NK, NKT, CD4 and CD8 cells [81]. Other activated cell types include endothelial cells, dendritic cells, and macrophages. Activation of neutrophils by IL-12 has been proposed to cause microhemorrhage and thrombosis associated with its antitumor activity [85]. In most experimental models, antitumor activity of IL-12 was shown to require IFNγ. In addition to augmentation of cellular responses, IL-12, by inducing Th1 responses, also augments the production of opsonizing antibodies, also having antitumor activity. It has been demonstrated that the antiangiogenic effect of IL-12 is mediated by activating the downstream effectors of IFNγ such as IP-10 and MIG. However, in spite of its antitumor effect, IL-12 is toxic and has resulted in the death of patients during phase II clinical trials. Numerous protocols and methods have been proposed to allow for safe and effective application of this potent cytokine. If successfully applied to humans, IL-12 could be a powerful therapeutic agent against cancer.

I.2 Gene transfer methods and adenoviral vector systems

I.2.1 Vectors and cancer gene therapy

Vectors are vehicles for the introduction of nucleic acids into cells. They are either viral or nonviral in nature. Viral vectors used routinely for gene transfer belong to the family of retrovirus, adeno-associated virus (AAV), adenovirus and herpes simplex virus (HSV). Retrovirus is a RNA virus containing genes namely gag, pol and env that encodes for viral proteins, reverse transcriptase/integrase and viral envelope glycoprotein respectively [86]. Retroviral vectors are used extensively for introducing genes into dividing cells, such as tumor cells and hematopoietic cells. Retroviral vectors are constructed by providing the genes gag/pol and env in trans separately in packaging cells. The vector RNA, which has the packaging signal alone, is packaged and the vector is released from the cell by budding. Retroviruses have been extensively modified which includes modification of envelopes to improve its infectivity and generation of transcriptionally controlled vectors such as self-inactivating vectors in which all the viral promoter activity is lost upon integration and the transcription of the transgene is under the control of a heterologous promoter. The main limitation of retroviral vectors has been their inability to infect non-dividing cells and loss of transgene expression in transduced cells upon transplantation. The use of retroviral vectors has leaded the way to the technological production, storage, and distribution of commercial vectors on a scale that is required for the human clinical trials [87]. However, in the recent years lentiviral vectors, which also belong to the retroviral family, have been extensively used. Lentiviral vectors have the unusual property of transducing non-dividing cells and therefore may have wider application.

Adeno associated virus (AAV) is a small, nonpathogenic, single stranded DNA virus and requires the expression of genes from a helper virus such as Ad viruses or HSV for replication [88]. AAV contains two genes namely rep and cap. Rep encodes for replication and integration function of the virus and cap encodes for the structural components of the virus. The viral DNA also has two inverted terminal repeats, which contain the sequences needed for the packaging of the virus. The viral vector is produced by replacing the rep and cap gene with the therapeutic gene [89]. The rep and cap genes are expressed in trans in a packaging cell line along with the adenoviral genes needed for replication of the virus. Long-term expression of AAV vector has been observed in tissues such as muscle, liver and brain after transduction. The major limitations of the AAV vector are titer and the size of the transgene, which is limited to about 4.5 kb [89].

Adenoviruses are double stranded DNA viruses that may cause in general mild diseases of respiratory tract and gastro intestinal tract depending on the serotypes [90]. Replication defective Ad vectors for gene transfer are generated by deleting multiple genes or by complete removal of all viral genes. Ad vectors are very desirable for gene transfer because they can be produced in high titers, do not integrate in to the host genome, can transfer large DNA sequences, can infect both dividing as well as non-dividing cells and have broad tropism. The characteristics of adenovirus and its vectors are discussed in detail below.

Numerous gene transfer strategies have been devised to combat cancer including transfer of tumor suppressor genes (TSG) or cell cycle genes, direct attack on tumor cells, activation of the immune system and or blocking angiogenesis [91, 92]. The idea to use TSG was based on the observation that tumor tissues frequently have mutations in genes regulating cell cycle and apoptosis. Tumor suppressor genes which have for example been used are p53 or RB [93]. A second broad approach to selectively kill cancer cells is based on the transfer of suicide genes [94]. These suicide genes express enzymes, which convert a harmless drug into a potent cytotoxin, which apart from killing the tumor cell can also diffuse and kill the neighboring cells, thereby creating a bystander effect. Suicide genes that have been employed are for example HSV-thymidine kinase, cytosine deaminase or nitroreductase. The cytotoxins generated by these enzymes kill the cancer cell by mechanisms such as blocking DNA synthesis, DNA cross linking, or inhibition of topoisomerase activity. Thus, the transfer of suicide genes in contrast to transfer of TSG results not only in the

death of directly transduced neoplastic cells but also the surrounding cells. Another kind of gene transfer method involves the transfer of cytokines to activate the immune system or to promote the recovery of haematopoietic cells during chemotherapy [95]. A fourth commonly used approach is the use of vectors referred to as oncolytic viruses, which selectively replicate in tumor cells. Commonly used oncolytic viruses belong to the HSV or adenovirus family [96]. The commercially developed oncolytic vector Onyx 15 has a mutation in the E1B 55K gene and was believed to replicate selectively in p53 defective tumor cells [97].

I.2.2 Regulation of gene expression

Another important requirement for the expression of transgenes is the specific promoter. The choice of a promoter depends on the application and can be either constitutive or regulatable. In general strong constitutive promoters such as hCMV, MCMV and EF-1α are preferred for gene transfer experiments [98]. These promoters express transgenes ubiquitously and the expression is improved by the use of upstream enhancers and the inclusion of introns. In special applications such as cancer gene therapy, the expression of suicide genes or TSGs needs to be restricted to the tumor tissue to avoid systemic toxicity. Numerous tumor specific promoters are available which have some degree of selective activity in tumor cells. A promoter that is considered relatively specific for cancer cells is the telomerase promoter since telomerase is over-expressed in most tumors. Promoters of oncofetal origin such as the carcinoembryonic antigen (CEA), the α fetoprotein and the ErbB2 promoter have increased activity in breast tumors and in pancreatic tumors. Promoters, which are upregulated in the tumor microenvironment such as hypoxia responsive promoters, endothelial specific promoters and glucose specific promoters, are also currently being tested. Another strategy involves the use of tissue specific promoters for cancer gene therapy and is restricted to tissues in which the damage is not critical for the survival of the host. Some of the commonly used tissue specific promoters are the albumin promoter for hepatoma, tyrosinase promoter for melanoma, and prostate specific antigen (PSA) promoter for prostate carcinoma [99].

Regulation of gene expression is important, when toxic genes are expressed and expression should be limited for a short time. Several systems, which depend on the addition of exogenous chemicals such as antibiotics (doxcycline) and progesterone analogues (RU 486) have been developed. Apart from these methods of regulable/controllable gene expression, systems using promoters responding to UV, heavy metal and temperature have been tested. A system based on the progesterone analogue RU 486 is versatile and is recognized for its superior expression kinetics and lack of expression in the absence of the drug RU 486 [100]. RU 486 based systems consist of two expression cassettes. The first expression cassette expresses pSwitch. pSwitch is a fusion protein consisting of three domains: a DNA binding region, a RU 486 binding domain and a transcription activation domain. The DNA binding domain is derived from the yeast GAL 4 protein. The RU 486 binding domain is a mutated progesterone receptor and the transcription activation domain is derived from p65, a component of the NFkB complex. pSwitch is 86% human in sequence and is therefore less immunogenic when compared to an earlier form of regulator proteins, which used VP16 derived from HSV as the activation domain. The second cassette consists of a cDNA placed downstream of the UAS-TATA box-binding region. The UAS region consists of a tandemly arranged 17mer sequence to which the GAL4 DNA binding region of pSwitch binds efficiently in the presence of the drug RU 486. In the absence of RU 486, pSwitch resides in the cytosol as an inert complex with heat shock protein and other molecular chaperones. Binding of RU 486 triggers a conformational change that causes pSwitch to translocate to the nucleus where it initiates transcription of the target gene. Apart from RU 486 other progesterone analogues such as Org31376, Org 313806, ZK 98,229, ZK98.734 have been used, but detailed dose-response studies have not been reported. RU 486 is used as antiprogestin and antiglucorticoid at a dose of 10mg/kg. In contrast the doses sufficient to achieve gene induction studies are in the range of 0.1 to 0.8 mg/kg [101].

RU 486 mediated inducible transgene expression has been achieved both in vitro and in vivo using viral vectors and plasmids. High levels of erythropoietin in the presence of RU 486 was reported in mice upon intramuscular injection of a pGeneswitch plasmid designed to express erythropoietin [102]. Similarly, a lentiviral vector based on the pGeneswitch system demonstrated a 50-200 fold increase in EGFP expression upon RU 486 induction in vitro [103]. Tail vein injection of a HC-Ad vector expressing hGH under the control of the liver specific promoter TTRB followed by induction with RU 486 resulted in high level expression of hGH. Apart from gene transfer experiments, effective and tissue specific, anitprogestin-dependent regulation of gene expression has also been achieved in transgenic mice [104].

I.2.3 Adenovirus structure and characteristics

Adenoviruses are a large group of DNA viruses that infect vertebrates. They constitute the Adenoviridae family of viruses, which is divided into four genera, *Mastadenovirus, Aviadenvirus, Atadenovirus and Siadenovirus* [105]. So far more than 50 human adenovirus serotypes have been identified based on sequence comparison and neutralization assays. The serotypes are further classified into 6 species. Most vectors are based on adenovirus serotype 5 (Ad5) and Ad2. Adenoviruses are icosahedral particles with a size of 70-100 nm in diameter. The virion consists of a protein capsid surrounding a DNA-containing core. The capsid is composed of 252 subunits (capsomeres), of which 240 are hexons and 12 are pentons (241). Each penton consists of a base, which forms part of the surface of the capsid, and a projecting fiber whose length varies among different serotypes. Additional structural and non-structural include V, VI, VII, VIII, IX, III and IVa2 and a virus-encoded protease. The virus genome is a linear double stranded DNA of 36 kb with a terminal protein covalently attached to the 5′ termini. The MW of a single particle is 150-180 x 10^6. Virions have a buoyant density in CsCl of 1.32-1.35 g cm^{-3}.

Adenoviral genomes of different serotypes have the same or similar general organization. The viral genome consists of five early transcription units (E1A, E1B, E2, E3, and E4), two delayed early units (IX and IVa2) and one late unit (major late), which is processed to generate five families of late mRNAs (L1 to L5). The replication origins of adenoviruses are present in the first 50 base pairs of the about 100 bp inverted terminal repeats (ITRs) located at each end of the viral genome. A cis acting sequence required for the packaging is present at the left end and is responsible for the polar encapsidation of the viral DNA.

Proteins generated by the early transcription units are involved in cell transformation, replication and transactivation of viral and cellular transcription units and in immunosuppressive functions. Adenoviral entry into the cells involves the binding of the fiber to the Coxsackie Adenovirus Receptor (CAR) and the interaction of the RGD sequence in the penton base with α_v integrins [106]. This process is very efficient and rapid and involves the sequential uncoating of the virion before the ending up of DNA in the nucleus within 30 minutes to a few hours. After nuclear entry, the virus expresses the E1A proteins, which activate other transcription downstream proteins, which play a role in induction of apoptosis and bind to numerous cellular protein involved in transcriptional regulation [90]. The E2 region unit encodes the viral proteins involved in adenovirus DNA replication such as Ad DNA polymerase, pre-terminal protein (pTP) and DNA binding protein (DBP). The E3 region encodes multiple proteins that function to inhibit multiple pathways of cell death induced by host innate and cellular immune responses to the infected cells. Proteins encoded by the E4 region have been shown to play important roles in viral DNA replication, viral mRNA transport and splicing, shut off of host cell protein synthesis and regulation of apoptosis. Replication of adenoviral DNA occurs after accumulation of replication proteins encoded from the E2 region and requires as cis element the origin of replication present within the ITR region. Following DNA replication the major late promoter is activated resulting in the transcription of the late transcription units and in the production of the virus structural proteins followed by capsid formation and DNA encapsidation [90]. The encapsidation process is governed by the presence of a packaging signal located at the left end of the virus DNA. An infectious cycle is completed in 36-48 hours with the release of about 10,000 virions per permissive cell.

I.2.4 Adenoviral vector systems

First or second generation adenoviral vectors are replication deficient and are characterized by deletion of viral sequences. First generation Ad vectors were generated by the deletion of E1 genes, allowing introduction of about 8.0 kb of foreign DNA under the control of heterologous promoters. Without the E1 function the E2 transcription unit is inactive. Thus proteins necessary for viral DNA replication are not expressed. First generation Ad vectors are propagated in a permissive cell line such as 293 cells, which provides E1 functions in trans [107]. Numerous systems have been developed for the generation of first generation Ad vectors. In general, these systems are based on in vivo recombination between shuttle plasmids containing a gene of interest flanked by homologous sequences such as Ad E1 or E3 and a second plasmid containing essentially the entire Ad genome in a circular form [108]. The shuttle plasmids differ in size and location of the Ad deletion, the regulatory sequences present, and unique restriction sites available for the insertion of a foreign gene. The generated first generation adenoviral vector is further selected by several rounds of plaque purification. In many studies with first generation Ad vectors performed in vivo in mice, expression has peaked about one week after vector administration and returned to background levels at 2-4 weeks. The transient expression has been attributed to immune response against capsid proteins and the expressed transgenes. Also the elimination of E3 proteins from the vector may contribute to the elimination of defenses against host responses. Short term transgene expression from first generation Ad vectors make this vector type unsuitable for most gene therapy applications in which continuous expression of a therapeutic protein is required. However, because of their immunostimulatory activity it is likely that this vector will be used in the future in vaccination studies.

Second generation adenoviral vector were generated by further deletion of parts of the E2 region and E4 regions, increasing somewhat the capacity for gene transfer. In some cases, the E3 function of the vector has been restored to augment prolonged transgene expression. The advantages of second generation over first generation adenoviral vector are controversially discussed.

In an attempt to improve the expression kinetics and the safety profile a new generation of Ad vectors called high capacity adenoviral (HC-Ad) vectors has been generated [109]. These vectors unlike earlier generation vectors are completely devoid of viral genes. They contain only the ITRs, which are required as cis-elements for initiation of replication and packaging. The HC-Ad vectors are also referred to by different names such as helper dependent Ad vectors, gutless vectors, gutted vectors, and mini adenoviruses [110]. HC-Ad vectors can carry transgenes up to a maximum capacity of 37 kb thereby facilitating the transfer of complete genomic fragments. In the case of an expression cassette having a smaller size, stuffer DNA is used to bring the total vector genome size to at least 27 kb to prevent rearrangement during production [111]. In one system stuffer DNA was derived from the non-coding region of the hypoxanthine guanine phosophoribosyl transferase (HPRT) locus or from the human cosmid C346 [112]. Stuffer DNA may contain matrix or scaffold attachment regions, which are believed to have positive influences on vector and/or expression stability in transduced cells. The influence of stuffer sequence on transgene expression was demonstrated when a CpG rich stuffer DNA derived from phage lambda was used. These vectors showed a significantly shorter hepatic expression of a lac Z transgene when compared to a vector containing HPRT stuffer sequences [112].

Generation of a HC-Ad vector requires three components, a helper virus, a permissive cell line expressing Cre-recombinase and a linear plasmid to be rescued as a vector. The helper virus is a first generation vector having deletions in the E1/E3 region and two LoxP sites flanking the packaging signal. The permissive cell line Cre66 expresses cre recombinase and E1a and E1b protein constitutively. Cre recombinase is derived from the bacteriophage P1 and is responsible for recombination between the two LoxP sites. The plasmid to be rescued as HC-Ad vectors requires free terminal ITRs and a size between 27-36 kb. HC-Ad vector is generated by transfecting the linear plasmid and infection with helper virus into Cre66 cells. Replication is initiated by the E1a protein expressed in trans by Cre66 cells. Along with the helper virus, the vector DNA also

replicates to high numbers. However, in the presence of Cre recombinase, the packaging signal from the helper virus genome is excised. In contrast, the vector DNA containing the ITRs is packaged efficiently. The HC-Ad vector is released by freeze thawing and the lysates containing the HC-Ad vector are serially passaged for about six times to yield high titers. As a result of serial passaging, the helper virus contamination is reduced to 1%.

First and second generation adenoviral vectors have been used extensively for gene transfer in different rodent models and in clinical trials. These vectors have shown efficacy in different animal models of liver diseases, hemophilia, Duchenne muscular dystrophy (DMD), cystic fibrosis (CF) and cancer [113]. In general, the results from these vectors were characterized by short-term expression of transgenes due to clearance of transduced cells by infiltrating lymphocytes and by ADCC against the transgene [90]. In contrast, HC-Ad vectors administered intravenously show improved expression kinetics and significantly less toxicity compared to first generation adenoviral vectors. HC-Ad vectors have been also been used in preclinical models of liver diseases, hemophilia, and DMD. HC-Ad vectors have also been used in the successful gene transfer to the eye and the CNS. An HC-Ad vector containing the complete locus for α-antitrypsin gene expressed the protein in immuno-competent mice for more than a year with negligible toxicity [12]. In a similar study another HC-Ad vector expressed leptin for a longer time compared to first generation vector demonstrating the superiority of the HC-Ad vector [11]. In another example, high levels of RU 486 dependent expression of hGH were observed in immunocompetent mice. The expression of hGH could be induced over time by repeated RU 486 administration during the 50-days study period [10]. HC-Ad vectors have also been used in animal models for hemophilia, which causes prolonged bleeding into joints, muscle, and internal organs. An HC-Ad vector expressing the F VIII human cDNA under the control of the 12.5 kb AAT promoter showed correction of the phenotype in a mice model [114]. However, it was also observed that the levels of F VIII decreased which was believed to be due to antibodies generated against the transgenic F VIII protein.

Adenoviral vectors have also been tested for efficacy in different murine models of cancer. First and second generation adenoviral vectors have been constructed to incorporate TSGs, suicide genes or cytokine genes. The vectors have been injected either intravenously by tail vein injection or by direct injection into the tumor site. Ad vectors incorporating p53 showed efficacy with thyroid cancer, malignant gliomas, and breast cancer[115-118]. Adenoviral vectors incorporating suicide genes such as thymidine kinase or cytosine deaminase were tested *in situ* for head and neck tumors and phase 1 trials have been completed for malignant mesothelioma and for prostate carcinoma [119, 120]. A trimodal therapy involving a double suicide vector of HSV-tk and CD combined with radiotherapy has proved very effective in tumor reduction in a cervical carcinoma xenograft model [121]. Also, adenoviruses replicating in tumor tissues called oncolytic vectors have been developed. The commercially developed vector called Onyx 15 has a mutation in the E1B 55K gene and was supposed to replicate selectively in p53 defective tumor cells [97].

Numerous methods have been shown to improve the kinetics of transgene expression using Ad vectors. The methods include retargeting of virus, injection of immunosuppressive agents, use of tissue specific promoters, use of alternate serotypes, improvement of stuffer regions and depletion of Kupffer cells. Thus the advancement in the development of adenoviral vectors shall aid in the delivery of transgenes, which are known to inhibit cancer growth. Also the modification of viral tropism may increase the tumor infectivity of adenoviral vectors in the future. Taken together, these strategies offer new hope in the treatment of susceptible tumors.

II Objective

Conventional tumor therapy is frequently unsuccessful in the eradication of distant metastases and recurrent tumors. Therefore, new strategies are required to supplement current therapies. Some of the recent efforts have been directed to the activation of the immune system and to the suppression of tumor angiogenesis. We reasoned that long-term expression of immunomodulatory or anti-angiogenic molecules at significant levels might represent a promising strategy to control malignant tumor growth.

As vector delivery system we chose HC-Ad vectors since they allow long-term gene expression from hepatocytes following systemic administration.

As therapeutic molecules, we focused on IL-12, sflt1 and stie2, which are well-studied proteins with potent immunomodulatory and anti-angiogenic functions, respectively.

A first aim was the generation of HC-Ad vectors expressing sflt1 and stie2 in a constitutive manner. Since constitutive high-level expression of murine IL-12 and sflt1 was expected to have toxic side effects, a further safety level was introduced by constructing additional vectors that expressed IL-12 and sflt1 in a drug-inducible manner. Because the RU 486-inducible pGeneSwitch system has been shown to allow tight transcriptional control in vivo, this system was used as the basis for these studies.

A second aim consisted in the characterization of the generated vectors in vitro and in vivo with respect to expression kinetics and functional activity. Since the human IL-12 is not functional (and not toxic) in mice, this molecule was used as a reporter to follow expression from a RU486 inducible and liver-specific vector format in vivo.

Finally, a third aim was the testing of the different vectors in two different syngenic tumor models in mice, the subcutaneous LLC model and the orthotopic MC-38 model. The former is a relatively simple model that allows rapid screening of antitumor effects of biologicals. The latter is a physiological model of liver metastases, in which tumor cells are implanted directly into the liver and anti-tumor effects of proteins expressed in normal hepatocytes in the tumor environment can be studied.

Together, these studies were designed to contribute to an improved understanding of the potential of vector-mediated expression of anti-angiogenic and immunomodulatory functions for tumor therapy.

III Materials and Methods

III.1 Materials and Instruments

III.1.1 Materials

All chemicals, when not specially mentioned, were purchased from the company Applichem GmbH (Germany). The solutions were prepared using water obtained from EASY pure instrument (Werner water purification system, Germany). The bacterial media and agar was purchased from Invitrogen (Germany). The enzymes were purchased from NEB (Germany). Oligonucleotides were purchased from Invitrogen (Germany). Cell culture media, when not specially mentioned, were purchased from Invitrogen (Germany). All cell culture materials (cell culture dishes, pipettes etc.,) were purchased from Renner (Germany). The secondary antibodies used in western blot analysis were purchased from Jackson Immunochemicals (USA). The ELISA plates were purchased from NUNC (Germany).

III.1.2 Instruments and equipment

Autoclave	Systec (Germany)
Cell culture hood	Clean Air Technik (Netherlands)
Cell culture incubator	Forma Scientific, (USA)
Centrifuges	Biofuge fresco (Germany)
	Eppendorf 5417C (Germany)
	Sigma 6K15 (Germany)
Gel chamber for protein gels	"Mini-protean II Electrophoresis Cell"
	Bio-Rad Laboratories GmbH (Germany)
Heating block	VWR (Germany)
Hitachi Auto analyzer	Roche/Hitachi 904/911: ACN 166 (USA)
Incubator (Bacterial culture,	
enzyme reactions, pipette sterilization)	VWR (Germany)
Minihybridization oven	Biometra biomedizinische Analytik GmbH
	(Germany)
Micro Plate reader	Model 550.Bio-Rad Laboratories GmbH
	(Germany)
PCR thermocycler Uno II	Biometra biomedizinische Analytik GmbH
	(Germany)
pH-meter pH526	WTW GmbH (Germany)
Spectrophotometer	Pharmacia Biotech (Germany)
Ultracentrifuge	Beckman, L7-65 with SW41-Rotor (USA)

III.1.3 Buffers and Solutions

Agarose overlay medium	
0.5%	autoclaved agarose (FMC products, USA)
1 x	MEM
0.5%	penicillin/streptomycin
0.05%	yeast extract
5%	FCS

DNA-loading buffer (6x)
30%	Glycerin
60 mM	EDTA
0.1%	Bromophenol blue
0.1%	Xylene cyanol

HBS-Buffer (2x)
50 mM	HEPES
280 mM	NaCl
1.5 mM	Na_2HPO_4
pH	7.13

Hybridization buffer for slot blot
2 x	SSC
10%	Milk powder solution
0.5 mg/ml	Herring sperm
10%	Dextran sulfate

Laemmli Buffer with SDS (4x)
20%	Glycerin
0.7 M	Mercaptoethanol
4%	SDS
0.25 M	Tris-HCl (pH 7.0)
0.1%	Bromophenol blue

Milk powder solution for slot blot
5%	Low fat milk powder
10%	SDS

PCR-Mix
DNA	Plasmid DNA was used at concentration of 1-10 ng
	Genomic DNA was used at concentration of 1-2 µg
Pfu polymerase buffer	1x
Pfu polymerase	1.25 units (Stratagene, Netherlands)
dNTP-Mix	40 nmol (Roche, Germany)
dH_2O	made up to a volume of 50 µl

Sodium phosphate-buffer
46.6 ml	1M Na_2HPO_4
3.4 ml	1M NaH_2PO_4
8.8 gm	NaCl
500 ml	dH_2O
pH	8.0

Stacking gel for SDS PAGE
5%	Acrylamide/Bisacrylamide
125 mM	Tris-HCl, pH 6.8
0.1%	SDS
0.1%	APS
0.1%	TEMED

Separation gel for SDS PAGE
5-10%   Acrylamide/Bisacrylamide
375 mM   Tris-HCl, pH 8.8
0.1%   SDS
0.1%   APS
0.1%   TEMED

SDS-Running buffer (10x)
250 mM   Trisbase
2.5 M   Glycine
1%   SDS

SSC solution (20x)
3 M   NaCl (tri-sodium citrate)
0.3 M $Na_3H_5C_6O_7$ (tri-sodium citrate)
pH   7.0 (adjusted with NaOH)

Substrate solution for ELISA
0.024 M $C_6H_8O_7$
0.052 M Na_2HPO_4
pH   5.0 (adjusted with HCl)
1 tablet TMBD (3,3′, 5,5′-Tetramethyl benzidine) for 10 ml
21 µl of 30% H_2O_2 for 10 ml
The solution was filtered through a 0.22 µm filter

TAE-Buffer (50x)
2 M   Tris-Base
0.05 M   Acetic acid
0.05 M   EDTA

TBE Buffer
0.225 M   Tris base
0.225 M   Boric acid
0.02 M   EDTA

TBST Buffer for the ELISA
0.05 M   Tris-HCl, pH 7.5
0.1 M   NaCl
0.05%   Tween-20

TBS-Buffer (1x) for resuspension of virus
137 mM   NaCl
2.7 mM   KCl
25 mM   Tris-Base
pH 7.4 (adjusted with HCl)
(The solution was sterilized by autoclaving)

TE Buffer (1x)
10 mM   Tris-HCl, pH 7.5
1 mM   EDTA

TELT Buffer
50 mM	Tris-HCl, pH 8.0
62.5 mM	EDTA
2.5 M	LiCl
0.6%	Triton X-100

One spatula of Lysozyme

Transfer buffer for Western blot analysis
25 mM	Tris-Base
150 mM	Glycine
20%	Methanol

TTBS for Western blot analysis
10 mM	Tris-Base
150 mM	NaCl
0.1%	Tween-20
pH	7.6 (adjusted with HCl)

Transfer buffer for Southern blot analysis
0.1 N	NaOH

III.1.4 Oligodeoxyribonucleotides

The oligodeoxyribonucleotides were purchased from Invitrogen (Germany). The lyophilized oligonucleotides were dissolved in 1x TE buffer and were stored at –20 $^{\circ}$C. Oligodeoxyribonucleotides used for ligation were dissolved in 10 mM Tris buffer.

Actin-s   5´- GACGGCCAGGTCATCACTATTG-3´

Actin-as   5´-CCACAGGATTCCATACCCAAGA-3´

Fiber I   5´-ATGAAGCGCGCAAGACCGTCTG-3´
                   binds to nucleotides 31042-31063 of the Ad 5 sequence

Fiber II   5´-CCAGATATTGGAGCCAAACTGCC-3´.
                   binds to nucleotides 32368-32390 of the Ad 5 sequence

ITR I   5´- AACGCCAACTTTGACCCGGAACGCGG- 3´
                   binds to nucleotides 438-413 of the Ad 5 sequence

ITR II   5´- CATCATCAATAATATACCTTATTTTG-3´
                    binds to nucleotides 1-26 of the Ad 5 sequence

GLp65F   5´-AGCCAGATCTGAAGCTAC-3´
                   binds to nucleotides 3476-3493 of plasmid pRS 17

GLp65R   5´-TGCTTGATATATCTCGTCGA-3´
                   binds to nucleotides 4562-4579 of plasmid pRS 17

17merf2   5´-GGGACCGATCCAGCCTCCGCG-3´
                   binds to nucleotides 2452-2464 of plasmid pRS 17

BGHPA1	5′-GCAACTAGAAGGCACAGTCGA-3′ binds to nucleotides 2681-2702 of plasmid pRS 17
BGHPA2	5′-GCCCTCGACCTGCAGCCCAAGCTT-3′ binds to nucleotides 2971-2995 of plasmid pRS 17
MCMV1	5′-ATCGATGCGGCCGCTACGTAAGGCCTCTCGAG-3′ was generated to insert a *Not I* and *SnaB I* site into plasmid pRS 34
MCMV2	5′-CTCGAGAGGCCTTACGTAGCGGCCGCATCGAT-3′ was generated to insert a *Not I* and *SnaB I* site into plasmid pRS 34
Oligo 78	was generated by annealing complementary oligos V01 and V02
Oligo V01	5′-ATTTAAATATCGAT-3′ Contains a *Swa I* and *ClaI* site
Oligo V02	5′-ATCGATATTTAAAT-3′ contains a *Swa I* and *Cla I* site
Oligo 79	was generated by annealing oligos V03 and V04
Oligo V03	5′TATGTCGCGGCCGC TCGCC-3′ Contains a *Not I* site
Oligo V04	5′GGCGAGCGGCCGCGACATA-3′ Contains a *Not I* site
SG TTRB	5′-GGCTTCTGAGGCGGAAAGAAC-3′ binds to nucleotides 2908-2927 of plasmid pRS 17
SG PSwitch	5′-GCGGACATGGACTTCTCAGCCC-3′ binds to nucleotides 5339-5361 of plasmid pRS 17

III.1.5 Plasmids

The following plasmids were constructed during the work. The plasmids were constructed according to the protocols described in Chapter III.3. The plasmids obtained as a gift are specially mentioned. When non-cohesive ends of DNA were ligated, the ends were treated with Klenow enzyme to fill up the 5′ends. All the plasmids used, when not specially mentioned, were based on pBluescript II KS (Stratagene). pBluescript II KS has an ampicillin resistance gene, Co1E1 and f1 (+) origin of replication. pBluescript II KS also has a multiple cloning site for the insertion of DNA fragments.

a) Construction of plasmid pRS 14
The plasmid pRS 14 expresses the transactivator GLp65 under the control of transthyretin promoter (TTRB). The plasmid pRS 14 was generated from the plasmid pSTK 119 TA End TTRB and plasmid pPAP CMV GLp65 SV40. The plasmid pRS 14 was generated by subcloning the *Asc I/Pac I* fragment (expresses the transactivator under the control of TTRB promoter) from the plasmid pSTK 119 TA End TTRB GLp65, into the *Asc I/Pac I* site (by replacing the DNA fragment expressing the transactivator GLp65 under the control of CMV promoter) of the plasmid pPAP CMV GLp65 SV40. The plasmid pSTK 119 TA End TTRB GLp65 was obtained as a kind gift from Dr. Mark Burcin. The plasmid pSTK 119 TA End TTRB GLp65 expresses the transgene

endostatin, upon induction with RU 486, in a liver specific manner. The plasmid pPAP CMV GLp65 SV40 was obtained as a kind gift from Dr. Mark Burcin. The plasmid pPAP CMV GLp65 SV40 expresses the transactivator p Switch protein (pGLp65) under the control of the CMV promoter. The plasmid pRS 14 was later used in the construction of plasmid pRS 17. The cloning scheme for the construction of plasmid pRS 14 is shown in Figure III.1.
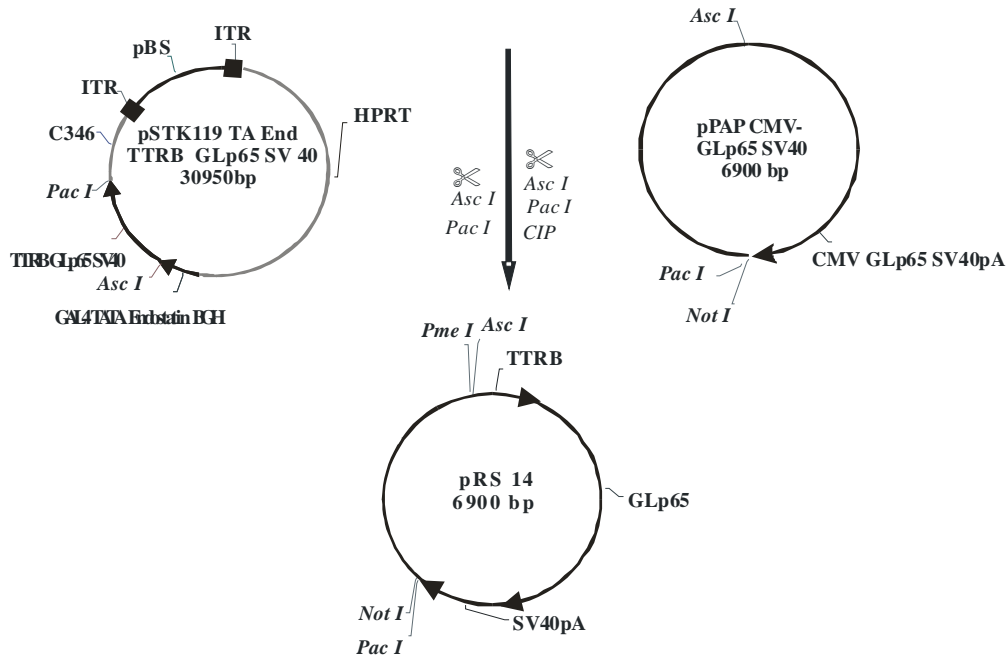

Figure III.1: Cloning scheme for the generation of plasmid pRS 14. The plasmid pRS 14 was generated by the insertion of the expression cassette TTRB GLp65 SV40 from the plasmid pSTK 119 TAEnd TTRB GLp65 SV40 into the plasmid pPAP CMV GLp65 SV40.

b) Construction of plasmid pRS 15

The plasmid pRS 15 has a unique *Cla I* and *Swa I* site for cloning the transgene for inducible expression, under the control of the TTRB promoter and RU 486. The plasmid pGene V5/His A was cleaved with enzymes *Hind III* and *Pme I* to release the multiple cloning site. The linear plasmid was isolated by agarose gel electrophoresis and was ligated to Oligo 78 containing *Swa I* and *Cla* I sites. The cloning scheme for the construction of plasmid pRS 15 is shown in Figure III.2.

c) Construction of plasmid pRS 16

The plasmid pRS 16 was generated from the plasmids pRS 15 and pPNA Δ *Sal* I/*Kpn*-CAT (a kind gift of Dr. Mark Burcin). The plasmid pRS 15 was digested with *Sal I* and *Pvu II* to release the insert containing the TATA box, cloning site and bGH poly A. The insert was made blunt by Klenowing and after agarose gel extraction the insert was subcloned into the *Sal I*/*Sma I* site of the plasmid pPNA Δ Sal I/*Kpn*-CAT. The plasmid pPNA Δ *Sal I*/*Kpn*-CAT contains the cDNA chlorophenicol acetyl transferase enzyme inserted downstream of the 17 mer TATA box. The plasmid pPNA Δ Sal I/*Kpn*-CAT contains a SV 40 poly A cloned downstream of the transgene. The plasmid pRS 16 was later used in the construction of plasmid pRS 17. The cloning scheme for the construction of plasmid pRS 16 is shown in Figure III.3.

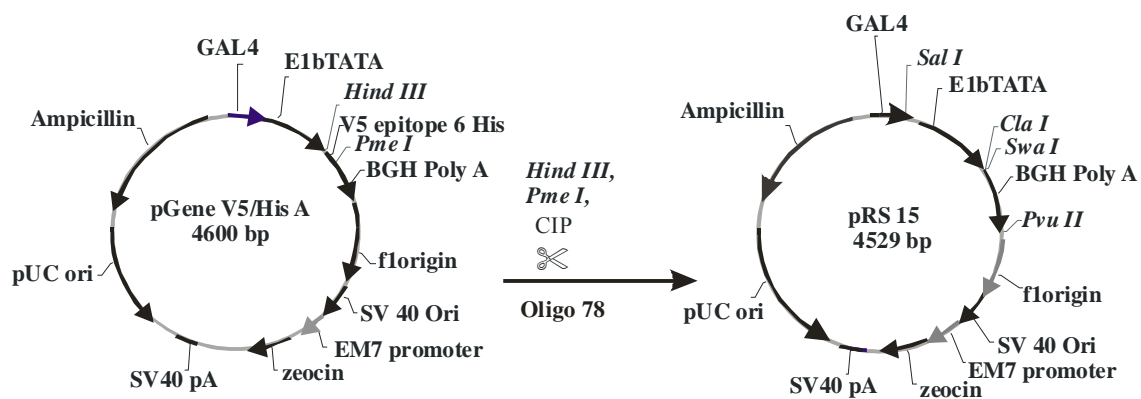**Figure III.2:** Generation of plasmid pRS 15. The plasmid pRS 15 was generated by replacing the MCS with the Oligo 78 containing restriction sites for *Cla I* and *Swa I*.
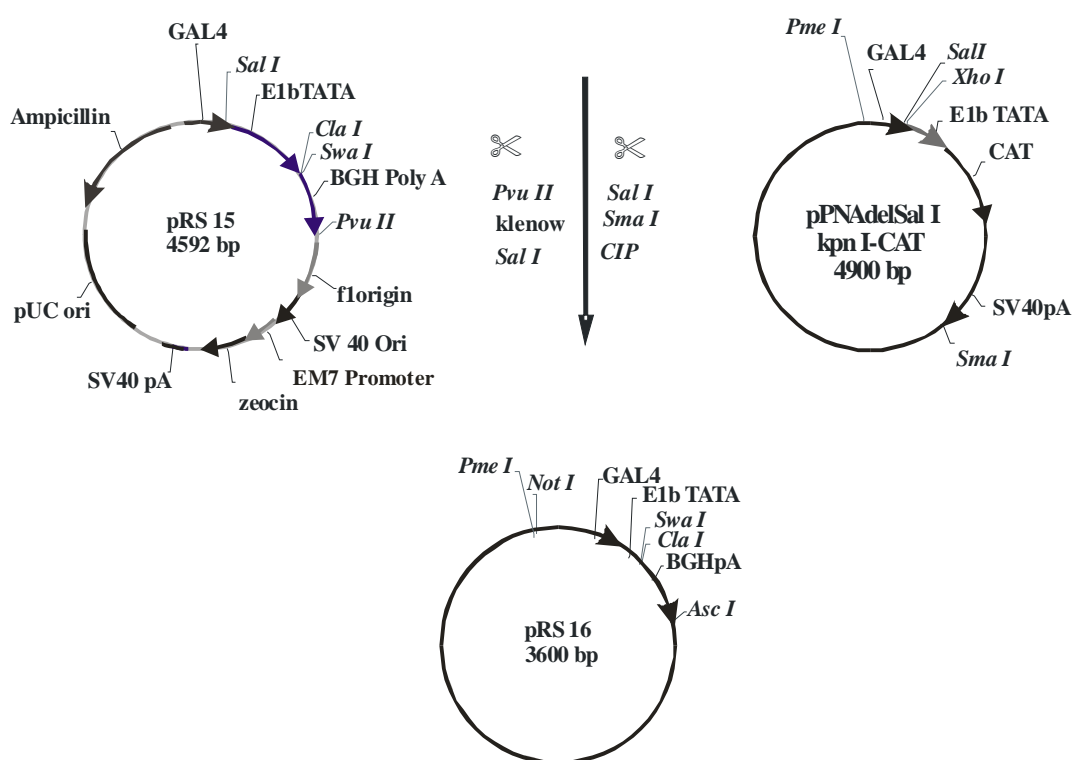
Figure III.3: Generation of the plasmid pRS 16. The plasmid pRS 16 was generated by inserting the *Pvu II* and *Sal I* fragment (Klenowed) derived from the plasmid pRS 15 into the *Sal I* and *Sma I* sites of plasmid pPNA del SalI / KpnI-CAT.

d) Construction of plasmid pRS 17

The plasmid pRS 17 has the two expression cassettes required for inducible expression of transgenes. The plasmid pRS 17 was generated from the plasmids pRS 14 and pRS 16. The plasmid pRS 17 was generated by insertion of the *Pme I/Asc* I fragment from plasmid pRS 16 into the *Pme I/Asc I* site of plasmid pRS 14. The oligos used for sequencing the pSwitch protein were GLp65F and GLp65R (Chapter III.1.4). The oligo used for sequencing the GAL4 region was 17merf2 (Chapter III.1.4). The oligos used for sequencing the BGHpA region were BGHPA1 and BGHPA2 (Chapter III.1.4). The cloning scheme for the construction of plasmid pRS 17 is shown in Figure III.4.

Figure III.4: Generation of plasmid pRS 17. The plasmid pRS 17 was generated by inserting the *Asc I/Pme I* fragment from desired plasmid pRS 16 into the *Asc I/Pme I* site of plasmid pRS 14.

e) Construction of plasmid pRS 20

The plasmid pRS 20 expresses sflt1 upon induction with RU 486 in a liver specific manner. The plasmid pRS 20 was generated from plasmids pRS 17 and pBS SK+flt1 D1-6 (a kind gift of Dr. Hubert Weich). The plasmid pRS 20 was generated by the insertion of the sflt1 cDNA, derived from the plasmid pBS SK+flt1 D1-6, into the *Swa I* site of plasmid pRS 17. pBS SK+flt1 D1-6 was digested with enzymes *Bam HI* and *Xho I* to release the sflt1 cDNA. The cloning scheme for the construction of plasmid pRS 20 is shown in Figure III.5.

Figure III.5: Generation of plasmid pRS 20. The plasmid pRS 20 was generated by inserting the *Bam HI/Xho I* fragment derived from plasmid pBS SK+flt1D1-6 into the *Swa I* site of plasmid pRS 17.

f) Construction of plasmid pRS 21

The plasmid pRS 21 expresses the hIL-12 upon induction with RU 486 in a liver specific manner. The plasmid pRS 20 was generated from the plasmids pRS 17 and pBS/hIL-12. The plasmid pRS 21 was generated by insertion of the hIL-12 cDNA into the *Swa I* site of plasmid pRS 17. The plasmid pBS/hIL-12 was digested with the enzymes *Xba I* and *Spe I* to release the hIL-12 cDNA. The released cDNA was made blunt by using the Klenow enzyme. The DNA was separated on a 0.8 % agarose gel, and was purified by using the Qia quick gel extraction kit (Qiagen, Germany). The blunt ended cDNA was cloned into the *Swa I* site of plasmid pRS 17. The cloning scheme for the construction of plasmid pRS 21 is shown in Figure III.6.
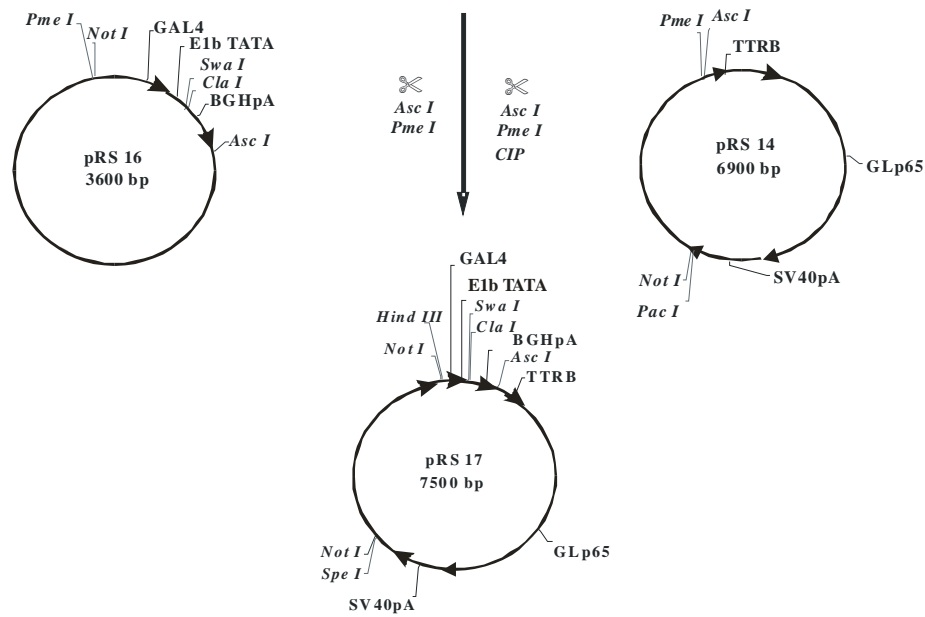
Figure III.6: Generation of plasmid pRS 21. The plasmid pRS 21 was generated by inserting the *Spe I/Xho I* fragment from the plasmid pBS hIL-12 into the *Swa I* site of plasmid pRS 17.

g) Construction of plasmid pRS 22

The plasmid pRS 22 expresses mIL-12 upon induction with RU 486 in a liver specific manner. The plasmid pRS 22 was generated by insertion of mIL-12 cDNA into the *Swa I* site of plasmid pRS17. The plasmid pBSmIL-12 was initially digested with enzymes *Xh*o I and *Spe I* to release the mIL-12 cDNA. The cloning scheme for the construction of plasmid pRS 22 is shown in Figure III.7.
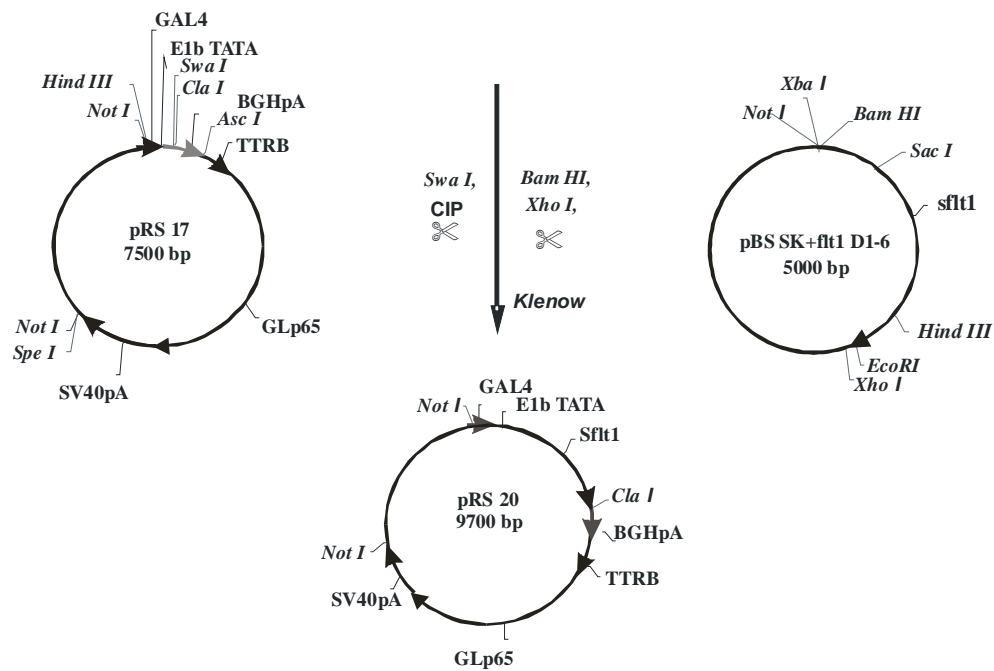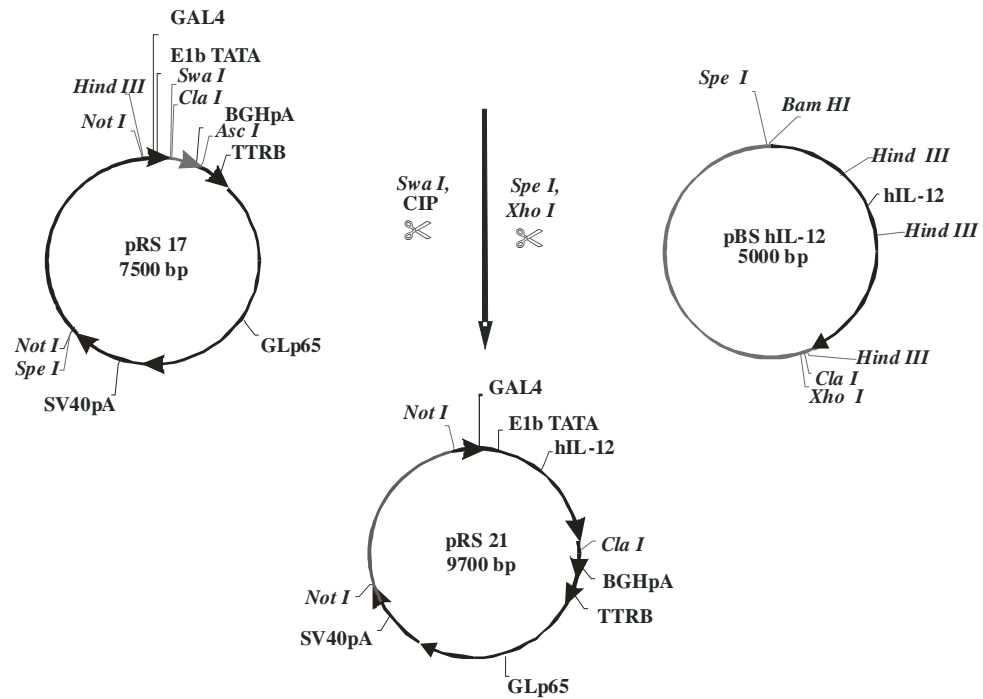

Figure III.7: Generation of plasmid pRS 22. The plasmid pRS 22 was generated by inserting the *Spe I/Xho I* fragment from plasmid pBS mIL-12 into the *Swa I* site of plasmid pRS 17.

h) Construction of plasmid pRS 23

The plasmid pRS 23 expresses the sflt1 upon induction with RU 486 in a liver specific manner. The pRS 23 was generated from the plasmids pRS 20 and pSTK 119. The plasmid pRS 23 was generated by the insertion of the *Not I* fragment (expresses sflt1 upon induction in hepatic cells) from the plasmid pRS 20 into the *Ecl XI* site of plasmid pSTK 119. The cloning scheme for the construction of plasmid pRS 23 is shown in the Figure III.8.

Figure III.8: Generation of plasmid pRS 23. The plasmid pRS 23 was generated by inserting the *Not I* sequence from plasmid pRS 20 into the *Ecl X I* site of plasmid pSTK 119.

i) Construction of plasmid pRS 24

The plasmid pRS 24 was constructed to express the hIL-12 upon induction with RU 486 in a liver specific manner. Plasmid pRS 24 was generated from the plasmids pRS 21 and pSTK 119. The plasmid pRS 24 was generated by the insertion of the *Not I* fragment (expressing hIL-12 upon induction in hepatic cells) from the plasmid pRS 21 into the *Ecl XI* site of plasmid pSTK 119. The cloning scheme for the construction of plasmid pRS 24 is shown in Figure III.9.

j) Construction of plasmid pRS 25

The plasmid pRS 25 expresses the mIL-12 upon induction with RU 486 in a liver specific manner. The plasmid pRS 25 was generated from the plasmids pRS 22 and pSTK 119. The plasmid pRS 24 was generated by the insertion of the *Not I* fragment (express mIL-12 upon induction in hepatic cells) from the plasmid pRS 22 into the *Ecl XI* site of the plasmid pSTK 119. The cloning scheme for the construction of plasmid pRS 21 is shown in Figure III.10.

31
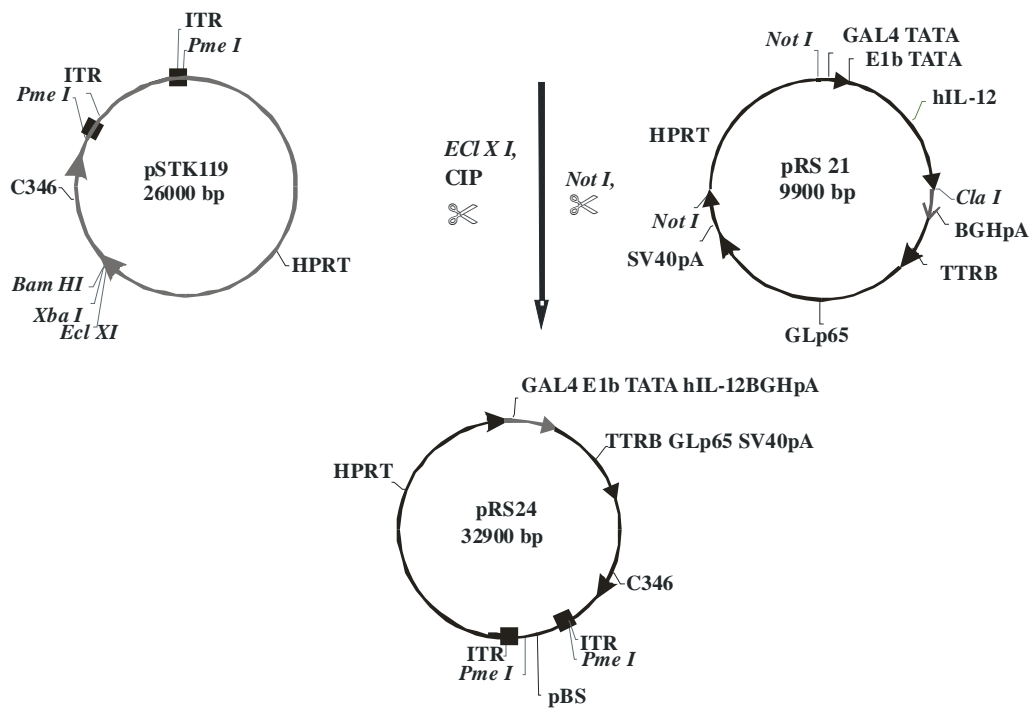
Figure III.9: Generation of plasmid pRS 24. The plasmid pRS 24 was generated by inserting the *Not I* sequence from plasmid pRS 21 into the *Ecl XI* site of plasmid pSTK 119.
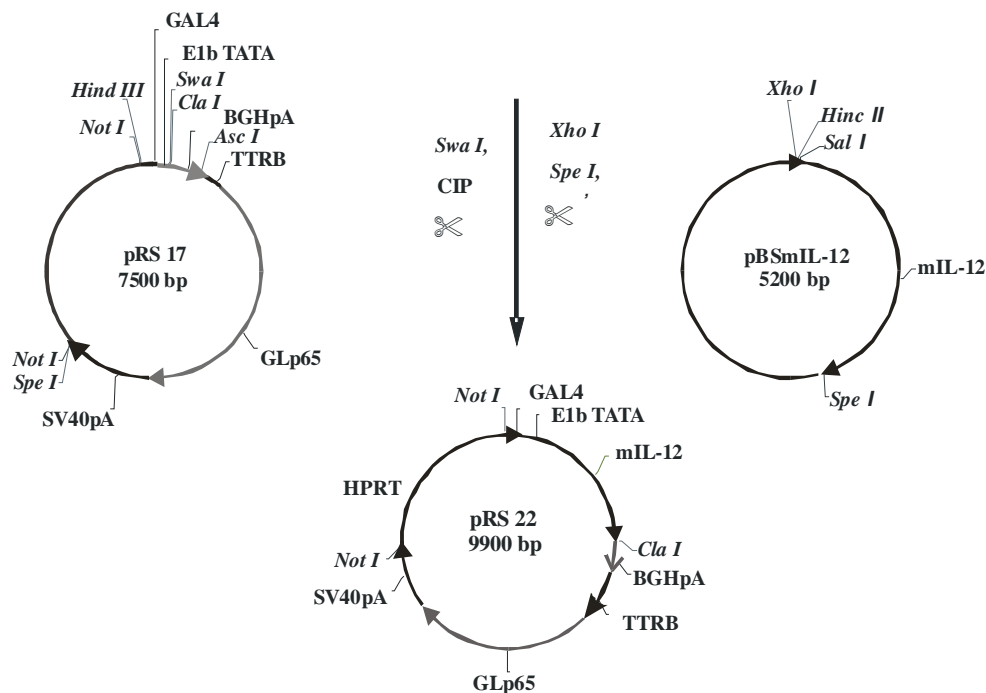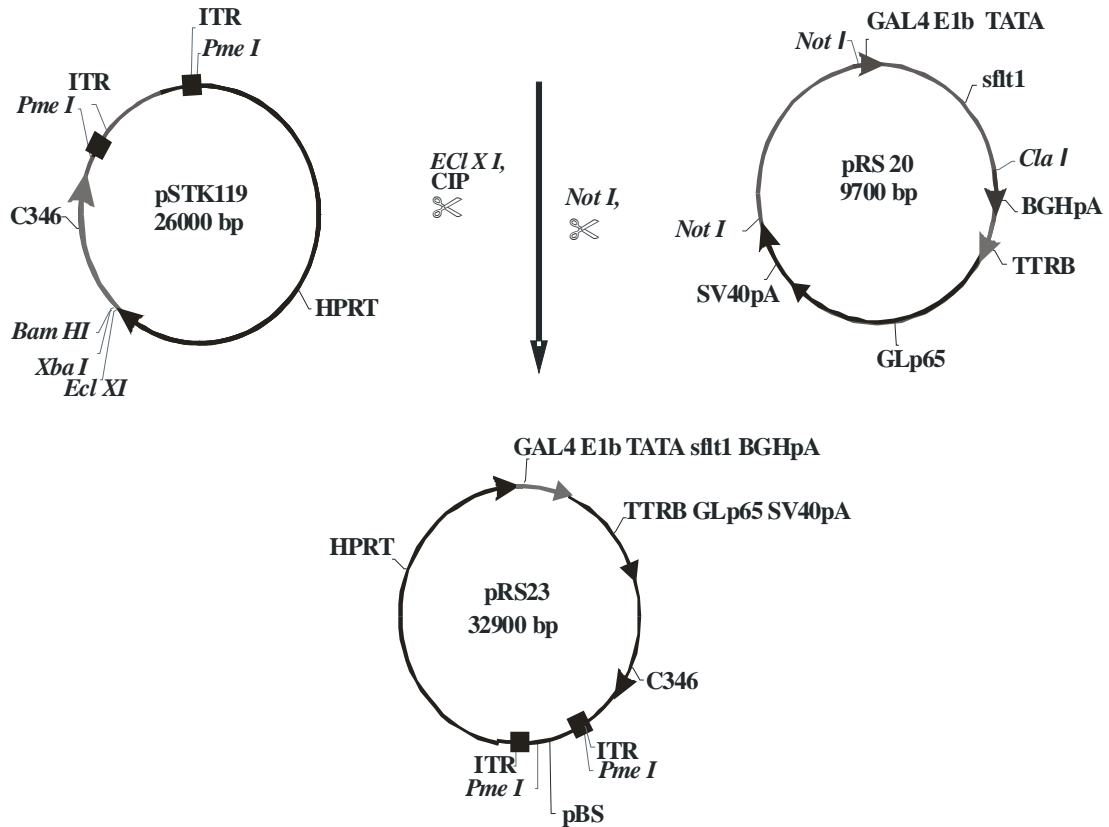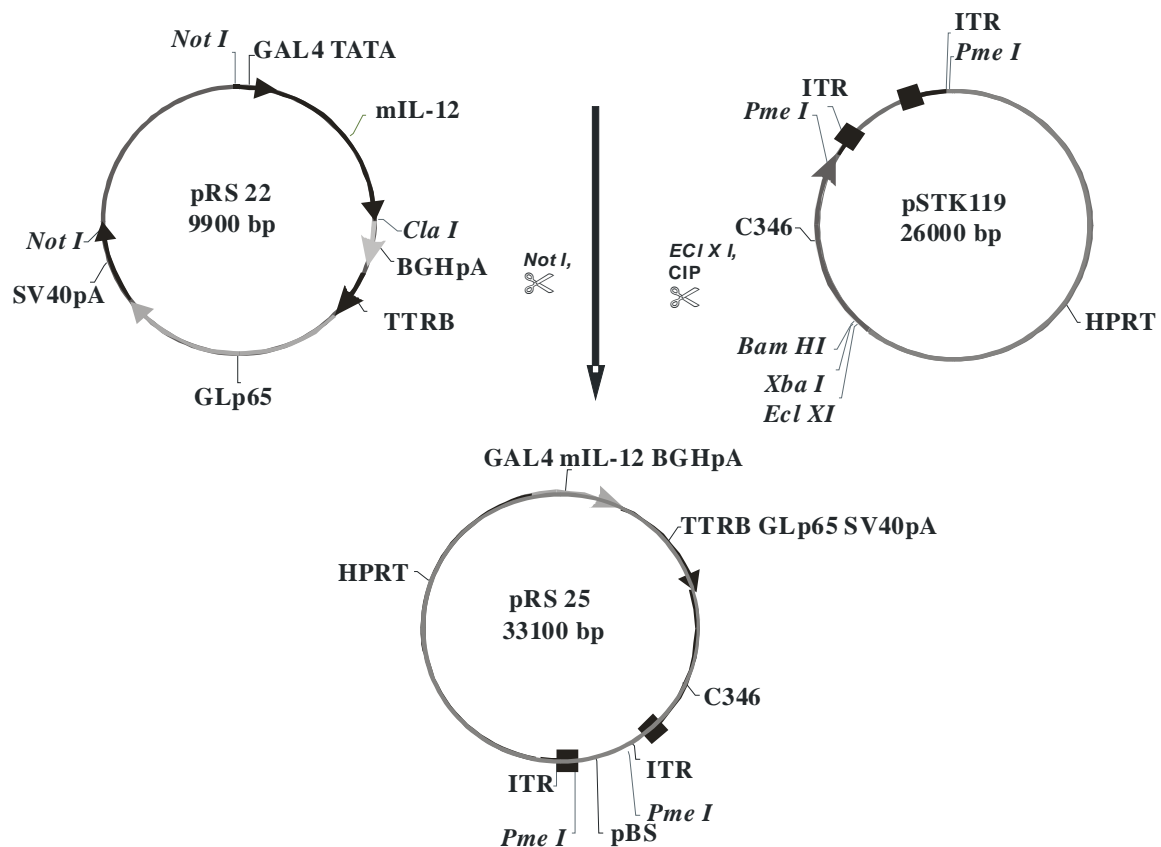

Figure III.10: Generation of plasmid pRS 25. The plasmid pRS 25 was generated by inserting the *Not I* sequence from plasmid pRS 22 into the *Ecl XI* site of plasmid pSTK 119.

k) Construction of plasmids pRS 28 and pRS 29

The plasmid pRS 28 was used for the generation of plasmid pRS 29. The plasmid pRS 28 was generated from plasmid pRS 17. The plasmid pRS 17 was digested with enzymes *Asc I/ Spe I* (to remove the sequence TTRB GLp65 SV40 pA) and was religated to generate the plasmid pRS 28. The cloning scheme for the construction of plasmid pRS 28 is shown in Figure III.11.
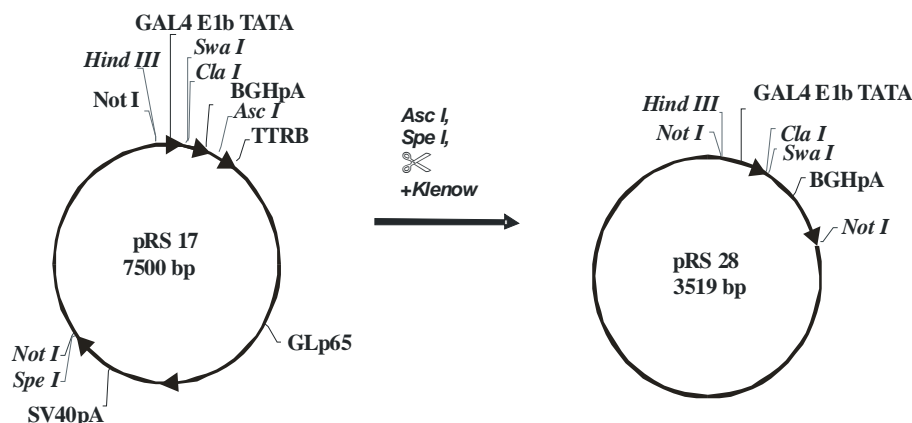
Figure III.11: Generation of plasmid pRS 28. The plasmid pRS 28 was generated by digesting the plasmid pRS 17 with the enzymes *Asc I* and *Spe I* and self-ligating the linear plasmid.

The plasmid pRS 29 was designed to express transgenes under the control of the elongation factor 1α (EF1α) promoter. It has a bovine growth hormone poly A. The plasmid pRS 29 was constructed from plasmids pRS 28 and pEF-BOS. The plasmid pEF-BOS was digested with the enzymes *Hind III* and *Xba I* to release the EF1α promoter containing fragment. This fragment was inserted into the *Hind III / Swa I* site of plasmid pRS 28 to generate plasmid pRS 29. The generation of plasmid pRS 29 is shown in Figure III.12.

Figure III.12: Generation of plasmid 29 The plasmid pRS 29 was generated by inserting the *Xba I / Hind III* fragment from plasmid pEF-BOS into the *Hind III / Swa I* site of the plasmid pRS 28.

33

l) Construction of plasmid pRS 31

The plasmid pRS 31 was designed to express transgenes under the control of the murine CMV (MCMV) promoter. The plasmid pRS 31 was generated from plasmid pPDK6 (a kind gift of Dr.J.M.Sallenave) and plasmid pPAP CMV GLp65.

The plasmid pPDK6 was digested with *Bam HI* and *Xba I* to release the DNA fragment containing the MCMV promoter. This sequence was cloned into the *BamH I* and *Sal I* site of the plasmid pPAP CMV GLp65. The cloning scheme for the construction of plasmid pRS 31 is shown in Figure III.13.

Figure III.13: Generation of plasmid pRS 31. The plasmid pRS 31 was generated by inserting the *Xba I / Bam HI* fragment from the plasmid pPDK6 into the *Sal I /Bam HI* site of the plasmid pPAP CMV GLp65 SV40pA.

m) Construction of plasmid pRS 33

The plasmid pRS 33 expresses sflt1 under the control of the EF1α promoter. The plasmid pRS 33 was based on plasmid pRS 29 and plasmid pBSK + flt1 D1-6. The sflt1 cDNA was released from plasmid pBSK+ flt1 D1-6 by digesting with the enzymes *Bam HI* and *Xho* I. This DNA fragment was inserted into the *Spe* I site of plasmid pRS 29. The cloning scheme for the construction of plasmid pRS 33 is shown in Figure III.14.

Figure III.14: Generation of plasmid pRS 33. The plasmid pRS 33 was generated by inserting the *Xho I/Bam HI* fragment from plasmid pBS SK+fltD1-6 into the *Spe I* site of plasmid pRS 29.

n) Construction of plasmids pRS 34 and pRS 42

The plasmid pRS 34 expresses the murine tie2 under control of the MCMV promoter. The plasmid pRS 34 was based on plasmids pRS 31 and pBS II KS Tie2 EC His. The tie2 cDNA was excised from plasmid pBS II KS Tie2 EC His using the enzymes *Eco RI* and *Not I*. The released cDNA was cloned into the *Hind III* site of plasmid pRS 31. The cloning scheme for the construction of plasmid pRS 34 is shown in Figure III.15

The plasmid pRS 42 expresses stie2 under the control of the MCMV promoter. The plasmid pRS 42 was based on plasmid pRS 34. The plasmid pRS 34 was digested with the enzyme *Asc I*. Oligo 79 containing a *Not I* site was inserted into the *Asc I* site of plasmid pRS 34 to generate plasmid pRS 42. The cloning scheme for the construction of plasmid pRS 42 is shown in Figure III.15.
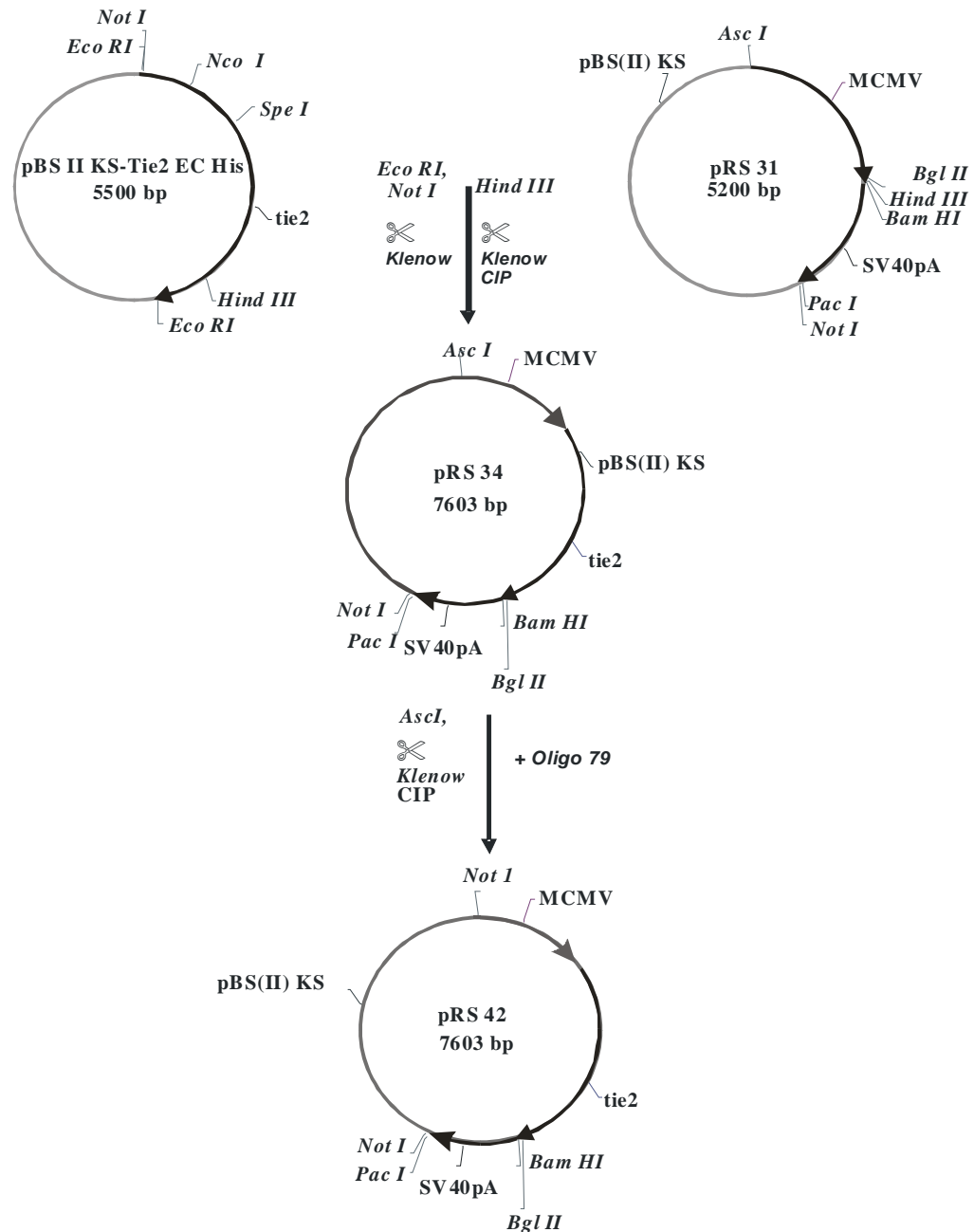
Figure III.15: Generation of the plasmid pRS 34 and 42. The plasmid pRS 34 was generated by digesting the plasmid pBS II KS-Tie2 EC His with the enzymes *Eco RI* and *Not I* and inserting the DNA fragment into the *Hind III* site of plasmid pRS 31. The plasmid pRS 42 was generated by inserting oligo 79 into the *Asc I* site of plasmid pRS 34.

o) Construction of plasmid pRS 44

The plasmid pRS 44 was based on plasmids pSTK 129 and pRS 33. The plasmid pRS 33 expresses the sflt1 protein under the control of the EF1α promoter. The plasmid pRS 33 was digested with *Not I* to release the cassette expressing sflt1 under the control of EF1α promoter. This fragment was inserted into the *Not I* site of plasmid pSTK 129 to generate plasmid pRS 44. The cloning scheme for the construction of plasmid pRS 44 is shown in Figure III.16.

p) Construction of plasmid pRS 45

The plasmid pRS 45 was based on plasmids pSTK 129 and pRS 42. The plasmid pRS 42 expresses the stie2 protein under the control of the MCMV promoter. The plasmid pRS 42 was digested with *Not I* to release the cassette expressing stie2 under the control of the MCMV promoter. This fragment was inserted into the *Not I* site of plasmid pSTK 129 to generate plasmid pRS 45. The cloning scheme for the construction of plasmid pRS 45 is shown in Figure III.17.

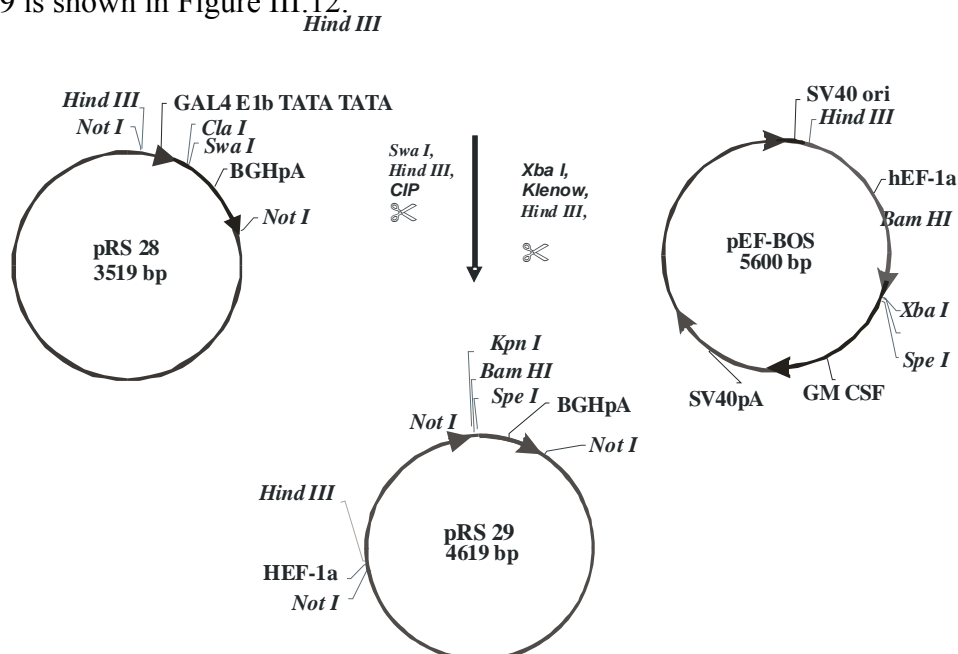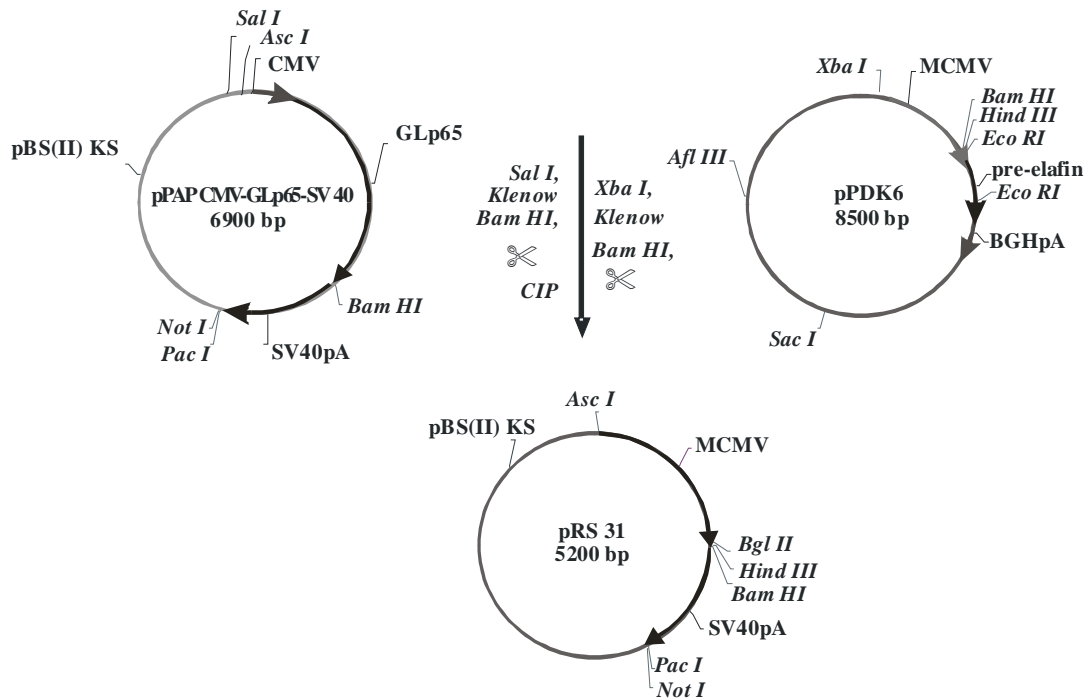**Figure III.16:** Generation of plasmid pRS 44. The plasmid pRS 44 was generated by inserting the *Not I* fragment from plasmid pRS 33 into the *Not I* site of plasmid pSTK 129.
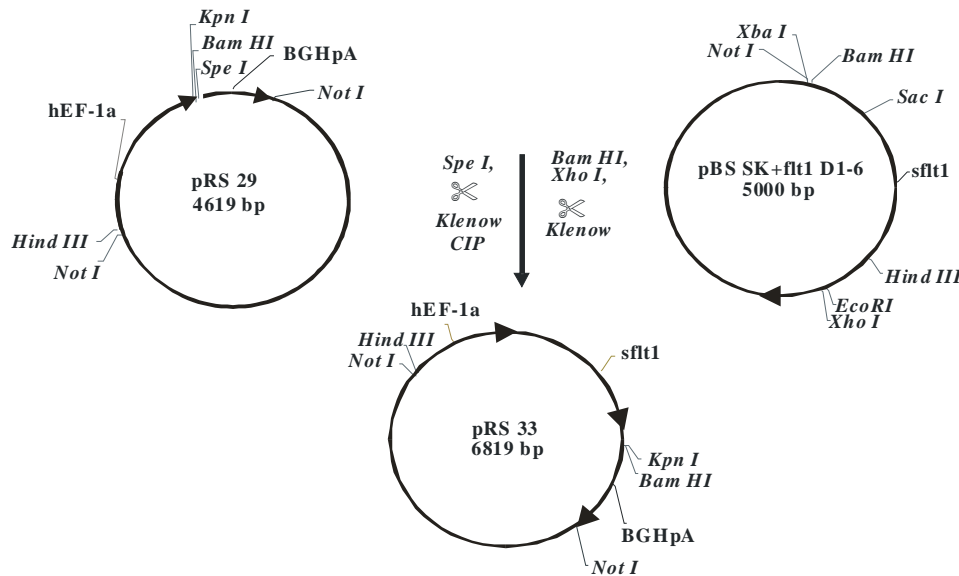

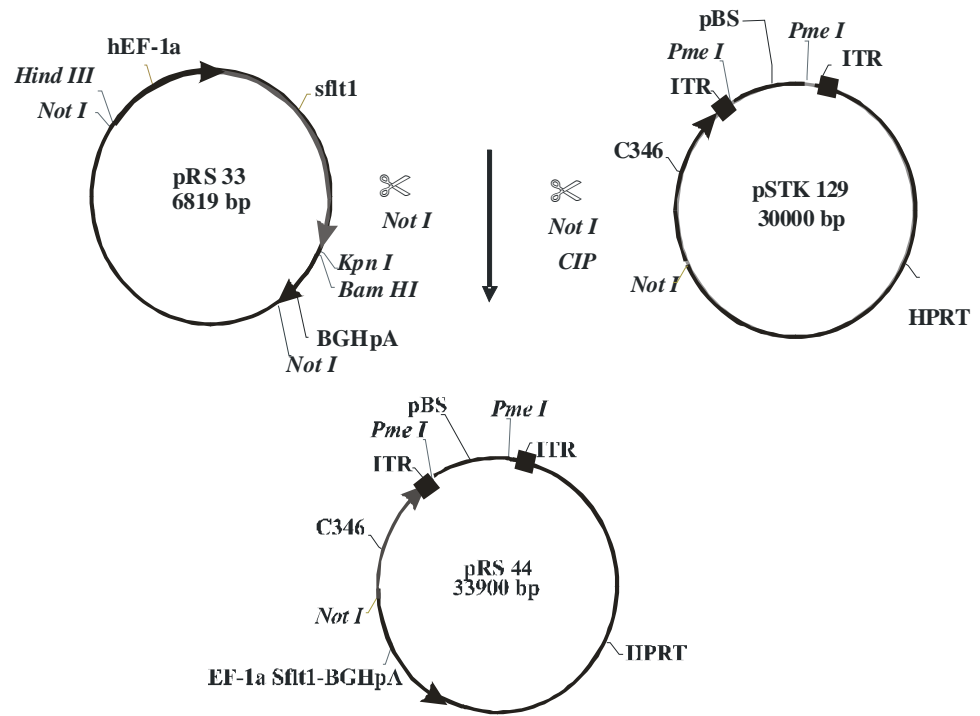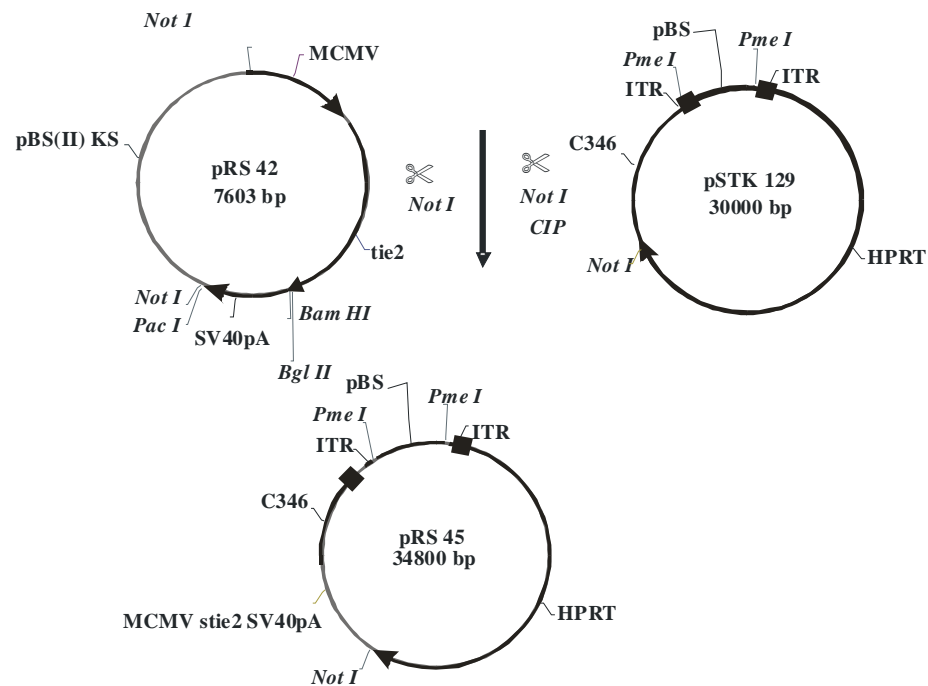**Figure III.17:** Generation of plasmid pRS 45. The plasmid pRS 45 was generated by inserting the *Not I* fragment from plasmid pRS 42 into the *Not I* site of plasmid pSTK 129.

III.2 Bacterial methods

III.2.1 Bacterial culture techniques

Culture of bacteria in Luria Broth Base
E.coli was cultured in Luria Broth Base in the presence of the antibiotic ampicillin at a concentration of 100 μg/ml. For small-scale preparation 1.5 ml Eppendorf tubes with a capacity of 2.0 ml were used. For large-scale preparation (200 ml), Erlenmeyer flasks with a capacity of 500 ml were used. The cultures were incubated for 12 hours with shaking at 250-300 rpm at 37°C.

Culture of bacteria in Luria Broth Agar
E.coli was cultured in 10 cm plates containing 20 ml of Luria Broth Agar (LBA) containing ampicillin at a concentration of 100 μg/ml.

III.2.2 Transformation of E. Coli

Transformation with plasmid DNA
Transformation of E.coli with plasmid DNA was performed by incubating 20 μl of XL-2 blue ultra competent bacteria (Stratagene, Germany) with 10-100 ng of plasmid in a 1.5 ml Eppendorf reaction tube for 5 minutes in ice. After five minutes incubation in ice, the bacteria were placed in a water bath having a temperature of 42°C for 45 seconds. The bacteria were then immediately placed in ice for 2 minutes and SOC medium was added. The bacteria were incubated for 1 hour at 37°C. After 1 hour, the bacteria were transferred to LBA plates containing ampicillin and were incubated for 12 to 16 hours.

Transformation with plasmid DNA from ligation
To transform bacteria using a ligation mix, 50 μl of XL-2 blue ultra competent bacteria (Stratagene, Heidelberg) were incubated with 0.5 μl of 2-Mercaptoethanol (1.42 M) for 10 minutes on ice. After 10 minutes, 2 μl of ligation mix was added and the bacteria were further incubated for 30 minutes in ice. The bacteria were placed in a water bath having a temperature of 42°C for 45 seconds. The bacteria were then immediately placed in ice for 2 minutes and 200 μl of SOC medium was added. The bacteria were incubated for 1 hour at 37°C before being transferred to LBA plates containing antibiotic and were incubated for 12 to 16 hours.

III.2.3 Isolation of plasmids

Analytical plasmid isolation ("Mini prep")
Mini prep of DNA was performed to analyze the integrity of DNA by restriction digestion. Isolated bacterial clones picked from Luria Broth Agar plates were grown over night (12-14 hours) in 1.5 ml of LB shaker culture containing ampicillin at 100 μg /ml. The bacteria were pelleted by centrifuging at 5000 RPM for 3 minutes at RT. The bacterial pellet was re-suspended in a volume of 200 μl of TELT buffer. The re-suspended bacterial pellet was incubated at 96ºC for 3 minutes followed by incubation in ice for 5 minutes. The supernatant containing DNA was collected by centrifugation at 14,000 RPM for 10 minutes. The DNA present in the collected supernatant was precipitated by mixing the supernatant with an equal volume of isopropanol and centrifuging at 20000 g for 10 minutes. The precipitated DNA was washed once with 300 μl of 70% ethanol. The DNA was finally suspended in a volume of 30 μl of TE and was stored at 4ºC until further use. 3 μl of the re-suspended DNA was used for restriction digestion.

Preparative plasmid Isolation ("Maxi prep")

Maxi prep of DNA was performed to obtain large quantities of DNA for transfection, cloning etc. The DNA was prepared using the Qiagen Maxi Plasmid Kit (Qiagen, Germany). The protocol prescribed by the manufacturer was followed.

III.3 Molecular Biology Methods

III.3.1 Determination of the concentration of DNA

The concentration of DNA was determined using a spectrophotometer. The concentration of the DNA present in the solution was calculated using Lambert Beers Law which states concentration of double stranded DNA in mg/ml= A_{260} x 50 x dilution factor, whereby A is the absorption coefficient of DNA at 260 nm. The solution was also measured to determine the absorption at 280 nm for proteins. DNA samples containing A_{260}/A_{280} values of 1.7-2.0 were used for experiments.

III.3.2 Storage of DNA

For routine use, plasmid DNA was stored in TE buffer at 4°C. Plasmids having a size of larger than 8 kb were stored in TE buffer having a pH of 8.5. Plasmids having a size less than 7 kb were stored in TE buffer having a pH of 7.5. For long-term storage, plasmid DNA was dissolved in 70% ethanol and was stored at -20°C. Oligodeoxynucleotides and vector inserts used for ligation were stored in 10 mM Tris buffer.

III.3.3 Precipitation of DNA

Ethanol precipitation
Ethanol precipitation of solution containing DNA was performed by adding 0.1 volume of sodium acetate solution (3 M, pH 5.2) and two volume of 100% ethanol. After mixing, DNA was collected by centrifuging at 20,000 g for 30 minutes at 4°C. The supernatant was discarded and the pellet was washed with 70% ethanol by centrifuging at 20,000g for 30 minutes at 4°C. The supernatant was discarded and the pellet was air dried at RT for 5-10 minutes. The pellet was dissolved in TE buffer. Vector inserts and oligodeoxynucleotides were dissolved in 10 mM Tris buffer.

Isopropanol precipitation
Isopropanol precipitation of solution containing DNA was performed by adding 0.1 volume of sodium acetate solution (3 M, pH 5.2) and 0.5 volume of isopropanol. After mixing, the DNA was pelleted by centrifugation at 20.000 g for 20 minutes at RT. After discarding the supernatant, the pellet was washed with 70% ethanol for 30 minutes at 4°C. The supernatant was discarded and the DNA was air dried at RT for 5 minutes before being resuspended in TE buffer.

III.3.4 Phenol chloroform extraction of DNA.

Phenol-chloroform extraction of DNA was performed for purification of DNA from proteins. 200 μl of DNA containing solution was mixed with an equal volume of TE equilibrated phenol (Invitrogen, Germany). After mixing the aqueous and organic phase were separated by centrifugation at 20,000 g for 4 minutes at RT and the organic phase was discarded. The aqueous phase was mixed with an equal volume of chloroform/isoamyl alcohol (24:1) and the phases were separated by centrifuging at 20.000 g for 4 minutes at RT. The DNA present in the aqueous phase was finally precipitated with ethanol.

III.3.5 Restriction digestion of DNA and agarose gel electrophoresis

Restriction analysis was performed with 10 μg or 200 ng of DNA for preparative or analytical digest respectively. DNA was digested with restriction enzyme (5 IU/μg of DNA) in the prescribed buffer for 2 hours. DNA was digested in a total volume of 20 μl or 200 μl. In the case of double

digestion of DNA with enzymes having different prescribed buffers, the digested DNA was precipitated with ethanol and was re-suspended in Tris-HCl (pH 8.5), before being re-digested. The digested DNA fragments were dissolved in DNA loading buffer, and were electrophoreticaly separated in a 0.8% agarose gel. The agarose gel used for the separation of DNA bands contained ethidium bromide for visualizing the DNA. TBE running buffer was used for analytical preparation of DNA. TAE running buffer was used in the case of preparative digests of DNA, when a DNA fragment was to be isolated from the gel.

III.3.6 Isolation of DNA fragments from agarose gels

Digested DNA for preparative analysis was separated by agarose gel electrophoresis. The separated DNA was visualized under UV light. The desired DNA band was cut out using a sharp knife. DNA bands having sizes of less than 5 kb were isolated using the QIAEX II Gel extraction kit. DNA bands having a size of more than 5 kb were isolated by electroelution using Elu trap electrophoretic system (Schleicher & Schuell, Germany). The isolated DNA was precipitated using ethanol and was re-suspended in 20 µl of 1x TE buffer.

III.3.7 Filling up of 5´ends ("Klenowing")

Filling up of 5´ends of DNA fragments was performed when non-compatible ends were to be ligated. DNA (50 ng/µl) was incubated with two units of Klenow enzyme for 15 minutes in Klenow buffer. After 15 minutes, the Klenow enzyme was inactivated by adding EDTA to a final concentration of 5 mM followed by incubation at 75ºC for 10 minutes. The DNA was purified by phenol/chloroform extraction and ethanol precipitation. Following centrifugation, the precipitated DNA was re-suspended in 20 µl of 10 mM Tris-HCl (pH 8.5).

III.3.8 Dephosphorylation of DNA fragments

Dephosphorylation of digested vector DNA was performed to prevent selfligation. One to two µg of DNA were incubated with 1 unit of calf intestinal phosphatase (CIP) at 37ºC for 1 hour. After 1 hour, CIP was inactivated by adding EDTA to a concentration of 5mM followed by incubation at 75ºC for 10 minutes. The dephosphorylated DNA was purified by phenol/chloroform extraction and ethanol precipitation. Following centrifugation, the precipitated DNA was re-suspended in 20 µl of 10 mM Tris-HCl (pH 8.5).

III.3.9 Ligation of DNA fragments.

Ligation of DNA fragments and dephosphorylated vector DNA was performed in a volume of 10µl in 1x T4 ligase buffer, for 2 hours at room temperature, in the presence of five units of T4 DNA ligase. The amount of vector DNA and DNA fragments were in molar ratios of 1:3, 1:6 and 1:12.

III.3.10 Polymerase Chain Reaction

Construction of primers for PCR
In general, the primers used for PCR had around 18 nucleotides. The melting temperature for the oligonucleotide primer used in PCR was determined using the formula
Tm[C] = ((A+T) x 2)+((G+C) x 4)
T represents thymine base, G represents guanine base, C represent cytosine base and A represent adenine base.

Performance of PCR

Polymerase chain reaction was performed in a total volume of 50 µl. The equipment used for PCR was a PCR – Automat Uno II (Biometra, Germany). The dNTPs were used in a concentration of 200 µM, primers at a concentration of 300 nM and $MgCl_2$ at an end concentration of 1.5 mM. When not specially mentioned Taq polymerase (Invitrogen, Germany) was used for preparation of probes and pfu polymerase (Stratagene, Germany) was used for sequencing and for cloning purposes. Genomic DNA was used at a concentration of 1-2 µg and plasmid DNA was used at a concentration of 1-10 ng. The denaturing temperature was set at 95°C for 5 minutes. The annealing temperature was set at 5°C below the melting temperature of the primers. In general, 25–30 cycles were used for amplification of desired fragments.

Purification of PCR products

PCR products were purified using a PCR purification kit (Qiagen, Germany). The PCR product was analysed using agarose gel electrophoresis.

III.3.11 Generation of DNA probes for slot blot analysis

The probes for slot blot analysis namely the ITR and the fiber probes were prepared using PCR. The 438 bp long ITR probe binds to the Ad-ITR (nucleotide 1 to 438). The primers used for the generation of the ITR probe were ITR I and II. The 1348 bp long fiber probe binds to the Ad–fiber DNA (nucleotide 31042 to 32390). The primers used for the generation of the fiber probe were fiber I and fiber II. PCR amplification, was carried out for 2 minutes at 94ºC followed by 20 cycles of 1 minute at 94ºC, 1 minute at 55ºC, and 1 minute at 72ºC, followed by a final extension of 10 minutes at 72ºC. The probes generated by PCR were purified using the QIA quick PCR purification Kit (Qiagen, Germany). The probes were stored at –20ºC. The concentration of the probes was determined spectroscopically and by agarose gel electrophoresis.

III.3.12 Detection of Ad RS 24 presence in tissues using PCR

PCR was used for the detection of the tissue distribution of the vector Ad RS 24. The primers used for the PCR were GLp65F and GLp65R. The size of the PCR product was 1103 bp. Total DNA and RNA from the tissues of the animal was isolated using the TRI reagent (Sigma, Germany) according to the instruction of the manufacturer. The PCR was performed using 0.5 µg of DNA from tissues of mice, in a volume of 25 µl, using 1 unit of Red Taq polymerase (Sigma, Germany). The PCR amplification steps were 5 minutes at 94ºC followed by 30 cycles of 30 seconds at 94ºC, 30 seconds at 48ºC and 1 minute at 72ºC, followed by a final extension of 5 minutes at 72ºC. 5µl of the amplification product was separated by agarose gel electrophoresis on 2% agarose and the product was visualized under UV light.

III.3.13 Detection of GLp65 expression from Ad RS 24 in tissues using RT-PCR

16µg of total RNA from each tissue was treated with 15 units of RNAse-free DNAse (Roche, Germany) and 20 units of RNAse inhibitor (Invitrogen, Germany) for 15 minutes at room temperature. After extraction with phenol/chloroform and precipitation with ethanol, RNA was redissolved in 20 µl of DEPC-treated H_20. 1 µg of RNA was subjected to reverse transcription using 100 units of M-MLV Reverse Transcriptase (Invitrogen, Germany) in a 12 µl volume for 60 minutes at 37ºC and followed by 5 minutes at 95ºC. 6 µl of this mixture were used for PCR amplification in a 50 µl total volume containing 10 pmol of primers GLp65F and GLp65R and 2 units of Red Taq DNA polymerase (Sigma, Germany). PCR conditions were the same as described in Chapter III. 3.10. 10 µl of PCR products were analyzed by electrophoresis on 2% of agarose gels and visualized with ethidium bromide. RT-PCR for mouse ß actin was used as control. The primers

used for the amplification of ß actin were Act-s and Act-as. The PCR conditions were the same as described in Chapter III. 3.10. The size of the ß actin product is 182 bp.

III.4 Cell culture techniques

III.4.1 Cell lines and media

The cell culture media and fetal calf serum (FCS), when not otherwise mentioned, were purchased from Invitrogen (Germany). Minimum essential medium (MEM) and α-MEM powder were dissolved at room temperature in 4.5 L of water. 11 g of $NaHCO_3$ was added to the prepared media and the medium was adjusted to pH 7.1 with 1 N HCl. The media was made up to a volume of 5 L and was sterile filtered through a 0.2 μm filter.

All cell culture and viral techniques were performed in the S2 laboratory facility. The cells were harvested by centrifugation at 250g. The cell lines were passaged once or twice per week. For passaging of cells plated in 15 cm cell culture dishes, the medium was aspirated, and the cells were washed once with 10 ml of PBS. After washing, the PBS was aspirated and the cells were detached using 3.0 ml of Trypsin-EDTA solution. After detachment, the trypsin was neutralized with 10 ml of medium containing 10% FCS. The cells were centrifuged and were resuspended in new medium for passaging.

293 Cre 66: The cell line is based on HEK 293. 293 Cre 66 expresses Cre recombinase constitutively. The cell line was used for the amplification of HC-Ad vectors. It was a kind gift from our colleague Dr. Gudrun Schiedner. The cell line was cultured in MEM/10% FCS/1x penicillin-streptomycin. The cell line was passaged 1:3, twice every week.

A549: The cell is derived from a human lung carcinoma. The cell line was purchased from Cell line services, Germany. The cell line was cultured in DMEM/10% FCS/1x penicillin-streptomycin. The cell line was passaged 1:5 once every week.

HEK 293: The cell line is derived from embryonic kidney cells [107]. The cell line has been stably transformed with the E1 function of Adenovirus type 5. The cell line was used for the production of helper virus before being replaced by N52E6. The cell line was a kind gift from Dr. Frank Graham, Toronto General Research Institute, Canada. The cell line was cultured in MEM/10% FCS/1x penicillin-streptomycin. The cell line was passaged 1:5 twice every week.

HeLa: The cell line is derived from of a human tumor of cervical epithelial origin. The cell line was purchased from Cell line services, Heidelberg. The cell line was used for transduction with HC-Ad vector to estimate the levels of transgene expression in vitro. The cell line was passaged 1:5 once every week.

HUVEC: Human umbilical venous endothelial cells (HUVEC) are primary endothelial cells derived from human umbilical cord. The cells were purchased form Promocell GmbH (Germany). The cells were cultured with Macro vascular media purchased from Promocell GmbH (Germany). The cells were passaged 1:3 once every week. Cells were used until passage 5.

HepG2: The hepatic cell line is human in origin. The cell line was a kind gift from Dr. Cheng Qian, University of Navarra, Pamplona, Spain. The cell line was used for transduction with HC-Ad vectors to estimate the levels of transgene expression. The cell line was cultured in RPMI/10% FCS/1x penicillin-streptomycin. The cell line was passaged 1: 8 once every week.

HUH 7: The hepatic cell line was a kind gift of Dr. Cheng Qian. The cell line was used for transduction with HC-Ad vectors to estimate the levels of transgene expression. The cell line was cultured in MEM/10% FCS/1x penicillin-streptomycin. The cell line was passaged 1:5 once every week.

PLC/PRF/5: The hepatocarcinoma cell line was a kind gift of Dr. Cheng Qian. The cell line was used for transduction with HC-Ad vectors to estimate the levels of transgene expression. The cell line was cultured in MEM/10% FCS/1x penicillin-streptomycin. The cell line was passaged 1:8 once every week.

LLC: The Lewis Lung Carcinoma cell line is a syngenic cell line derived from a lung carcinoma of C57BL mice. The cell line was a kind gift from Dr. Cheng Qian. The cell line forms aggressive tumors in C57BL mice (LLC tumor model). The LLC tumor model was used for determining the anti-cancer properties of the generated HC-Ad vectors. The cell line was cultured in MEM/10% FCS/1x penicillin-streptomycin. The cell line was passaged 1:4 twice every week.

MC-38: The colon carcinoma cell line was derived from a colon carcinoma of C57BL mice. The cell line was a kind gift from Dr. Cheng Qian. The MC-38 cell line forms aggressive subcutaneous tumors or colonic tumor, which is metastatic to liver in C57BL mice. The cell line was cultured in MEM/10% FCS/1x penicillin-streptomycin. The cell line was passaged 1:4 twice every week.

N52E6: The cell line is based on human amniocytes [122]. The cell line was stably transformed with the E1 function of Ad type 5. The cell line was used for the production of helper virus. The cell was a kind gift of our colleague Dr. Gudrun Schiedner. The cell line was cultured in MEM/10 % FCS/1x penicillin-streptomycin. The cell line was passaged 1:5 once every week.

III.4.2 Freezing of eukaryotic cells

For freezing, early passages of cells were used. The cells were washed twice with PBS and were detached using trypsin-EDTA solution. The cells were pelleted and resuspended using freezing mix. The freezing mix was aliquoted in 2 ml cryotubes (Nunc, Germany). The cryotubes were placed at RT for 15 minutes and were placed in an isopropanol bath, which was frozen at -80° C for overnight. The cryotubes were then placed in a liquid nitrogen container until further use. The freezing mix used was 90% FCS, 10% DMSO (Sigma-Aldrich, Germany).

III.4.3 Transfection of eukaryotic cells

The transfection of eukaryotic cells was performed using Fugene transfection reagent (Roche, Germany) as described by manufacturer. The cell lines were plated at a density of 50 to 80% confluency for 24 hours before transfection. The DNA used for transfection was purified using phenol-chloroform extraction method (Chapter III.3.4). For transfecting cells in 6 well plates, 1.5 µg of DNA was added to transfection solution containing 6 µl of Fugene reagent diluted in 100 µl of serum free medium. The transfection solution was incubated at RT for 15 minutes for complex formation. The transfection solution was added dropwise to the cells and was swirled to equally distribute the DNA complex. The volume of the culture supernatant was increased to 1 ml. The medium containing the expressed proteins was collected at 48 hours post transfection.

III.4.4 Matrigel assay

A Matrigel assay was performed to determine the biological activity of sflt1 and stie2. It is a semi-quantitative assay based on the principle that tube like structures formed on a matrigel by HUVECs can be inhibited by anti-angiogenic agents. To perform the assay, the matrigel was thawed overnight in ice at 4°C. Culture plate and pipettes were placed at -80°C for four hours before usage. The thawed matrigel was coated on cell culture plates and the matrigel was allowed to gel at 37°C for 1 hour. Early passage HUVECs were mixed with control medium or medium containing

the anti-angiogenic principle and were plated on the matrigel for 9 hours. The formation of tubes was visualized under a microscope and the number of branch points was counted visually.

III.4.5 Proliferation assay for determination of sflt1 activity

The assay was performed to confirm the biological activity of sflt1 expressed from the vectors Ad RS 23 and Ad RS 44. The assay was performed in two steps. In the first step, the sflt1 containing supernatant was obtained by infecting HepG2 cells with the vector Ad RS 23 or Ad RS 44 at a moi of 100. A control supernatant was obtained by infecting the HepG2 cells with the vector Ad SLS 14. The levels of sflt1 were estimated by ELISA and were then diluted to a concentration of 100 ng/ml before the supernatants were used in the experiment. In the second step, the serum-starved HUVECs (2% FCS) were stimulated to proliferate by addition of VEGF at a concentration of 10 ng/ml. The stimulated HUVECs were incubated for further 48 hours with the supernatant from the HepG2 cells that had been transduced with the vectors HC-Ad RS 23, HC-Ad RS 44 and HC-Ad SLS 14. The serum-starved HUVECs, which had not been stimulated with VEGF, acted as a control for VEGF- mediated proliferation. Recombinant sflt1 at concentration of 100 ng/ml was the positive control for assaying the inhibition of VEGF mediated proliferation. The extent of proliferation was estimated using the WST-1 reagent (Roche, Germany), which measures the mitochondrial dehydrogenase enzyme.

III.4.6 Preparation of RU 486 for cell culture

For use in cell culture, a 1mM stock solution of RU 486 (Invitrogen, Germany) was prepared by dissolving 4 mg of RU 486 in 9.3 ml of 100% ethanol. The stock solution was stored at –20°C. A 10 μM working solution of RU 486 was prepared by diluting 100 μl of the RU 486 stock solution in 10 ml of 100% ethanol.

III.5 Adenovirus methods

III.5.1 Isolation of plaques

N52E6 or 293 cells were plated at 60-70% confluency in a 6 well plate. 24 hours after seeding, the cells were either transfected with a plasmid used for the generation of first generation vector or infected with the first generation vector. After 16 hours, the transfected or infected cells were overlaid with agarose overlay medium (Chapter III.1) and were incubated at 37ºC in a cell incubator containing 5% CO_2 for a maximum period of two weeks. The cells were observed for two weeks under a light microscope for focal areas of lysed cells called plaques. Individual plaques representing single rescue events of vector were picked using sterile Pasteur pipettes. The plaques were re-suspended in 1 ml of TBS and were frozen at –80ºC.

III.5.2 Generation of high capacity adenoviral (HC-Ad) vectors

Cre 66 cells were used for the generation of HC-Ad vectors. The plasmid used for the generation of the HC-Ad vector was digested with *Pme* I to release the ITRs. For the first amplification, the Cre66 cells ($2x10^6$ cells in a 6 cm plates) were transfected with the plasmid using effectene reagent (Qiagen, Germany). 16 hours after transfection, the cells were infected with 5 moi of helper virus. The infected cells showing a CPE at 48 hours were harvested. The harvested Cre 66 cells were re-suspended in 2 ml of TBS followed by three times freeze thawing to release the vector particles. During the second and the third amplification, Cre 66 cells ($3x10^6$ cells in 6 cm plate) were infected with half the supernatant from the cell lysate of the earlier amplification, and 5 moi of helper virus. During the fourth and fifth amplifications, Cre 66 cells, plated at a density of $3x10^7$ cells in 15 cm plates were infected with half the supernatant (from the cell lysate of the earlier

amplifications) and 5 moi of helper virus. For a large-scale preparation, 293 Cre 66 (ten 15 cm plates having a cell density of $3x10^7$) were infected with the supernatant (containing the vector) from the fifth amplification or 10 moi of HC-Ad vector (if the titer had previously been determined) and 5 moi of helper virus. The infected cells were harvested at 48 hours and were re-suspended in TBS containing glycerol.

III.5.3 Purification of adenoviral vectors using CsCl density gradient ultracentrifugation

The re-suspended cells were freeze thawed for vector release. The vector containing supernatant was collected by centrifugation at 200g to remove the cell debris. The supernatant was made up to a volume of 20 ml and CsCl was added at a concentration of 0.5 gm/ml. The virus was centrifuged twice at 32,000 RPM at 4ºC for 22 hours in an ultracentrifuge (Ultracentrifuge L7-65 with SW41-Rotor, Beckman, USA). The adenoviral vector floats as a band in the CsCl gradient at a density of $1.34gm/cm^3$. The virus was aspirated using a 2 ml syringe fitted to a needle. After the second gradient, the virus was desalted in PD 10 columns using TBS buffer. Glycerol was added to the eluted vector at a concentration of 10%. The virus was stored at -80ºC.

III.5.4 Titration of helper virus or first generation adenoviral vectors

N52E6 cells were used for determining the titer of first generation vectors and helper virus vectors. The cells were plated at a density of $2x10^6$ in 6 cm plates. The plated cells were infected with different dilutions of the vector. 16 hours after infection the cells were overlaid with 10 ml of agarose overlay medium for 15 minutes at room temperature. The cells were incubated at 37ºC in cell incubator containing 5% CO_2 for 5-14 days. The plates were observed with a light microscope for the appearance of plaques. The average number of plaques at a given dilution represents the plaque forming units (pfu) of the virus.

III.5.5 Titration of HC-Ad vectors using slot blot analysis

The slot blot method was used to determine the infectious units, total particle, and the helper virus contamination titers. A549 cells were used for the determination of infectious units of the HC-Ad vectors. The A549 cells were plated for overnight, at a density of $1x10^5$ cells, in a 24 well plate before infection with HC-Ad vector. HC-Ad vectors were diluted 1:20 in TBS, and 4 to 20 μl of the diluted HC-Ad vector was used to infect A549 cells in duplicates. 16 hours after infection, the A549 cells were washed intensively with PBS and were incubated with 200 μl of PBS/5mM EDTA for 15 minutes to detach the cells from the plate. The detached cells were incubated with 200 μl of 0.8 N NaOH for 30 minutes to lyse the cells. The plasmid pGS 46, added to uninfected A549 cells at copy numbers ranging from $1x10^6$ to $1x10^8$, acted as the standard.

The total particle titer of HC-Ad vectors was determined using a cell free system. The HC-Ad vector was diluted 1: 400 in TBS buffer. Four to 20 μl of the diluted HC-Ad vector was made up to a volume of 200 μl of TBS and was lysed with 200 μl of 0.8 N NaOH for 30 minutes at room temperature. The plasmid pGS 46 was used as the standard and was diluted in TBS (to a volume of 200 μl) to represent copy numbers ranging from $1x10^6$ to $1x10^8$. The diluted standards were mixed with 200 μl of 0.8 N NaOH and were incubated for 30 minutes at room temperature.

The helper virus contamination was determined using a cell free system. The HC-Ad vector was diluted 1: 200 in TBS. Four - 20 μl of the diluted virus was made up to a volume of 200 μl of TBS and was lysed with 200 μl of 0.8 NaOH for 30 minutes at room temperature. The plasmid pGS 46 was used as the standard and was diluted in TBS (to a volume of 200 μl) to represent copy numbers ranging from $1x10^6$ to $1x10^8$. The diluted standards were mixed with 200 μl of 0.8 N NaOH and were incubated for 30 minutes at room temperature.

300 µl of cell or particle lysate was transferred to a Bio Dyne nylon membrane, (PALL corporation, USA) using a slot blot apparatus (Hoefer PR 648, Bio-Rad laboratories, Germany). After transfer, the membrane was washed with 2x SSC buffer followed by backing at 120ºC for 30 minutes. The baked membrane was pre-hybridized with hybridization buffer for 4 hours at 68ºC. The probe used for the determination of infectious units and total particle binds to the left ITR of the adenovirus (nucleotide 1- 438). The probe used for the determination of the helper viral particle binds to the fiber (nucleotide 31042 to 32390) The PCR probe was radioactively labeled with 50 µCi ^{32}[P] dCTP (Amersham Pharmacia, Germany) using a DNA Labeling Kit (Amersham Pharmacia, Germany). The membrane was hybridized using the radioactive probe for 16 hours at 68ºC. The membrane was washed at 68ºC with buffer containing 2 x SSC/0.1 % SDS for 15 minutes followed by a second wash with buffer containing 0.1% SSC / 0.1% SDS for 20 minutes. The membrane was transferred to a phosho-imager cassette and the signal was read using Phospho imager 445SSI (Molecular Dynamics, USA). The titer of the HC-Ad vector was estimated by comparing the signal intensity between the HC-Ad vector and the plasmid standards.

III.5.6 Storage of adenovirus

Adenovirus desalted after double cesium chloride centrifugation with a PD 10 column was eluted in TBS and was mixed with 10% glycerol. The virus was stored at −80ºC until further use.

III.6 Biochemical methods

III.6.1 SDS-Polyacrylamide gel electrophoresis (PAGE)

The supernatant, obtained by infecting the cells with viral vector was diluted in 4x Laemmli buffer in a total volume of 40 µl and was boiled in a water bath at 95ºC for 5 minutes. The proteins were separated using a discontinuous buffer system. The proteins were initially run in a stacking gel (5%, pH 6.8) and were separated in a running gel (6 or 8% gel, pH 8.8) at 100V for 2 hours. A molecular weight marker (Rainbow marker, BioRad, Germany) was used as a standard.

III.6.2 Western blot analysis

The proteins were initially separated using a discontinuous PAGE. The separated proteins were transferred to a nitrocellulose membrane (Hybond ECL, Amersham Pharmacia, Germany) in a western blot apparatus (BioRad, Germany). The proteins were transferred to a nitrocellulose membrane for 1 hour using 100 V in a cold room (temperature maintained at 4ºC). The nitrocellulose membrane was blocked overnight using TBS containing 5% milk powder in a cold room with shaking. The blocked membrane was incubated successively with the primary antibody, secondary antibody and detection antibody (having a tagged peroxidase enzyme) for 1 hour at room temperature respectively. After each incubation step, the membrane was washed thrice with TBST for 15 minutes. The final wash of the membrane was extended for further 15 minutes. The membrane was finally incubated with 3 ml of peroxidase substrate solution (ECL detection kit, Amersham Pharmacia, Germany) for one minute. The bands were visualized using a chemiluminescence sensitive film (Biomax ML, Kodak, Germany).

III.6.3 Biochemical analysis of serum parameters

Determination of concentrations of urea, total protein, albumin, creatinine, SGOT, SGPT in serum of mice was performed using Hitachi Auto analyzer. (Roche/Hitachi 904/911: ACN 166).

III.6.4 Enzyme linked immunosorbent assay (ELISA) for determination of sflt1, stie2, hIL-12 and mIL-12

A sandwich ELISA technique was used for detecting hIL-12, mIL-12, sflt1 and tie2 proteins present in the cell supernatant or in serum of mice. Kits were used for the detection of sflt1 (Bender MedSystems, Austria), mIL-12 (Pharmingen, Germany) and hIL-12 (Pharmingen, Germany). The protocol described by the manufacturer was followed.

Detection of hIL-12 by ELISA

Rat monoclonal antibody specific for the human IL-12 p75 heterodimer from p35 and p40 subunits was coated on a 96 well plate (Nunc Maxisorp) for overnight at 4ºC using PBS. The plate was blocked for 1 hour at room temperature using 10% FCS in PBS for 1 hour. The test fluid or standards containing hIL-12 were incubated for 1 hour. The plates were washed five times using TBST buffer (Chapter III.1.3). The captured hIL-12 was detected using working detector (conjugated detection antibody consisting of avidin and horse radish peroxidase). The plate was washed seven times and was developed using substrate solution for ELISA (Chapter III.1.3). The plates were read at 450 nm. The ELISA kit was purchased from Pharmingen, Germany.

Detection of mIL-12 by ELISA

Rat monoclonal antibody specific for the murine IL-12 p75 heterodimer from p35 and dp40 subunits was coated on a 96 well plate (Nunc Maxisorp) for overnight at 4ºC using PBS. The plate was blocked for 1 hour at room temperature using 10% FCS in PBS for 1 hour. The test fluid or standards containing hIL-12 were incubated for 1 hour. The plates were washed five times using TBST buffer (Chapter III.1.3). The captured mhIL-12 was detected using working detector (conjugated detection antibody consisting of avidin and horse radish peroxidase). The plate was washed seven times and was developed using substrate solution for ELISA (Chapter III.1.3). The plates were read at 450 nm. The ELISA kit was purchased from Pharmingen, Germany.

Detection of sflt1 by ELISA

Rat monoclonal antibody specific for human sflt1 was coated on a 96 well plate (Nunc Maxisorp) for overnight at 4ºC using PBS. The adsorbed plate was blocked for 1 hour at room temperature using blocking buffer (Bender med systems). The test fluid or standards containing hIL-12 and biotin conjugate were incubated for 1 hour. The plates were washed five times using TBST buffer (Chapter III.1). The captured sflt1 was detected using avidin-horse radish peroxidase. The plate was washed five times and was developed using substrate solution for ELISA (Chapter III.1.3). The ELISA kit was purchased from Bender Med Systems, Austria.

Detection of stie2 by ELISA

An ELISA for detection of stie2 protein was established. A rat monoclonal antibody specific to stie2 was used as a coating antibody (a kind gift from Dr. Urban Deutsch). The stie2 protein was purchased from R&D Systems, Germany. 5% albumin solution was used for blocking after overnight coating. As secondary antibody a mouse monoclonal antibody was used, specific to murine tie2 (Upstate, USA). Protein A-peroxidase conjugate (Sigma, Germany) was used as the detection antibody. The plates were developed using substrate solution (Chapter III.1.3).

III.7 Animal handling techniques

Female C57BL/6J (5-8 week old) mice were used in all the experiments. The animals were supplied by Harlan (Spain). The animals were maintained under pathogen free conditions at the animal facility of the University of Navarra. The mice were fed with standard diet (B&K universal) and sterilized water. All mice were cared for in compliance with the guidance prescribed by the University of Navarra.

III.7.1 Collection of blood from mice

Blood was collected by puncturing the retro-orbital plexus. The collected blood was centrifuged twice at 14,000 RPM for 8 minutes to separate serum. The serum was stored at -20ºC.

III.7.2 Preparation of RU 486 for mouse studies

For use in mice, a stock solution of RU 486 (Sigma, Germany) was prepared by dissolving 9 mg RU 486 in 18 ml of sesame oil (Sigma, Germany). Mice were injected intraperitonealy with RU 486 with a dose of 250 µg/kg of body weight in a total volume of 50 µl.
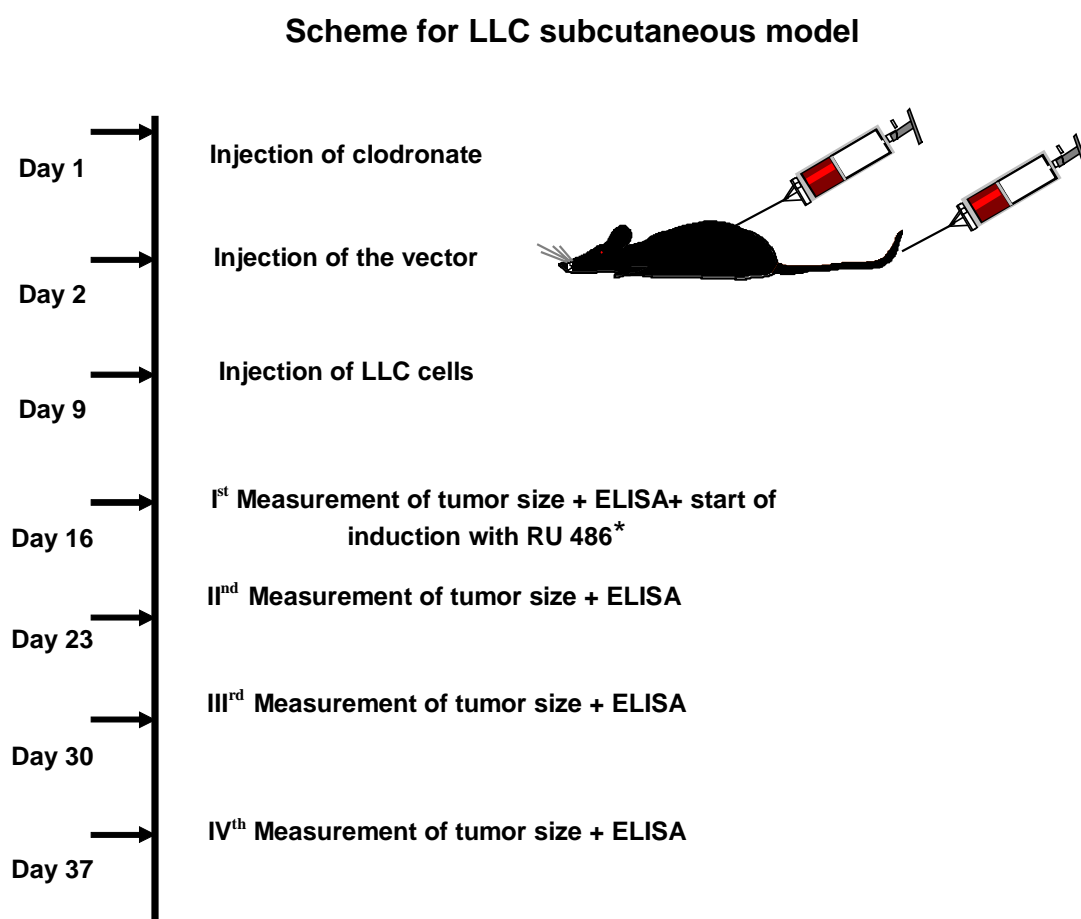
III.7.3 Injection of clodronate liposomes

Clodronate was a kind gift of Dr. Nico van Rooijen. Injection of clodronate liposomes through the tail vein of mice was done to deplete the Kupffer cells in the liver. Transient Depletion of Kupffer cells prior to Ad vector administration has been shown to increase and stabilize the transgene expression in mice [123-125]. It was suggested that improved expression kinetics upon Kupffer cell depletion was attributed to reduced humoral response to the transgenic protein [125].
Clodronate liposomes were injected at a dose of 20 µl/10 gm bodyweight in a total volume of 200 µl of PBS. The injection was performed 24 hours prior to the injection of the HC-Ad vectors. In this study, unless otherwise stated, Kupffer cells were depleted prior to the injection of sflt1 or stie2 expressing vectors. Kupffer cell depletion did not alter the tumor growth or survival time in both orthotopic MC-38 and heterotopic LLC mice model of cancer (not shown).

.

III.7.4 LLC heterotopic cancer model

C57BL/6J mice were injected first with vector by tail vein injection. In order to increase the efficiency of liver transduction, Kupffer cells were depleted by injecting clodronate liposomes 24 hours prior to vector injection (Chapter III.7.3). One week after injection of the vector, the mice were injected with 10^6 LLC cells subcutaneously. The sizes of the tumors and the levels of transgene expression were ascertained at weekly intervals. The volume of the tumor was calculated using the formula $V = D \times d^2/2$, where V is the volume of the tumor, D is the larger diameter of the tumor and d is the smaller diameter of the tumor. The animals were sacrificed when any of the diameters (major or minor) of the tumor exceeded 1.5 cm (800-1000 mm^3) or when the mouse became moribund.

Scheme for LLC subcutaneous model

Day 1	Injection of clodronate
Day 2	Injection of the vector
Day 9	Injection of LLC cells
Day 16	Ist Measurement of tumor size + ELISA + start of induction with RU 486*
Day 23	IInd Measurement of tumor size + ELISA
Day 30	IIIrd Measurement of tumor size + ELISA
Day 37	IVth Measurement of tumor size + ELISA

* Induction only for Ad RS 23 and Ad RS 25

Figure III.18: LLC heterotopic cancer model. The scheme displays the design of the LLC heterotopic cancer model.

III.7.5 MC-38 orthotopic cancer model

C57BL/6 mice were injected first with the vector by tail vein injection. Seven days after injection of the vector, the mice were implanted with $5x10^5$ MC-38 cells into the liver by laparotomy (Figure III.20). Five days after the implantation of the MC-38 cells, the initial size of the tumor was ascertained by laparotomy (Figure III.21 B). The animals were induced with RU 486 at a dose of 250 µg/kg for 10 days. Five days after the end of induction, the size of the tumor was determined by laparotomy. Serum was collected once during the 10-days induction period for estimating the levels of transgene expression. After the second laparotomy, mice either were induced or were left uninduced with RU 486. In mice not responding to the treatment, the tumor spreads and metastasizes to the peritoneum (Figure III.21 C). The volume of the tumor was calculated using the formula $V= Dx\ d^2/2$, where V is the volume of the tumor, D is the larger diameter of the tumor and d is the smaller diameter of the tumor. In animals injected with the vectors expressing sflt1, clodronate liposomes were injected 24 hours prior to the administration of the vector.
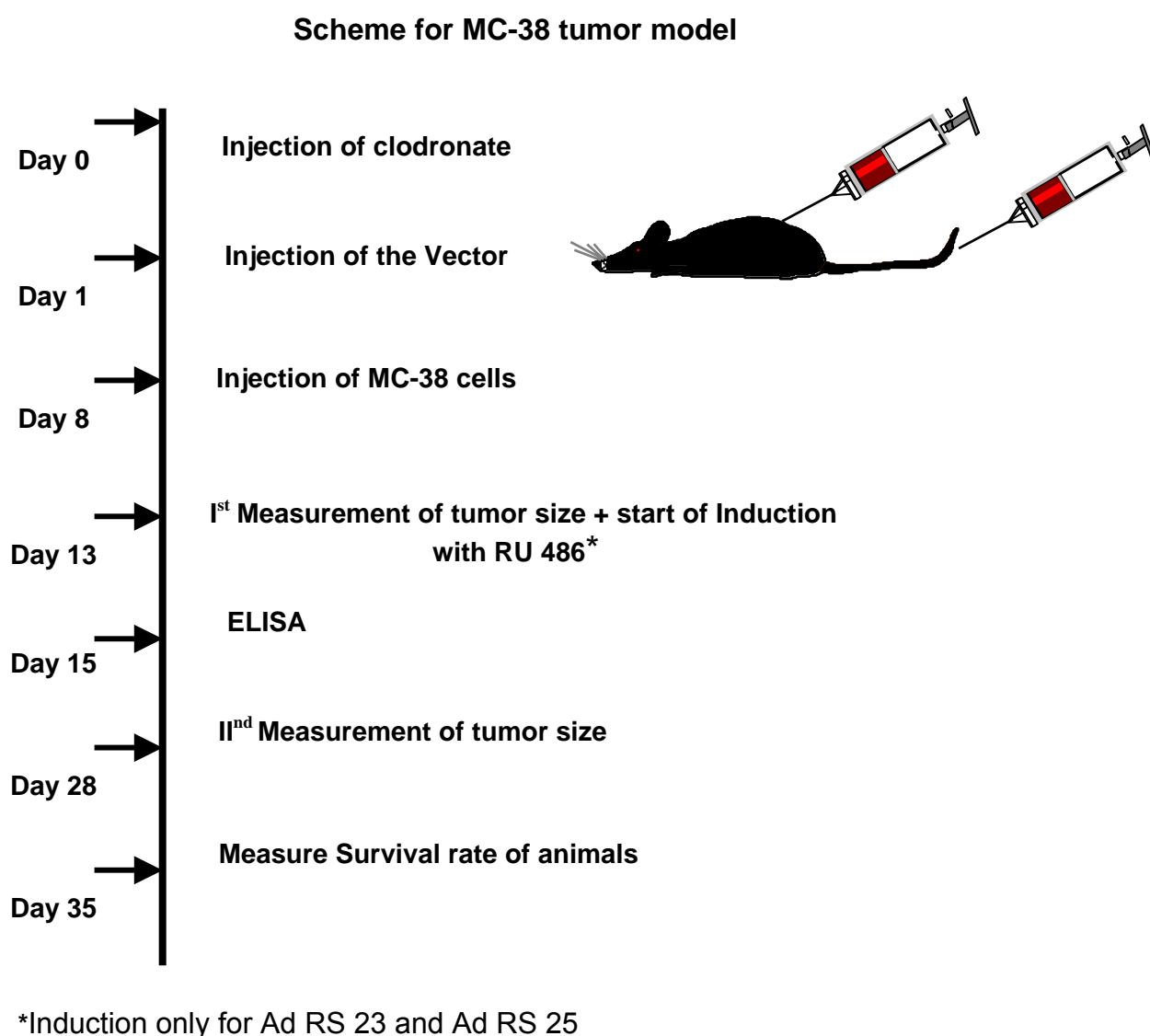
Scheme for MC-38 tumor model

Day 0 — Injection of clodronate

Day 1 — Injection of the Vector

Day 8 — Injection of MC-38 cells

Day 13 — Ist Measurement of tumor size + start of Induction with RU 486*

Day 15 — ELISA

Day 28 — IInd Measurement of tumor size

Day 35 — Measure Survival rate of animals

*Induction only for Ad RS 23 and Ad RS 25

Figure III.19: MC-38 orthotopic cancer model. The scheme displays the design of MC-38 heterotopic cancer model.
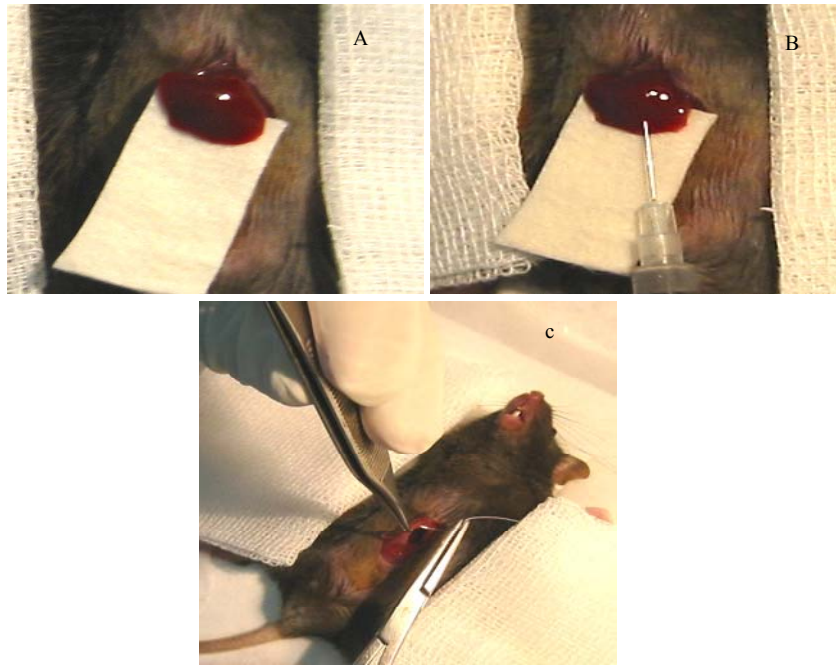
Figure III.20: Picture A shows the liver exposed for injection of MC-38 cells. Figure B shows the injection of MC-38 cells directly into the liver. Figure C shows the completion of laparotomy.
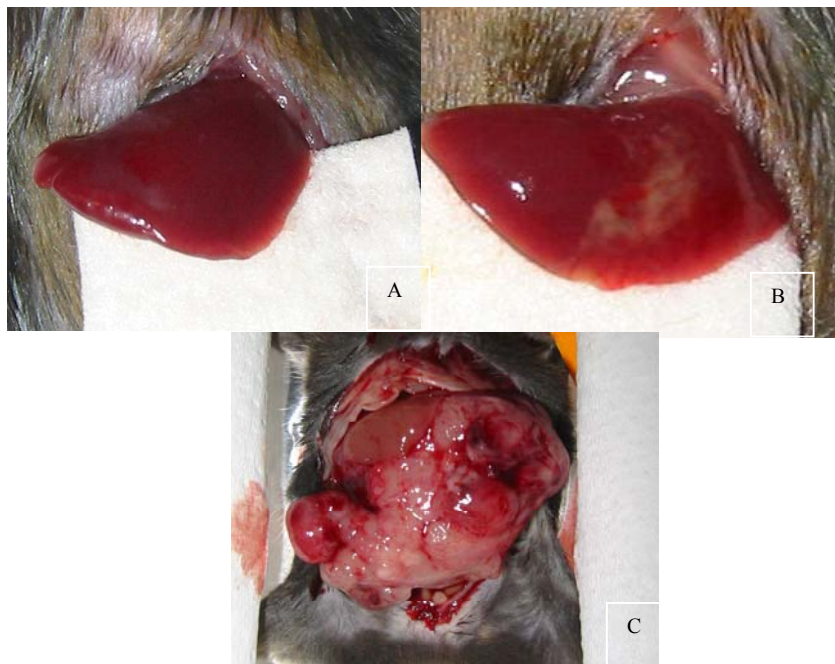

Figure III.21: Figure A shows the liver of the animal before the injection of the MC-38 cells. Figure B shows the development of tumor five days after the injection of MC-38 cells. Figure C shows the liver of a mouse with a prominent MC-38 tumor.

III.8 Statistical analysis

When indicated, the statistical differences were calculated by using a nonparametric test (Mann-Whitney U test, 2-tailed) for unpaired samples. P values smaller than 0.05 were considered significant.

III.9 Summary of the generated HC-Ad vectors

All HC-Ad vectors contain the left terminus of Ad5 (nucleotides 1 to 440; ITR), the right terminus (nucleotides 35818 to 35935; ITR), and the packaging signal from Ad5 (Ψ). pSTK 129 is a shuttle plasmid that can be used to generate high-capacity adenoviral vectors. pSTK 129 consists of the left terminus of the adenovirus type 5 (nucleotide [nt] 1-440), and the right terminus of adenovirus type 5 (nt 35818-35935) a 20-kb DNA fragment derived from the human HPRT locus 18 HUMHPRTB (gene map positions, 1777-21729), a 6.5-kb human fragment of C346 (locus, HUMDXS455A; cosmid map positions, 10205-16750). pSTK 119 is a shuttle plasmid that can be used to generate high-capacity adenoviral vectors. pSTK 119 consists of the left terminus of the adenovirus type 5 (nucleotide [nt] 1-440), and the right terminus of adenovirus type 5 (nt 35818-35935) a 16-kb DNA fragment derived from the human HPRT locus 18 HUMHPRTB (gene map positions, 1777-17777), a 6.5-kb human fragment of C346 (locus, HUMDXS455A; cosmid map positions, 10205-16750). The HC-Ad vectors generated during this study and the transgenes expressed by the vectors are shown in the Table 1.

Name of the HC-Ad vector	Name of the expressed transgene	Mode of expression	Based on plasmid
Ad RS 23	sflt1	Inducible	pSTK 119
Ad RS 24	hIL-12	Inducible	pSTK 119
Ad RS 25	mIL-12	Inducible	pSTK 119
Ad RS 44	sflt1	Constitutive	pSTK 129
Ad RS 44	stie2	Constitutive	pSTK 129

Table 1: HC-Ad vectors generated during the work. The HC-Ad vectors, the expressed transgene, and the shuttle plasmid are shown above.

IV Results

IV.1 Construction and characterization of hIL-12 expressing plasmids and vector

IV.1.1 Construction of pRS 21, pRS 24 and Ad RS 24

In certain human tumors hIL-12 has anti-metastatic effects [48, 81]. However, serious side effects have been regularly observed, when hIL-12 was given systematically. Therefore, we aimed to establish a system that enabled tissue specific and controlled release of hIL-12 following gene transfer. Since hIL-12 is inactive and nontoxic in mice, we used this human version of IL-12 as a reporter to study the in vivo pharmacokinetics of the RU 486 gene switch system.

To obtain inducible liver specific transgene expression, a primary plasmid pRS 17 based on Gene Switch was constructed (Figure III.4). Subsequently, hIL-12 cDNA was inserted into pRS 17 to generate reporter plasmid pRS 21 (Figure III.6). After confirming the integrity of pRS 21, it was used to construct pRS 24. pRS 24 was used to generate the HC-Ad vector Ad RS 24. Ad RS 24 consists of two expression cassettes (Figure IV.1). The first cassette consists of hIL-12 placed downstream of the GAL4 E1b TATA region and upstream of BGHpA. The second cassette consist of GLp65 placed downstream of the liver specific promoter TTRB and upstream of SV40pA. Ad RS 24 apart from the ITRs has two stuffer regions namely C346 and HPRT.
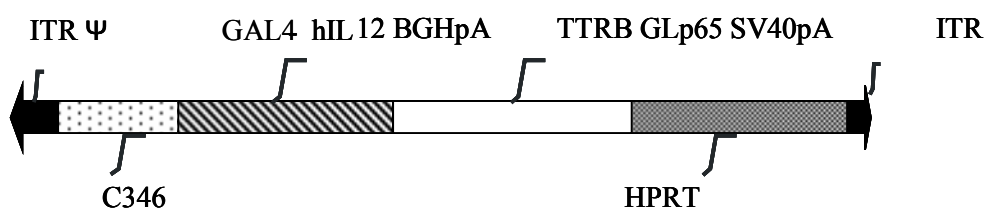

Figure IV.1: The vector Ad RS 24. Ad RS 24 expresses hIL-12 upon induction with RU 486 in a liver specific manner. The vector contains two expression cassettes. The first cassette expresses the regulator GLp65 under the control of the liver specific TTRB promoter and enhancer. GLp65 in the presence of RU 486 binds to the GAL4 region present in the second expression cassette and hIL-12 is transcribed. Ad RS 24 contains the left terminus, the right terminus of Ad5 and the packaging signal Ψ. In addition Ad RS 24 also contain C346 and HPRT stuffer sequences.

IV.1.2 hIL-12 is inducibly expressed upon transfection of pRS 21 in vitro

To investigate the liver specific regulable expression of hIL-12, pRS 21 was transfected into HepG2, PLC/PRF/5 and HeLa cell lines using Fugene reagent (Chapter III.4.3). The cell lines were seeded at a density of $3x10^5$ in six well plates and were cultured for 24 hours before transfection. pCMV hIL-12 expressing hIL-12 constitutively served as a control. 24 hours later, the cells transfected with pRS 21 were induced with 10^{-8} M of RU 486 or were left uninduced (Chapter III.4.6). The supernatants were collected at 48 hours post induction and were analyzed for the expression of hIL-12 using ELISA (Chapter III.6.4). As shown in Figure IV.2 high levels of hIL-12 expression and induction in hepatic cell lines were observed, when compared with the non-hepatic cell line HeLa. Having confirmed the functional integrity of the plasmid pRS 21, the two expression cassettes were sub-cloned into the plasmid pSTK 119 to generate the plasmid pRS 24 (Figure III.9).
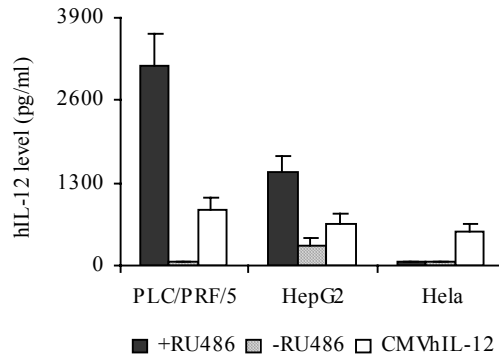
Figure IV.2: Inducible expression of hIL-12 from pRS 21 in vitro. 3×10^5 cells of PLC/PRF/5, HeLa and of HepG2 were cultured in 6 well plates for 24 hours before transfection. Transfection of cell lines with pRS 21 was performed using Fugene reagent. 24 hours later, the pRS 21 transfected cells were induced with 10^{-8} M of RU 486 or were left uninduced. pCMVhIL-12 expressing hIL-12 constitutively served as a control. The supernatants were collected 48 hours later, and the levels of hIL-12 were determined using ELISA. The legend - RU 486 and + RU 486 indicates the absence and presence of the drug RU 486. The legend CMV hIL-12 represents the plasmid expressing hIL-12 under the control of the hCMV promoter.

IV.1.3 hIL-12 is inducibly expressed upon infection of liver cell lines with Ad RS 24 in vitro

Ad RS 24 was tested for the expression of hIL-12 in vitro before being used in vivo. To test for dose dependent and liver specific expression of hIL-12, Ad RS 24 was tested on the cell lines HepG2, PLC/PRF/5, A549, and HeLa (Chapter III.4.1). The cells were seeded at densities of 5×10^5 in six well plates and were cultured for 24 hours before infection. The cells were infected with Ad RS 24 at a moi of 100 and were either induced or left uninduced with 10^{-8} M of RU 486 at 3 hours post infection. The first generation adenoviral vector Ad CMV hIL-12 expressing hIL-12 under the control of the hCMV promoter served as a control. The amount of hIL-12 present in the supernatants was determined using ELISA (Chapter III.6.4). As shown in Figure IV.3, HepG2 cells and PLC/PRF/5 cells in the presence of RU 486 expressed hIL-12 after transduction with 100 moi of Ad RS 24. The levels of hIL-12 were low or undetectable in the absence of RU 486. Interestingly, the levels of hIL-12 secreted by HepG2 cells upon infection with Ad RS 24 and induction with RU 486 were comparable to the expression levels obtained after transduction with
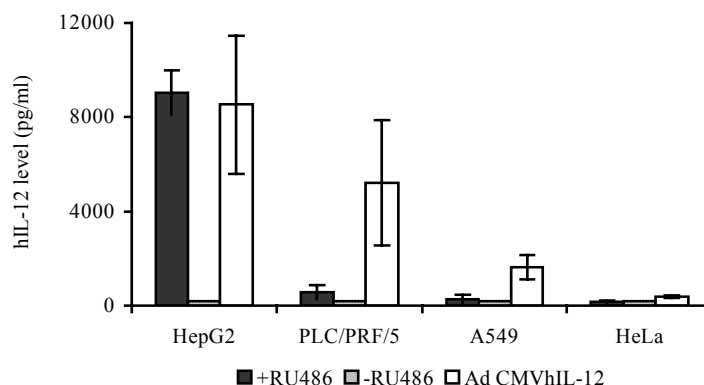

Figure IV.3: Inducible expression of hIL-12 from Ad RS 24 in vitro. 5×10^5 cells of PLC/PRF/5, A549, HeLa and HepG2 cells were seeded in 6 well plates. 24 hours later, the cells were infected with Ad RS 24 or Ad CMV hIL-12 at mois of 100. 3 hours after infection, Ad RS 24 infected cells were either induced with 10^{-8} of RU 486 or were left uninduced. The cell supernatants were collected after 48 hours and were assayed for hIL-12 expression. The legend - RU 486 and +RU 486 indicates the absence or presence of RU 486. The legend Ad CMV hIL-12 represents the virus Ad CMV hIL-12 expressing hIL-12 under the control of the hCMV promoter.

Ad CMV hIL-12. HeLa cells and A549 cells expressed low or undetectable levels of hIL-12 upon induction. In conclusion, inducible and liver cell specific hIL-12 expression from the vector Ad RS 24 was observed in cell lines HepG2 and PLC/PRF/5. In addition, the levels of hIL-12 were minimal or below the detection limit in the absence of RU 486.

IV.1.4 RU 486 induces hIL-12 expression in a dose dependent manner in vitro

Ad RS 24 expresses hIL-12 upon induction with RU 486 in a liver cell specific manner (Figure IV.3). To determine the effect of increasing concentrations of RU 486 on hIL-12 expression, HepG2 cells were infected with 100 moi of Ad RS 24 and were induced with increasing concentrations of RU 486. The supernatants from the infected HepG2 cells were collected at 48 hours post induction and the levels of hIL-12 were determined using ELISA. As shown in Figure IV.4, a RU 486 dose dependent (10^{-10} mol/L to 10^{-7} mol/L) increase in the expression of hIL-12 was observed. This experiment clearly demonstrates that varying the dosages of RU 486 can modulate the levels of hIL-12 expression in vitro.
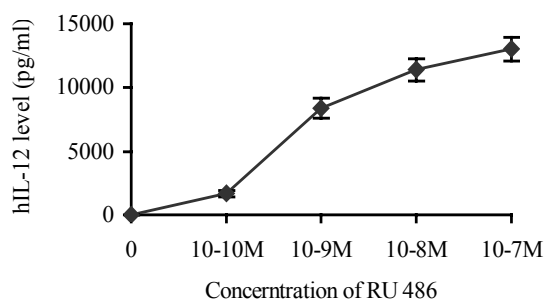

Figure IV.4: RU 486 dose dependent expression of hIL-12 in vitro. 1×10^5 cells of HepG2 cells were cultured in 24 well plates for 24 hours before infection. The HepG2 cells were infected with Ad RS 24 at a moi of 100 with Ad RS 24. 3 hours post infection, RU 486 was added to the culture medium at different concentrations. The supernatants were collected at 48 hours post induction and were assayed for the expression of hIL-12 by ELISA.

IV.1.5 hIL-12 is inducibly expressed upon injection with Ad RS 24 in vivo

The vector Ad RS 24 expresses hIL-12 upon induction with RU 486 in a liver specific manner in vitro (Chapter IV.1.3). To characterize the kinetics of hIL-12 expression in vivo, C57BL/6J mice were injected into the tail vein with the vector Ad RS 24 at a dose of 3×10^9 i.u (n=8). Two weeks post injection, hIL-12 expression was induced by a single intra-peritoneal injection of RU 486 (Chapter III.7.2) in Ad RS 24 injected mice (n=5). The control mice (n=3) were injected with sesame oil not containing RU 486. Blood samples were collected at 4, 10, 24 and 48 hours post induction for the determination of serum hIL-12. As shown in Figure IV.5, in the absence of RU 486, hIL-12 expression was not detected in the serum. Measurable expression of hIL-12 was observed at 4 hours post induction. High levels of hIL-12 expression were observed at 10 hours post induction. The expression of hIL-12 decreased sharply at 24 hours and dropped below the detection limit at 48 hours. This experiment demonstrated that inducible expression of hIL-12 from Ad RS 24 was achieved with administration of RU 486 in vivo.
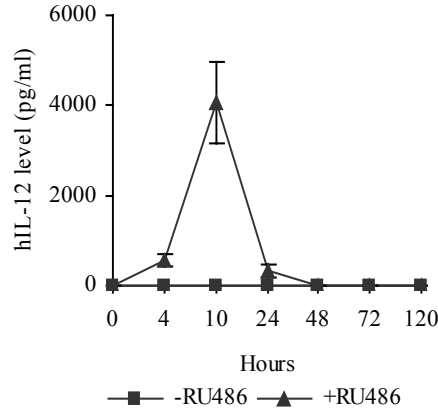
Figure IV.5: Inducible expression of hIL-12 from Ad RS 24 in vivo. C57BL/6 mice were injected with Ad RS 24 at a dose of $3x10^9$ i.u and were induced once with RU 486 at a dose of 250 µg/kg. Serum was taken at regular intervals. + and - RU 486 indicates presence or absence of drug .

IV.1.6 RU 486 and Ad RS 24 increases hIL-12 expression in a dose dependent manner

Modulation of hIL-12 expression in vivo is important to obtain hIL-12 levels within the therapeutic window. Increasing the dosages of RU 486 in vitro could modulate the levels of hIL-12 (Figure IV.4). To investigate the dose dependence of hIL-12 expression on RU 486 in vivo, C57BL/6J mice were injected with Ad RS 24 at doses of $1x10^9$ i.u (n=4) or $3x10^9$ i.u (n=4). Two weeks post injection, RU 486 was injected at 125, 250 and 500 µg per kg body weight. Ten hours after induction, serum was collected and hIL-12 was measured. As shown in Figure IV.6, a RU 486 dose dependent increase in the levels of hIL-12 was observed. In addition, mice injected with the vector Ad RS 24 at the higher dose of $3x10^9$ i.u showed RU 486 dose dependent increase of hIL-12. This experiment demonstrated that increasing the doses of both vector and RU 486 increased the levels of hIL-12 expression in vivo.
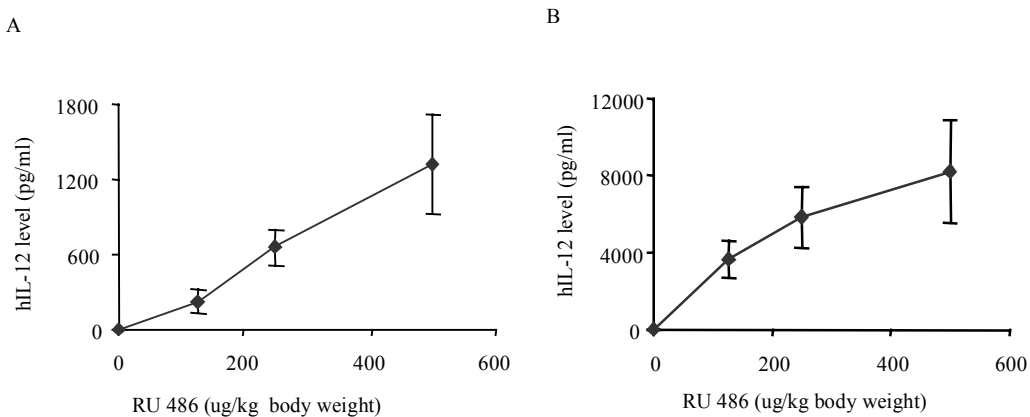

Figure IV. 6: Modulation of hIL-12 expression by Ad RS 24 and RU 486 doses in vivo. C57BL/6J mice (n=4) were injected with Ad RS 24 at a dose of $1x10^9$ i.u and $3x10^9$ i.u represented by Figure A and Figure B respectively. The mice were injected with increasing doses of RU 486 and the levels of hIL-12 expression were determined by ELISA.

IV.1.7 hIL-12 expression kinetics is dependent on intervals of RU 486 injection in vivo

For clinical application and in order to avoid toxic and potential lethal effects, it would be important to control IL-12 levels both qualitatively and quantitatively. The vector Ad RS 24 expresses hIL-12 only upon induction (Figure IV.5). To determine the optimal time intervals of RU 486 injection for maintaining a sustained level of hIL-12, C57BL/6J mice (n=8) were injected with Ad RS 24 at a dose of 3×10^9 i.u followed by induction (n=5) with RU 486 for six days either 12, 24 or 48 hour time interval respectively. Control mice were injected with sesame oil not containing RU 486.

Induction by injection of RU 486 every 12 hours

In week 9 post vector injection, RU 486 was given for six days every 12 hours. Serum was collected every 24 hours and 10 hours after the last induction. As shown in Fig IV.7, the levels of hIL-12 values were between 5000-7000 pg/ml in the first two days of induction and were at around 3000 pg/ml during the remaining four days. The levels of hIL-12 in the controls were below the detection limit.
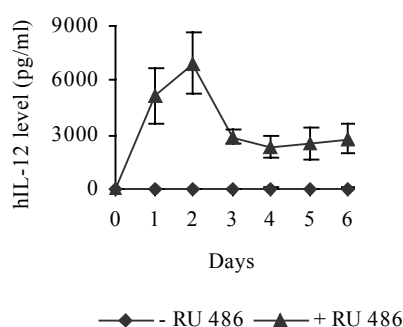

Figure IV.7: Inducible expression of hIL-12 by injection of RU 486 every 12 hours. Mice (n=8) injected with the vector Ad RS 24 at a dose of 3×10^9 i.u were injected (n=5) with RU 486 at time interval of 12 hours, for six days. The control mice (n=3) were injected with sesame oil. The serum was analyzed daily for levels of hIL-12. +RU 486 and – RU 486 indicates the presence and absence of RU 486 induction.

Induction by injection of RU 486 every 48 hours

In week 11 post vector injection, the same group of mice was induced again with RU 486, this time by injection every 48 hours for six days. Serum was collected every 24 hours and 10 hours after the last induction. As shown in Figure IV.8, the hIL-12 levels showed a saw like pattern with peak levels of hIL-12 of about 6000 pg/ml on the day of induction alternating with 6-8 fold lower values on the following day. The levels of hIL-12 in the controls were below the detection limit.
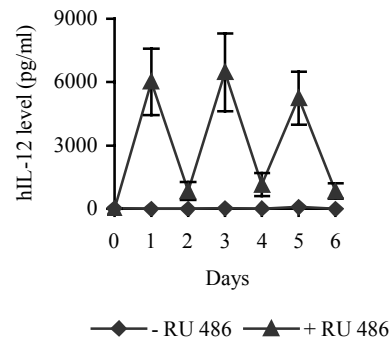
Figure IV.8: Inducible expression of hIL-12 by injection of RU 486 every 48 hours. C57BL/6J mice (n=8) injected with the vector Ad RS 24 at a dose of $3x10^9$ i.u were injected (n=5) with RU 486 at time intervals of 48 hours, for six days. The control mice were injected with sesame oil. The serum was analyzed daily for levels of hIL-12. +RU 486 and –RU 486 in the legend indicates the presence and absence of induction with RU 486.

Induction by injection of RU 486 every 24 hours

At week 14 post vector injection, the same group of mice was injected again with RU 486, now at time intervals of 24 hours for a period of 6 days. As shows in Figure IV.9, the levels of hIL-12 were 5000-6000 pg/ml for the first two days and followed by a relatively sustained level of approximately 3000 pg/ml for the remaining four days. Together these experiments indicated that hIL-12 expression could be sustained in mice by injecting RU 486 every 12 or 24 hours. Treatment for cancer varies depending on the type of tumor and sometimes prolonged expression of hIL-12 might be necessary. To investigate whether it was possible to sustain hIL-12 expression by repeated induction for a longer period of time Ad RS 24 injected C57BL/6J mice (n=4) were induced with the drug RU 486 every 24 hours for 21 days. Control mice (n=3) were injected with sesame oil without RU 486. As shown in Figure IV.10, the serum level of hIL-12 was kept constant at around 3000 pg/ml until the 9th day of induction and decreased moderately thereafter but was still above 1500 pg/ml on day 21. Thus, this experiment demonstrated that it was possible to sustain hIL-12 expression by repeated induction every 24 hours.
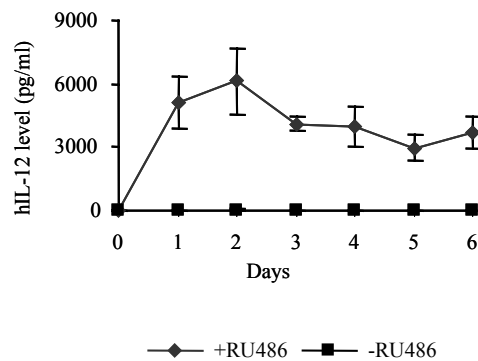

Figure IV.9: Inducible expression of hIL-12 by induction with RU 486 every 24 hours. C57BL/6J mice (n=8) were injected with Ad RS 24 at a dose of $3x10^9$ i.u followed by induction with RU 486 (n=5) at time intervals of 24 hours for six days. +RU 486 and –RU 486 in the legend indicates the presence and absence of induction with RU 486.
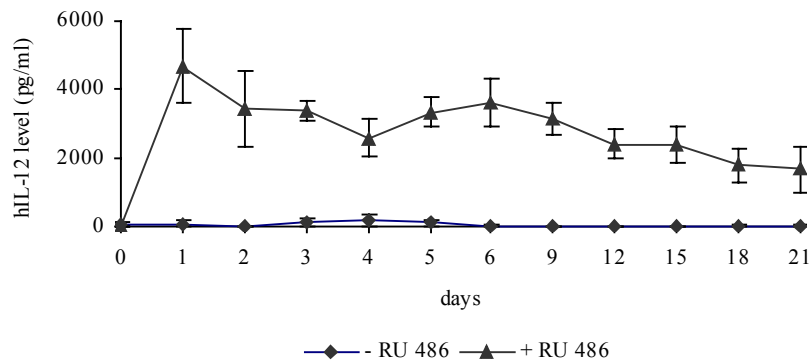
60

Figure IV.10: Inducible expression of hIL-12 for 21 days. C57BL/6J mice were injected with Ad RS 24 at a dose of $3x10^9$ i.u followed by daily induction with RU 486 for 21 days. Serum was collected at 10 hours post induction and the levels of hIL-12 were measured by ELISA. +RU 486 and –RU 486 in the legend indicates the presence and absence of induction with RU 486.

IV.1.8 hIL-12 is inducibly expressed for a long-term in vivo

The ability to induce hIL-12 expression at different time points might be essential for the treatment of recurrent tumors or for the eradication of residual tumors. To investigate whether long-term repeat induction in vivo of hIL-12 was possible for 48 weeks, RU 486 was injected at weeks 2, 9, 11, 14, 19, 28, 33 and 48 weeks. At these time points, hIL-12 was measured in serum before and 10 hours after RU 486 administration. In all cases, hIL-12 was undetectable in serum before induction and increased to values around 2000 pg/ml after induction, indicating that the system remained operative for at least 48 weeks. As shown in Figure IV.11, hIL-12 expression at week 28 was similar to that observed at week 2. At week 48, although the induction was quite significant, the levels obtained were about 43% of those of at week 2. This experiment demonstrated that inducible expression of hIL-12 could be observed for at least 48 weeks.
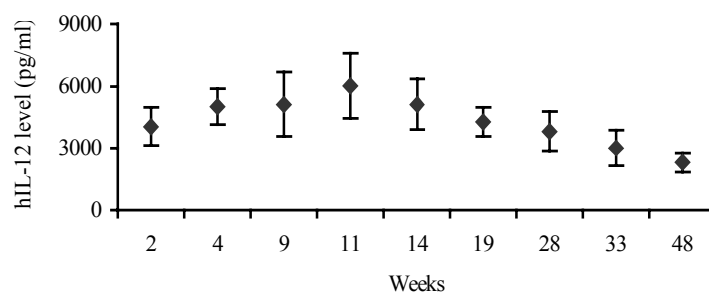

Figure IV.11: Long-term inducible expression of hIL-12 in vivo. C57BL/6J mice injected with Ad RS 24 at a dose of $3x10^9$ i.u were induced with RU 486 at different time points over a period of 48 weeks. Serum was collected at 10 hours post induction and the levels of hIL-12 were determined by ELISA.

IV.1.9 Ad RS 24 is widely distributed but expresses pGLp65 only in liver in vivo
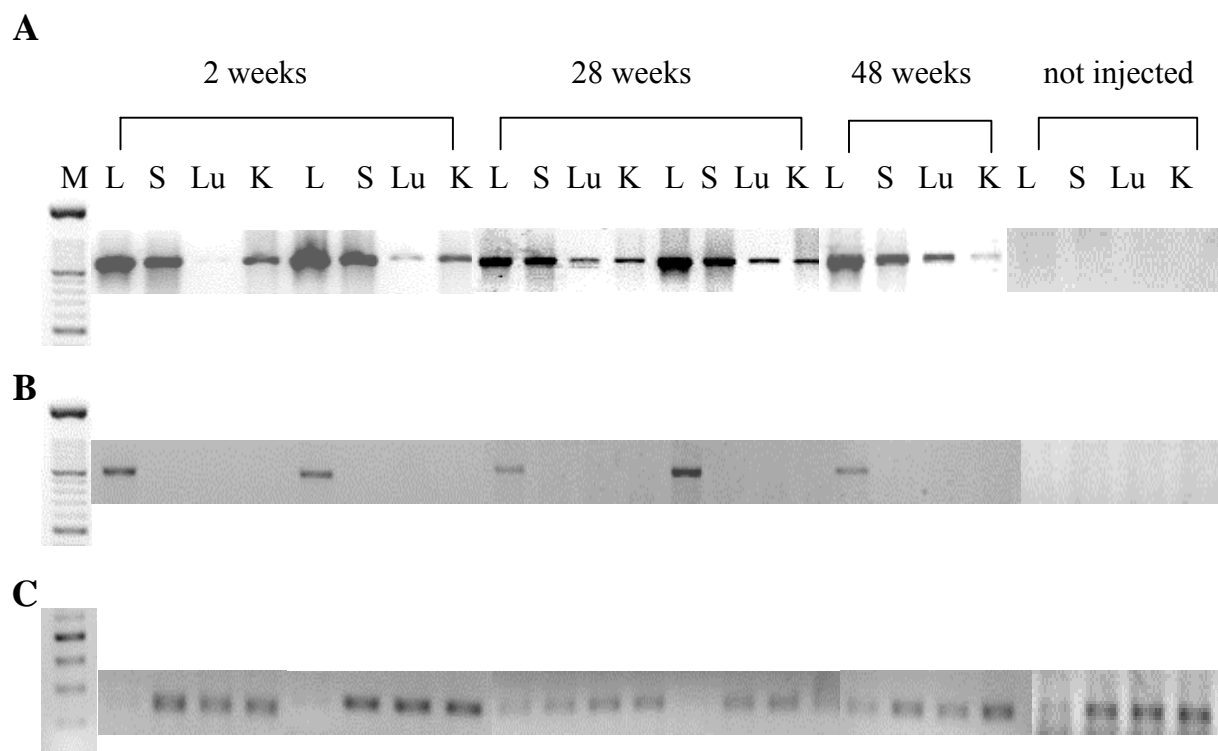

Figure IV.12: Distribution of Ad RS 24 and tissue RNA expression of the transactivator GLp65 in vivo. M, L, S, Lu, K refers to molecular weight marker, liver, spleen, lung and kidney. A) Total DNA was extracted from the organs to determine distribution of viral vector by PCR. B) Total RNA was extracted from the organs to determine tissue distribution of viral vector by RT-PCR. C) RT-PCR for amplification of the house keeping gene β actin was used for internal control of RNA.

The vector Ad RS 24 expresses hIL-12 upon induction in a liver specific manner. It is well known that the majority of Ad vector particles administered by tail vein injection will locate to the liver. To determine tissue distribution and expression of the transactivator GLp65 in vivo, mice were injected with Ad RS 24 at a dose of 3×10^9 i.u. The mice were sacrificed at weeks 2 (n=2), 28 (n=2) and 48 (n=1) post vector injection. Liver (L), lung (Lu), spleen (S) and kidney (K) were obtained from these 5 mice and 2 controls. Total DNA and RNA were extracted from the organs to determine vector distribution and RNA expression of the transactivator GLp65. (Chapter III.3.12 and III.3.13).

As shown in Figure IV.12 A, the presence of vector DNA was observed in all the organs, the signal being more intense in the liver, indicating vector DNA persisted in all tissues for a long period.

To demonstrate RNA expression from the vector, RT-PCR was performed to detect the expression of GLp65 in different tissues (Chapter III.3.13). As shown in Figure IV.12 B, GLp65 specific signals were detected in the liver even 48 weeks after vector administration. In control mice no PCR signals of the transactivator was found in any of the organs analyzed. This data indicated that the promoter and enhancer controlling GLp65 transcription allowed liver specific transgene expression for a long time. ß actin was used as internal control for the RT-PCR and is shown in Figure IV.12 C.

IV.2 Construction and characterization of mIL-12 expressing plasmids and vector

IV.2.1 Construction of pRS 22, pRS 25 and Ad RS 25

mIL-12 has been shown to have a profound anti-tumoral effect in different murine models of cancer [81]. However, sustained expression of mIL-12 for a long time is toxic in mice and human subjects [81, 126]. Therefore, the vector Ad RS 25 was designed to express mIL-12 upon induction with RU 486 in a liver specific manner. In order to generate Ad RS 25 the plasmids pRS 22 and pRS 25 were initially constructed. pRS 22 was generated by the insertion of the mIL-12 cDNA into the plasmid pRS 17 (Figure III.7). After confirming the integrity, pRS 22 was used to construct pRS 25 (Figure III.10). pRS 25 was used to generate Ad RS 25. A schematic diagram of Ad RS 25 is shown in Figure IV.13.
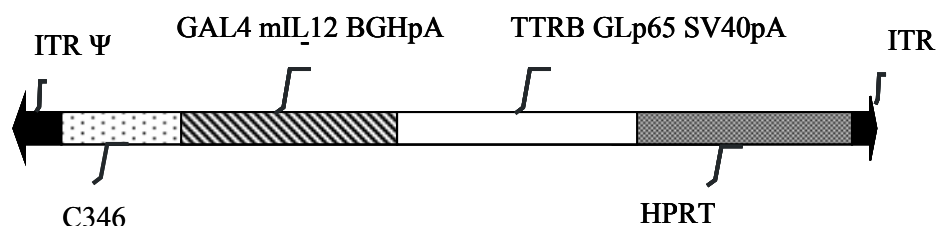

Figure IV.13: Vector Ad RS 25. The vector consists of two expression cassettes. The first cassette expresses the regulator GLp65 under the control of the liver specific TTRB promoter and enhancer. GLp65 in the presence of RU 486 binds to the GAL4 region present in the second expression cassette and mIl-12 is expressed. Ad RS 25 also contains the left terminus of Ad5, the right terminus of Ad 5, and the packaging signal from Ad5 (Ψ). In addition Ad RS 25 also contain C346 and HPRT stuffer sequences.

IV.2.2 mIL-12 is inducibly expressed in vitro upon transfection with pRS 22

pRS 22 was tested for liver specific and regulable expression of mIL-12 in vitro, before it was used for the generation of the vector Ad RS 25. To investigate the regulable liver specific expression of IL-12, pRS 22 was transfected into HepG2, PLC/PRF/5 and HeLa cell lines (Chapter III.4.1) using Fugene reagent. 24 hours post transfection the cells were induced with 10^{-8} M of RU 486 (III.4.6). The supernatants were analyzed 48 hours post induction for the expression of mIL–12 by ELISA (Chapter III.6.4). As shown in Figure IV.14, mIL-12 expression and induction in the hepatic cell lines was observed. However, expressions of mIL-12 was also observed in cell lines transfected with pRS22, but were left uninduced. The reason for background expression might be due to high GLp65 levels attained due to transfection of pRS 22, which results in spontaneous dimerization, and subsequent expression of the transgene downstream of the 17mer.
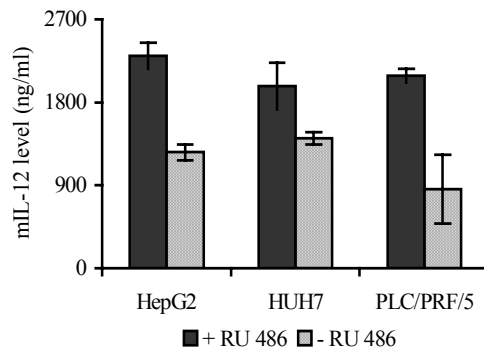
Figure IV.14: Inducible expression of mIL-12 following transfection of pRS 22 in vitro. $5x10^5$ cells of PLC/PRF/5, HUH 7 and HepG2 were cultured in 6 well plates for 24 hours before transfection. Transfection of cells with plasmid pRS 22 was performed using Fugene reagent. 24 hours later, the cells were induced with 10^{-8} M of RU 486 or were left uninduced. The supernatants were collected at 48 hours post induction and mIL-12 levels were determined using ELISA. The legend -RU 486 and +RU 486 indicates the absence or presence of RU 486.

IV.2.3 mIL-12 is inducibly expressed upon cell transduction in vitro with Ad RS 25

To test for dose dependent and liver specific expression of mIL-12, Ad RS 25 was tested on the cell lines HepG2, PLC/PRF/5, A549, and HeLa (Chapter III.4.1). The cells were seeded at densities of $5x10^5$ in six well plates and were cultured for 24 hours before infection. The cells were transduced with the vector Ad RS 25 at a moi of 100, and were induced with 10^{-8} M of RU 486 (Chapter III.4.6) at 3 hours post infection. The first generation adenoviral vector Ad CMV mIL-12 expressing mIL-12 under the control of the hCMV promoter at a moi of 100 served as a control. The amount of mIL-12 present in the supernatants was determined using ELISA. As shown in Figure IV.15, HepG2 cells and PLC/PRF/5 cells in the presence of RU 486 expressed mIL-12 after infection with 100 moi of Ad RS 25. The amount of mIL-12 secreted by HepG2 cells upon infection with Ad RS 25 was higher than after infection with vector Ad CMV mIL-12 expressing mIL-12 from the constitutive hCMV promoter. In contrast to HeLa cells, low levels of mIL-12 were observed in A549 cells upon induction. In conclusion, vector Ad RS 25 exhibited inducible mIL-12 expression upon transduction of the hepatic cell lines HepG2 and PLC/PRF/5.
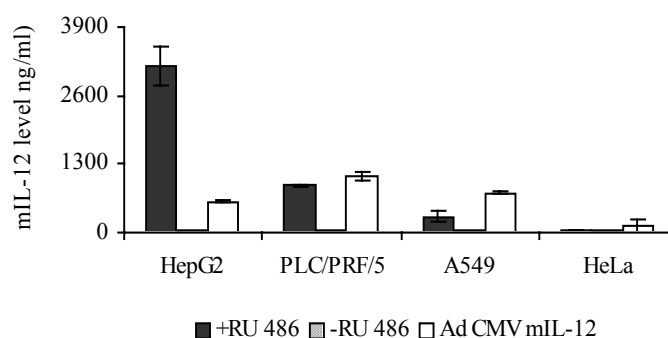
Figure IV.15: Inducible expression of mIL-12 following transduction with Ad RS 25 in vitro. 5×10^5 cells of PLC/PRF/5, A549, HeLa and HepG2 cells were seeded in 6 well plates. 24 hours later, the cells were infected with 100 moi of Ad RS 25 or Ad CMV mIL-12. 3 hours later, Ad RS 25 infected cells were induced with 10^{-8} M of RU 486 or were left uninduced. The first generation adenoviral vector Ad CMV mIL-12 infected at a moi of 100 served as a control. The cell supernatants were collected at 48 hours post induction and mIL-12 levels were determined. In the legend -RU 486 and +RU 486 indicates the absence or presence of RU 486. In the legend CMV hIL-12 represents the virus Ad CMV hIL-12 expressing hIL-12 under the control of the hCMV promoter.

IV.2.4 mIL-12 is inducibly expressed in vivo upon injection of Ad RS 25

The vector Ad RS 25 expresses mIL-12 upon induction with RU 486 in a liver specific manner in vitro (Chapter IV.2.3). To characterize the kinetics of mIL-12 expression in vivo, C57BL/6 mice were injected with Ad RS 25 at a dose of 2×10^9 i.u (n=6). Two weeks post injection, mIL-12 expression was induced by a single intra-peritoneal injection of RU 486 (n=3) at a dose of 250 µg/kg bodyweight. Control mice (n=3) were injected with sesame oil. Serum samples were collected at 0, 4, 10, 24, 48, 72 and 120 hours post induction to determine the levels of mIL-12. As shown in Figure IV.16, in the absence of the drug RU 486 mIL-12 expression was not observed. Measurable expression of mIL-12 was observed at 4 hours post RU 486 induction. High levels of mIL-12 expression were observed 10 hours after induction. The expression of mIL-12 decreased sharply at 24 hours and was below the detection limit at 48 hours. Thus, the in vitro and in vivo properties of vector Ad RS 25 resembled the vector Ad RS 24. Vector Ad RS 25 was used in murine cancer models as presented below in Chapters IV.6 and IV.7.
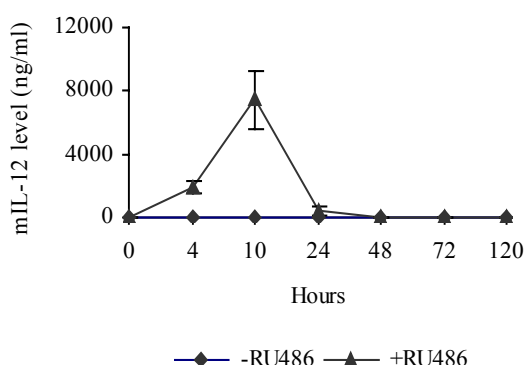

Figure IV.16: Inducible expression of mIL-12 following in vivo injection of Ad RS 25. C57BL/6J mice (n=6) were injected with Ad RS 25 at a dose of 2×10^9 i.u followed by a single injection of RU 486(n=3). Serum samples were collected at 0, 4, 10, 24, 48, 72, and 120 hours and levels of mIL-12 were determined using ELISA.

IV.3 Construction and characterization of stie2 expressing plasmids and vector

IV.3.1 Construction of pRS 42, pRS 45 and Ad RS 45

Tie2 is an endothelium specific tyrosine kinase having a crucial role during the development of the embryonic vasculature [127]. Tie2 knock out mice showed embryonic lethality characterized by a reduction in endothelial cell numbers and a defect in the morphogenesis of microvessels [59, 60]. Since angiogenesis is important for the development of tumors, it was plausible that blocking of Tie2 signalling would retard tumor growth. Recombinant soluble Tie2 receptor (stie2) expressed from a first generation adenoviral vector showed anti-tumor activity in murine models of cancer [128]. Therefore, we generated HC-Ad vector Ad RS 45 to express stie2 constitutively
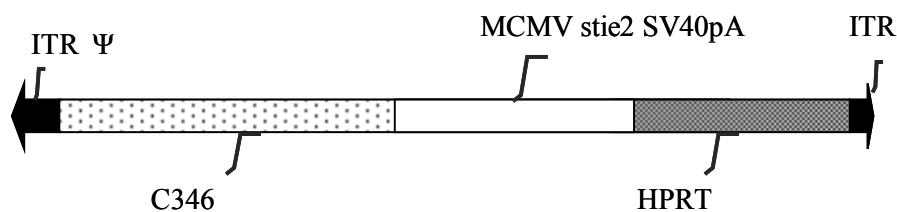

Figure IV.17: Vector Ad RS 45. The vector Ad RS 45 expresses stie2 under the control of the ubiquitously active MCMV promoter. Ad RS 45 was generated from plasmid pRS 45. Ad RS 45 also contains the left terminus of Ad5, the right terminus of Ad 5, and the packaging signal from Ad5 (Ψ). In addition Ad RS 45 also contain C346 and HPRT stuffer sequences.

under the control of the MCMV promotor. In order to generate Ad RS 45 a series of plasmids were constructed and tested for integrity. pRS 31 was constructed from the plasmids pPAPCMV-GLp65-SV40 and pPDK6 (Figure III.13). It consists of the MCMV promoter placed upstream of SV40pA. pRS 34 was generated from the plasmids pRS 31 and pBS II KS-Tie2 EC His. It consists of the stie2 cDNA placed downstream of the MCMV promoter (Figure III.15). pRS 42 was generated by an insertion of a *Not I* site into the plasmid pRS 34 (Figure III.15). pRS 45 was constructed from the plasmids pRS 42 and STK 129 (Figure III.17), and it was used for the rescue of Ad RS 45.

IV.3.2 stie2 is expressed in vitro upon transfection of pRS 42

The plasmid pRS 42 was tested for the expression of stie2 before being used for the generation of pRS 45. To investigate constitutive expression of stie2, pRS 42 was transfected into HepG2, PLC/PRF/5 and HeLa cell lines (Chapter III.4.1) The cells were plated at densities of $3x10^5$ in 6 well plates for 24 hours before transfection. The supernatants were analyzed 48 hours post transfection for the expression of stie2 by ELISA (Chapter III.6.4). As shown in Figure IV.18, stie2 expression was observed in all cell lines tested, the largest amount of stie2 secreted by PLC/PRF/5 cell line.
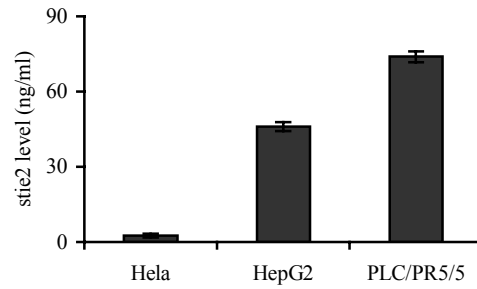
Figure IV.18: Expression of stie2 following transfection of pRS 42 in vitro. HepG2, PLC/PRF/5 and HeLa were plated at densities of 3×10^5 cells per well in 6 well plates. 24 hours later, the cells were transfected with pRS 42. The supernatants were collected 48 hours later and were analyzed for the expression of stie2 by ELISA.

IV.3.3 stie2 is expressed in vitro upon cell transduction with RS 45

Ad RS 45 was tested for expression of stie2 in vitro before being used in vivo. To test for the expression of stie2, cell lines HepG2, PLC/PRF/5 and HeLa cells (Chapter III.4.1) were transduced with Ad RS 45, rescued from the plasmid pRS 45 (Figure III.17), was transduced at a moi of 10 and 100. 48 hours post infection the amount of stie2 secreted into the supernatant was determined by ELISA (Chapter III.6.4). As shown in Fig IV.19 all tested cell lines expressed stie2 at significant levels. The experiment demonstrated a dose dependent expression of stie2 from Ad RS 45. The secreted stie2 protein was further tested for its activity in vitro as shown below.
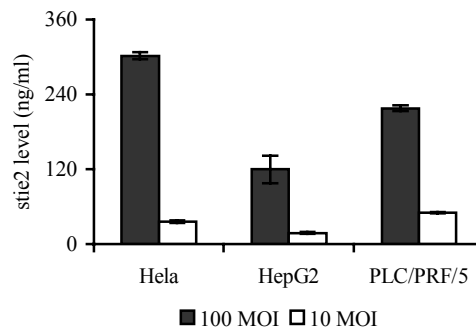

Figure IV.19: Expression of stie2 following transduction with Ad RS 45 in vitro. 5×10^5 cells of HepG2, PLC/PRF/5 and HeLa were plated in 6 well plates. 24 hours later the cells were transduced with 10 or 100 moi of Ad RS 45. The supernatants were collected 48 hours later and were analyzed for the expression of stie2 using ELISA.

IV.3.4 stie2 is detected as a 95 kD protein by Western blot analysis

To confirm the molecular size of the secreted stie2 protein, Western blot analysis was performed (Chapter III.6.2). HeLa and PLC/PRF/5 cells were transduced with vector Ad RS 45 at a moi of 100 and the supernatant was collected at 48 hours post infection. Controls were supernatants from HeLa and PLC/PRF/5 cells either left uninfected or infected with vector Ad SLS 14. To confirm
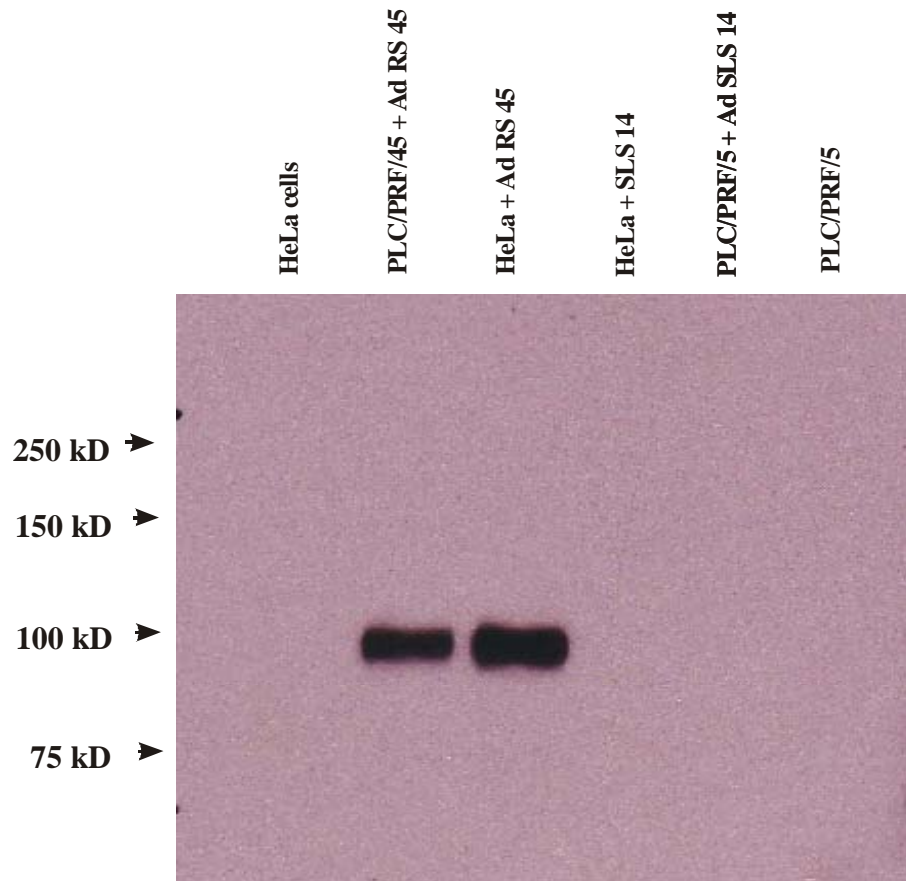

Figure IV.20: Western blot analysis of supernatants after cell transduction with different vectors. HeLa and PLC/PRF/5 cells were plated at densities of 5x105 in six well plates. 24 hours later the cells were either not infected or infected with 100 moi of vectors Ad RS 45 or Ad SLS 14. Supernatants were collected at 48 hours post infection. The stie2 protein present was visualized by Western blot analysis using murine anti-stie2 antibody.

the expression of stie2, murine anti-stie2 antibody (Upstate biotechnology) was used. As expected a specific 95 kD band was detected (Figure IV.20).

IV.3.5 stie2 inhibits tube formation of HUVECs in a matrigel assay

A matrigel assay was performed to confirm the biological activity of stie2 (Chapter III.4.4). Supernatants were collected at 48 hours from uninfected HeLa cells or from cells infected with either 100 moi of vector Ad RS 45 or control vector Ad SLS 14. HUVECs incubated with the supernatant containing stie2 showed incomplete tube formation (Figure IV. 21B). In contrast, HUVECs incubated with supernatants collected from uninfected cells (not shown) or cells infected with Ad SLS 14 showed clear tube formation (Figure IV.21 A). Since this experiment was done in parallel with supernatant containing sflt1 expressed by Ad RS 23 or Ad RS 44, Figure IV.21 A is shown again in Figure IV.30 A. To quantify tube formation, the numbers of branch points were counted per field, and the results are represented as an average value of 10 fields. As shown in Figure IV.22, the number of branch points in HUVECs incubated with the supernatant containing

stie2 as found to be reduced by half, when compared with HUVECs incubated with control supernatant.
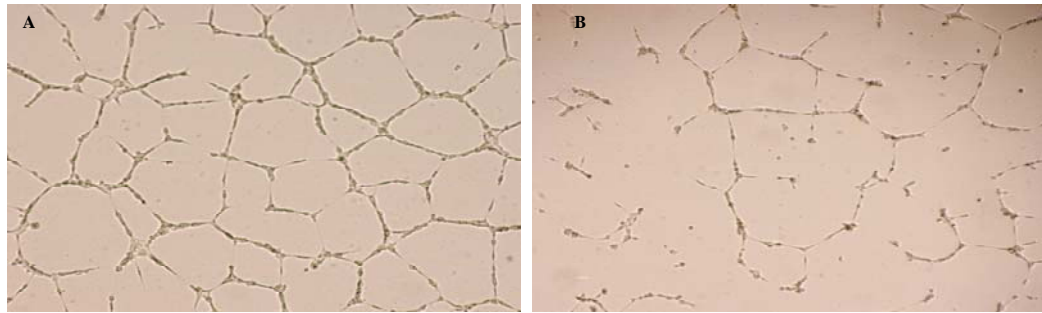

Figure IV.21: Inhibition of tube formation in a matrigel by stie2. HUVECs plated on a matrigel were incubated for 9 hours with supernatant from HeLa cells, which had been infected at mois of 100 with Ad RS 45 or Ad SLS 14, respectively. The pattern of tube formation was visualized under a microscope. Figure A and B represent HUVECs incubated with 100 µl of supernatant from cells transduced with Ad RS 45 (B) or Ad SLS 14 (A) respectively.
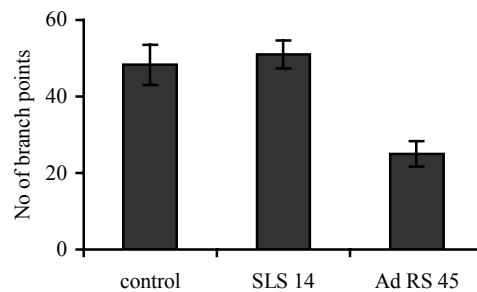

Figure IV.22: Semi quantitative determination of inhibition of tube formation by stie2. HUVECs plated on a matrigel were incubated for 9 hours with supernatants from HeLa cells. The supernatants were obtained by transducing HeLa cells at a moi of 100 with Ad RS 45 or Ad SLS 14, respectively. The supernatant from uninfected HepG2 cells was also used as control. The pattern of tube formation was visualized under a microscope. The number of branch points was counted manually. The figure IV.22 represents an average value obtained by counting of 10 fields.

IV.3.6 stie2 is constitutively expressed in vivo upon injection of Ad RS 45

To investigate the kinetics of in vivo expression, C57BL/6J mice (n=3) were injected into the tail vein with Ad RS 45 at a dose of 2×10^9 i.u. Control mice (n=3) were injected with saline. 24 hours prior to injection, both groups of mice were injected with clodronate liposomes to deplete Kupffer cells (Chapter III.7.3). One week after the injection of the vector, the sera from the mice were collected at weekly intervals and were assayed for the expression of stie2 by ELISA (Chapter III.6.4). As shown in Figure IV.23, stable stie2 expression was observed during the observation period. Control mice injected with saline did not exhibit expression of stie2 (not shown).
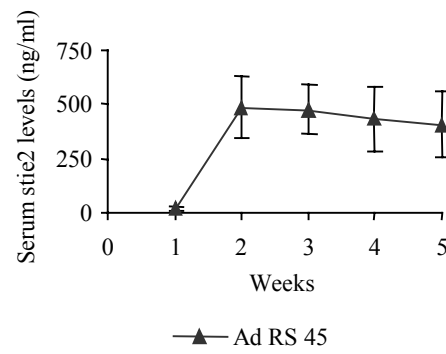
Figure IV.23: Expression of stie2 in vivo following injection of Ad RS 45. Kupffer cell depleted C57BL/6J (n=3) mice were injected with Ad RS 45 at a dose of $2x10^9$ i.u. Serum stie2 was determined by ELISA at weekly intervals.

IV.4 Construction and characterization of sflt1 expressing plasmids and vectors

IV.4.1 Construction of pRS 20, pRS23, pRS 33, pRS 44, Ad RS 23 and Ad RS 44

Growth of tumors requires angiogenesis. Angiogenesis is mediated by soluble growth factors like VEGF. VEGF is a potent stimulator of endothelial cell proliferation in vitro and in vivo. VEGF binds to endothelial cells through the high affinity receptor VEGFR1. Sequestration of VEGF is mediated by sflt1 in physiological conditions. Thus, the blocking of VEGF by sflt1 could be therapeutic for tumors that depend on VEGF function. Apart from embryonic and tumor growth, VEGF has been suggested to play important physiological roles [78]. Regulable expression of sflt1 therefore could be controlling levels of sflt1 within a therapeutic window. To investigate the potential of blocking tumor growth by sequestration of VEGF, vectors expressing sflt1, either constitutively or inducibly, were constructed.

To express sflt1 constitutively, plasmids pRS 29, pRS 33, pRS 44 and vector Ad RS 44 were generated and validated. For details of construction, see Chapter III.1.5. pRS 29 consists of an elongation factor 1-α (EF1-α) promoter placed upstream of the BGH cleavage and polyadenylating sequence (Figure III.12). pRS 33 was constructed by insertion of sflt1 cDNA into plasmid pRS 29 (Figure III.14). pRS 44 was constructed by inserting the sflt1 expression cassette from pRS 33 into STK 129 (Figure III.16). pRS 44 was rescued as HC-Ad vector Ad RS 44(Figure IV.24 A).

To express sflt1 upon induction in a liver specific manner pRS 20, pRS 23 and vector Ad RS 23 were generated and validated. For details of construction see Chapter III.1.5. pRS 20 was generated by the insertion of the sflt1 cDNA into pRS 17 (Figure III.5). pRS 20 was used to construct pRS 23 (Figure III.8). pRS 23 was rescued as HC-Ad vector Ad RS 23. Ad RS 23 contains as therapeutic principle two expression cassettes (Figure IV.24 B). The first cassette consists of the sflt1 cDNA placed downstream of the GAL4 E1b TATA region and upstream of BGHpA. The second cassette consist of GLp65 placed downstream of the liver specific promoter and enhancer TTRB, and upstream of the SV40 poly A sequence. In addition, Ad RS 23 contains the left and right termini of Ad5 and the C346 and HPRT stuffer sequences.
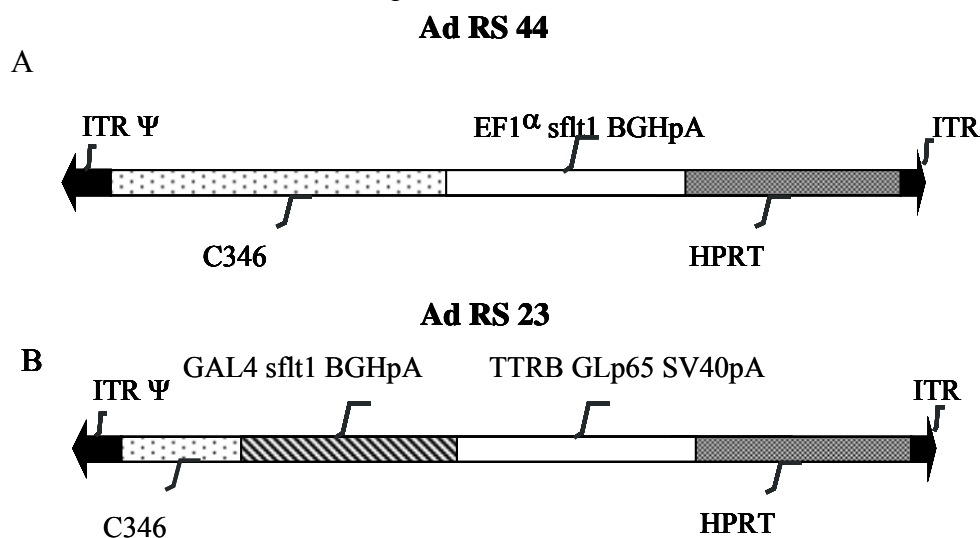
Figure IV.24:. Vector Ad RS 44 and Ad RS 23. A) Ad RS 44 expresses sflt1 constitutively under the control of ubiquitous promoter EF1α. B) Ad RS 23 expresses sflt1 upon induction with RU 486 in a liver specific manner. Ad RS 44 and Ad RS 23 also contain the left terminus of Ad5, the right terminus of Ad 5, and the packaging signal from Ad5 (Ψ). In addition, Ad RS 44 and Ad RS 23 also contain C346 and HPRT stuffer sequences. The adenoviral termini and the stuffer sequence are indicated.

IV.4.2 sflt1 is inducibly expressed upon transfection of pRS 20 or infection with Ad RS 23

To confirm regulable and liver specific expression of sflt1, pRS 20 was transfected into HepG2, PLC/PRF/5 and HeLa cells using Fugene transfection reagent (Chapter III.4.3). The cells were seeded at a density of $3x10^5$ in six well plates and were cultured for 24 hours before transfection. 24 hours later, the cells were transfected with pRS 20 followed by induction with 10^{-8} M of RU 486 or were left uninduced (Chapter III.4.6). The supernatants were collected 48 hours post induction and were analyzed for the expression of sflt1 by ELISA (Chapter III.6.4). As shown in Figure IV.25, inducible expression of sflt1 was observed in hepatic cell lines HepG2 and PLC/PRF/5. In HeLa cells the expression of sflt1 was below the detection limit. Having confirmed the functional integrity, pRS 20 was further used for the construction of pRS 23. Ad RS 23 generated from pRS 23 was tested for the expression of sflt1 in vitro, in HepG2, PLC/PRF/5, HUH -7, A549 and HeLa cells before being used in vivo (Chapter III.4.1). The cells were plated at densities of $5x10^5$ in 6 well plates for 24 hours before infection. The cells were infected with Ad RS 23 at a moi of 100 and were induced with 10^{-8} M of RU 486 3 hours post infection. The supernatants were collected at 48 hours post induction and ELISA (Chapter III.6.4) was used to determine the amount of sflt1 present. As shown in Figure IV.26, sflt1 expression was inducible in the hepatic cell lines by RU 486. HepG2 cells also expressed sflt1 even in the absence of RU 486, but the levels were lower than observed in the presence of RU 486. In contrast, the expression of sflt1 upon induction was not detected in A549 and HeLa cells infected with Ad RS 23. Ad RS 23 was further tested for expression in vivo below (Chapter IV.8).
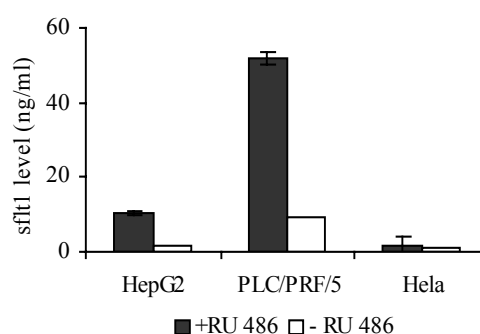

Figure IV.25: Inducible expression of sflt1 upon transfection of pRS 20 in vitro. $3x10^5$ cells of HepG2, PLC/PRF/5 and HeLa were plated in 6 well plates. 24 hours later the cells were transfected with plasmid pRS 20 using Fugene transfection reagent followed by RU 486 induction. The supernatants were collected 48 hours later and amount of sflt1 was determined using ELISA.
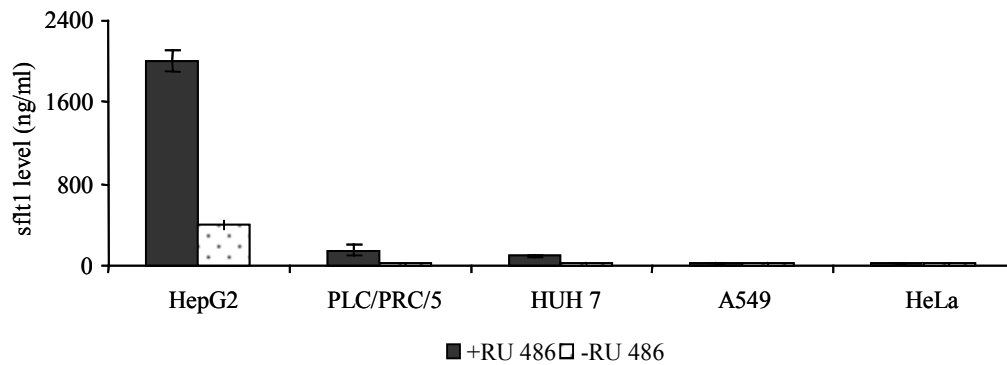
Figure IV.26: Inducible expression of sflt1 upon infection of Ad RS 23 in vitro in HepG2, PLC/PRF/5, HUH 7, A549 and HeLa cells. 24 hours after plating the cells were infected with 100 moi of Ad RS 23 followed by RU 486 induction. The supernatants were collected 48 hours later and were analyzed for the expression of sflt1 using ELISA. The symbols +RU486 or – RU 486 indicate the presence or absence of RU 486.

IV.4.3 sflt1 is constitutively expressed upon pRS 33 transfection or Ad RS 44 infection

To investigate constitutive expression of sflt1, pRS 33 (Figure III.14) was transfected into HepG2, PLC/PRF/5 and HeLa cells using Fugene transfection reagent (Chapter III.4.3) as described above. sflt1 amounts in the supernatants were determined by ELISA (Chapter III.6.4). As shown in Figure IV.27, expression of sflt1 was observed in all transfected cell lines, the levels being highest in the hepatic cell line PLC/PRF/5. Having confirmed the expression pRS 33 was used for the generation of pRS 44. Ad RS 44 was rescued from pRS 44. To test for the expression of sflt1 cell lines HepG2, PLC/PRF/5 and HeLa were infected with Ad RS 23 at 10 and 100 mois. The amount of sflt1 secreted into the supernatant 48 hours post infection was determined using ELISA. As shown in Figure IV.28 all the tested cell lines expressed sflt1 at significant levels. The experiment also demonstrated dose dependent expression of sflt1 in the infected cells, the highest being secreted by HeLa cells. The experiment confirmed the expression of Ad RS 44. The secreted sflt1 protein was further tested for activity in vitro as shown below.
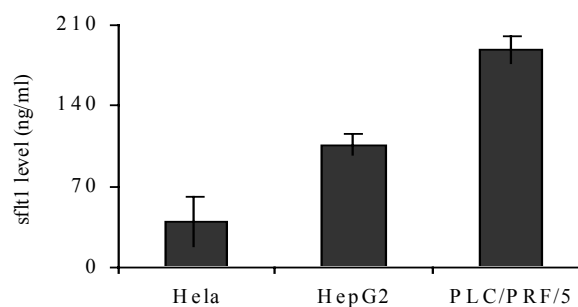

Figure IV.27: Constitutive expression of sflt1 upon pRS 33 transfection in vitro in HepG2, PLC/PRF/5 and HeLa cells. The supernatants were collected 48 hours after transfection and were analyzed for the expression of sflt1 by ELISA.
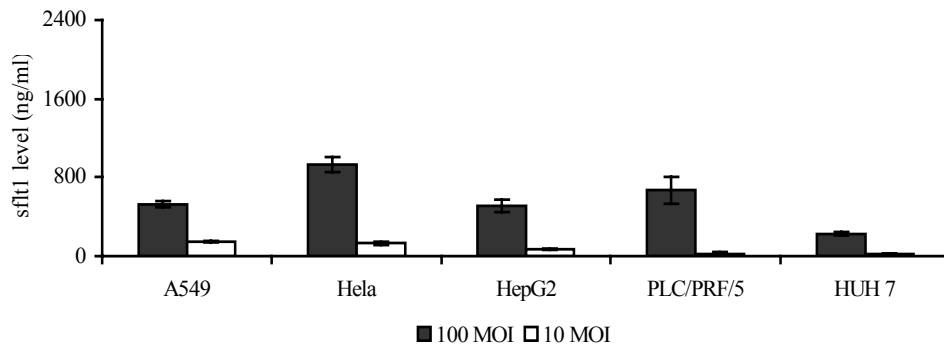
Figure IV.28: Constitutive expression of sflt1 upon Ad RS 44 infection in vitro. HepG2, PLC/PRF/5 and HeLa cells were plated in 6 well plates. 24 hours later the cells were infected with 10 or 100 moi of Ad RS 44. The supernatants were collected 48 hours later and were analyzed for expression of sflt1 by ELISA.

IV.4.4 sflt1 is detected as a 97 kD protein by Western blot analysis

To confirm the molecular size of the secreted sflt1 protein, Western blot analysis was performed. HepG2 cells were infected with control vector Ad SLS 14 or the sflt1 expressing vectors Ad RS 44 or Ad RS 23, at a moi of 100. Ad RS 23 infected cells were induced with 10^{-8} M of RU 486 at 3 hours post infection. Supernatants were collected at 48 hours post infection and were processed as described earlier (Chapter III .6.2). A recombinant sflt1-Fc chimera (R&D systems) having a Mwt of 123 kD was used as a control. As shown in Figure IV.29, HepG2 cells infected with Ad RS 23 or Ad RS 44 expressed sflt1 with a size of 97 kD as expected. The expressed sflt1 protein was further tested for biological activity.
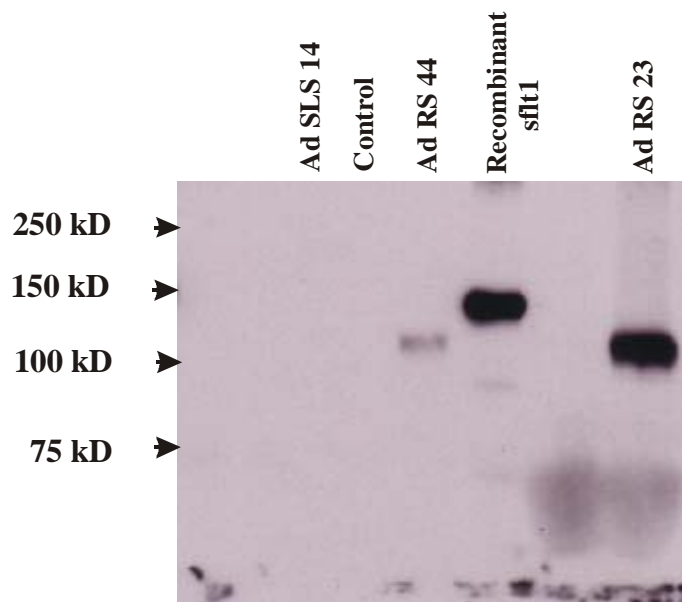
Figure IV.29: Western Blot analysis of supernatants after HepG2 cell transduction with different vectors. The cells were infected with Ad RS 44 or Ad RS 23 at a moi of 100. 4 hours post infection, the cells infected with Ad RS 23 were induced with 10^{-8} M of RU 486. Ad SLS 14 infected cells at a moi of 100 served as a control. Also a recombinant sflt1-Fc chimera was used to determine the specificity of the primary MAb. Supernatants were collected 48 hours post infection. The processed supernatants were run on a 6% SDS PAGE and were transferred to a nylon membrane for visualization. The sflt1 protein was visualized by western blot analysis using mice anti sflt1 antibody.

74

IV.4.5 sflt1 inhibits tube formation of HUVECs in a matrigel assay

A matrigel assay was performed to confirm the biological activity of sflt1 (Chapter III.4.4). HepG2 cells were infected with 100 moi of Ad RS 23, Ad RS 44 or Ad SLS 14 respectively. Cells infected with Ad RS 23 were induced with 10^{-8} RU 486 at 3 hours post infection and the supernatants were collected at 48 hours post infection. HUVECs plated on the matrigel were incubated with the supernatants for 9 hours. As shown in Figure IV.30.A, HUVECs incubated with the supernatant obtained from Ad RS 23 or Ad RS 44 infected cells containing sflt1 showed incomplete tube formation. In contrast, as shown in Figure IV.30 A, HUVECs incubated with supernatants from cells infected with Ad SLS-14 showed clear tube formation. Identical results were obtained with HUVECs incubated with supernatants collected from uninfected cells (data not shown). To quantify the pattern of tube formation, the average number of branch points per field was determined from an average of 10 fields (Figure IV.31).
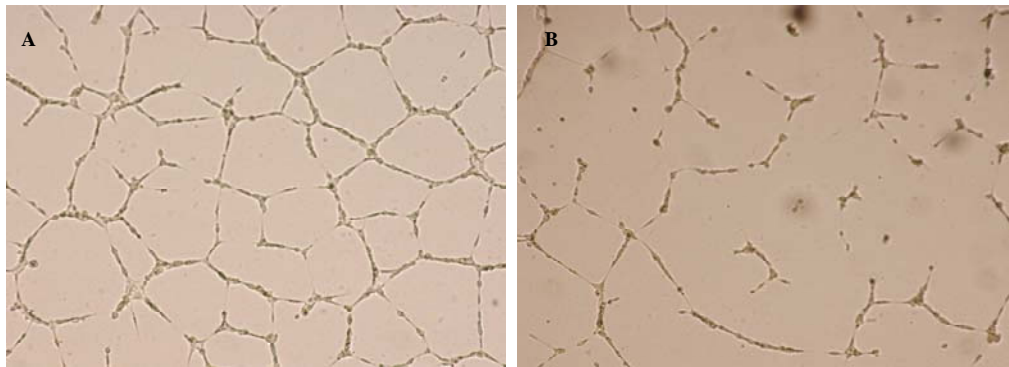
Figure IV.30: HUVECs plated on a matrigel were incubated for 9 hours with 100 µl of supernatant of HepG2 cells, infected with 100 moi of Ad RS 23 (B) and Ad SLS 14 (A) and induced with 10^{-8} M of RU 486. The pattern of tube formation was visualized under a microscope. Note that A is also shown in Figure IV.21 A.
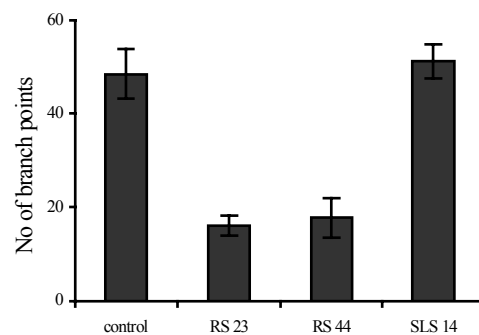
Figure IV.31: Semiquantitative determination of inhibition of tube formation by sflt1. HUVECs plated on a matrigel were incubated for 9 hours with supernatants from HepG2 cell infected with Ad RS 23, Ad RS 44 and Ad SLS 14 at a moi of 100. The supernatants from HepG2 cells were collected 48 hours post infection. The pattern of tube formation was visualized under a microscope. The number of branch points was counted visually. The figure represents an average value obtained from counting 10 fields.

IV.4.6 sflt1 inhibits VEGF induced proliferation of HUVECs

Endothelial cells proliferate in the presence of different growth factors [26]. Proliferation of HUVECs can be achieved by culturing them with low serum conditions and stimulating with VEGF. VEGF-mediated proliferation of serum-starved HUVECs can be specifically be blocked by its soluble receptor sflt1. The functional activity of sflt1 was determined using a HUVEC proliferation assay (Chapter III.4.5). To quantitatively determine the functional activity of sflt1, supernatants containing sflt1 were obtained by infecting HepG2 cells with vectors Ad RS 44, Ad RS 23 and Ad SLS 14 at a moi of 100. The supernatants were collected 48 hours later and were assayed for the levels of sflt1 protein using ELISA. The sflt1 containing supernatants were diluted to contain sflt1 at a concentration of 100 ng/ml in 2% total serum. Control supernatants were also diluted to contain 2% serum. The diluted supernatants from infected HepG2 cells were incubated with serum-starved HUVECs, which were stimulated with VEGF to proliferate. 48 hours post incubation, 10 μl of WST-1 reagent was added and the OD at 550 nm was measured 4 hours later. As shown in Figure IV.32, serum starved HUVEC proliferated in the presence of recombinant VEGF at a concentration of 10 ng/ml. VEGF induced proliferation of HUVECs was blocked by supernatant containing sflt1 or recombinant sflt1 at a concentration of 100 ng/ml.

The assay clearly demonstrated that VEGF induced proliferation of HUVEC was specifically blocked by sflt1 expressed from Ad RS 23 and Ad RS 44.
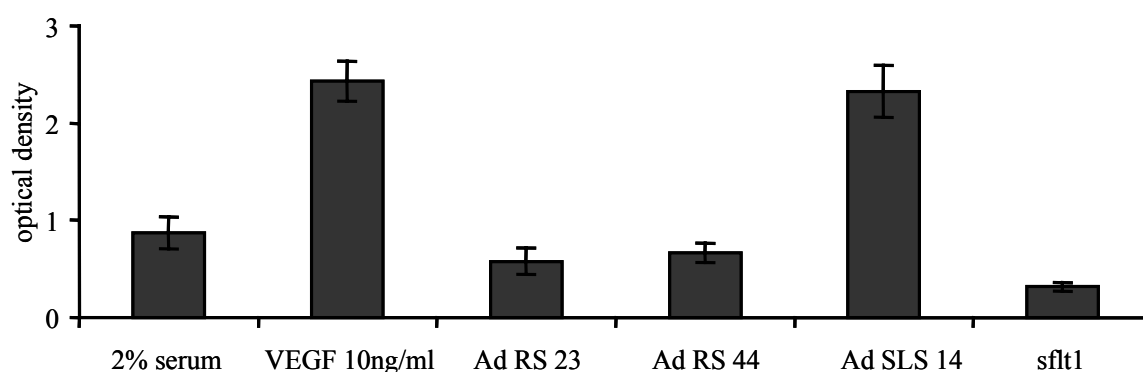
Figure IV.32: Inhibition of VEGF induced HUVEC proliferation by sflt1. 4×10^3. HUVECs were seeded in a 96 well plate and were incubated in endothelial cell media (ECM) containing 5% serum for 24 hours. The cells were further incubated in ECM containing 2% serum for 16 hours to undergo serum starvation. 16 hours later the medium was changed and HUVECs were incubated with supernatants from the HepG2 cells infected with Ad RS 23, Ad RS 44, Ad SLS 14. After the addition of supernatants, the HUVECs were stimulated with VEGF at a concentration of 10 ng/ml. HUVECs incubated only with 2% serum served as a negative control. HUVECs incubated only with VEGF at a concentration of 10 ng/ml served as a positive control. 48 hours post incubation with the supernatants the HUVECs were incubated for 2 hours with WST-1 reagent. The OD was read at 550 nm.

IV.4.7 sflt1 is constitutively expressed in vivo upon injection of Ad RS 44

The vector Ad RS 44 has been earlier shown to express active sflt1 in vitro (Figure IV.31 and Figure IV.32). To characterize the in vivo expression kinetics, Kupffer cell depleted C57BL/6J mice (n=3) were injected with 2×10^9 i.u of Ad RS 44 (Chapter III.7.3). Kupffer cell depleted control mice were injected with saline. Sera were collected at weekly intervals and serum sflt1 levels were measured (Chapter III.6.4). As shown in Figure IV.33 there was a gradual increase in the expression of sflt1 from the first week of measurement. Surprisingly, at the end of the fifth week after the injection of the vector, all mice were observed to have ascites. Ascites was not observed in mice injected with clodronate liposomes alone. All mice that had received Ad RS 44 died at the end of fifth week.

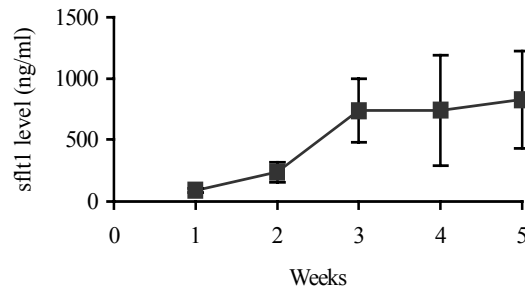**Figure IV.33:** Constitutive sflt1 expression upon infection of Ad RS 44 in vivo. Kupffer cells depleted C57BL/6J (n=3) mice were injected with the vector Ad RS 44 at a dose of $2x10^9$ i.u. Serum sflt1 levels were determined at weekly intervals by ELISA.

IV.4.8 sflt1 is inducibly expressed in vivo upon injection of Ad RS 23

Ad RS 23 has been shown to express sflt1 upon induction in a liver specific manner (Chapter IV.1.3). To investigate the kinetics of expression in vivo, C57BL/6J (n=3) mice were injected with Ad RS 23 at a dose of $5x10^8$ i.u. Two weeks post injection the mice received a single i.p. injection of RU 486 (250 µg/kg body weight). The levels of sflt1 were determined at 0 hour, 4 hours, 10 hours, 24 hours and 48 hours using ELISA. As shown in Figure IV.34 inducible expression of sflt1 was observed at 4 hours and was highest at 10 hours post induction. The levels of sflt1 were again low at 24 hours and were undetectable after 48 hours. To determine the levels of sflt1 upon daily induction for four weeks, C57BL/6J mice (n=5) were injected with Ad RS 23 at a dose of $5x10^8$ i.u. Starting at one week post injection, the mice received daily i.p. injections of RU 486 (250 µg/kg of body weight). Serum levels of sflt1 were determined at weekly intervals. As shown in Figure IV.35 A the levels of sflt1 were in the range of 75-300 ng/ml during the induction period. This experiment indicated that daily injection of RU 486 could maintain serum levels of sflt1. Ascites was not observed at any time in this group of mice. To investigate the expression kinetics of sflt1 expression in the presence of RU 486 pellets designed to release RU 486 at a dose of 250 µg/kg of body weight of mice for 30 days, C57BL/6J mice (n=5) were injected with Ad RS 23 at a dose of $5x10^8$ i.u . One week post injection the RU 486 pellets were subcutaneously implanted.
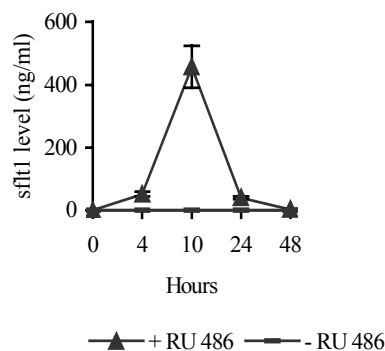
Figure IV.34: Inducible expression of sflt1 in vivo upon injection of Ad RS 23. C57BL/6J mice (n=3) were injected with $5x10^8$ i.u. of Ad RS 23. Two weeks post injection, the mice received a single dose of RU 486. Serum was collected at 0 hour, 10 hours, 24 hours and 48 hours after induction and sflt1 levels were determined by ELISA. The legend – and + RU 486 refers to absence and presence of induction.
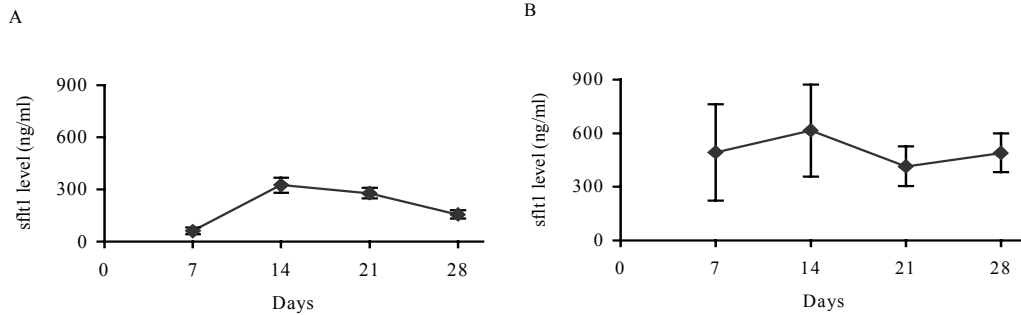
The levels of sflt1 were determined at weekly intervals for four weeks. All mice with implanted
RU 486 pellets showed ascites at the end of the fifth week. As shown in Figure IV.35B, sflt1 serum
levels were in the range of 150 to 700 ng/ml. This experiment indicated that subcutaneous
implantation of RU 486 pellets maintained relatively constant serum levels of sflt1. To summarize,
the vector Ad RS 23 expressed sflt1 upon induction in a liver specific manner. The levels of sflt1
were maintained by daily induction with RU 486 or by implantation of pellets releasing RU 486.
However, ascites was observed in mice that had received RU 486 pellets but not in mice that had
received daily i.p. injection of RU 486.

IV.5 Diagnostic work-up of sflt1 induced ascites

Constitutive expression of sflt1 from the vectors Ad RS 23 or Ad RS 44 caused ascites in C57BL/6J mice. The ascites became apparent at the end of the fifth week post vector injection. All mice died within few days thereafter. To investigate the causative factors for the development of ascites, C57BL/6J mice (n=3) were injected with 1.5×10^9 i.u of Ad RS 44. Control mice were injected with saline. 24 hours prior to the injection of the vector or saline, mice were injected with clodronate to deplete Kupffer cells. The mice were sacrificed at the end of the fifth week to collect sera and organs. Since liver or kidney malfunction generally causes ascites, a diagnostic work-up was performed. Levels of AST, ALT, urea, albumin, bilurubin, and total protein were determined from the serum (Chapter III.6.3). Haemotoxylin-Eosin (H&E) staining of organ was performed.

IV.5.1 Serum AST but not ALT levels are increased in RS 44 injected mice

AST and ALT are transaminases, which catalyze the interconversion of amino acids and α keto acids by transfer of amino groups. Presence of high levels of AST and ALT enzymes in the serum may signal myocardial infarction, hepatic diseases, muscular dystrophy or organ damage. Serum elevations of ALT activities are rarely observed except in parenchymal liver disease, because ALT is a more liver-specific enzyme than AST. To investigate the causative factor for ascites, AST and ALT levels were determined in the serum. As shown in Figure IV.36 AST levels were four fold higher in mice injected with vector Ad RS 44 when compared to mice injected with saline. No significant change was observed in ALT levels between control and Ad RS 44 injected mice. The absence of a significant change in ALT levels signaled an absence of liver damage as causative factor.
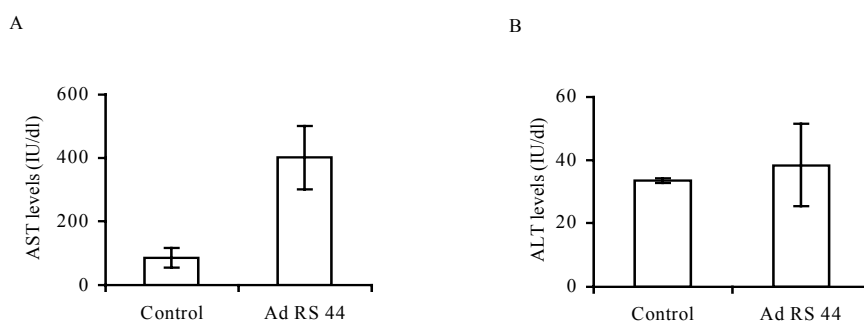
Figure IV.36: Determination of AST and ALT levels in serum of Ad RS 44 injected mice. Kupffer cell depleted C57BL/6J mice (n=3) were injected with Ad RS 44 at a dose of 1.5×10^9 i.u. Serum collected at the end of fifth week post infection was analyzed to determine the levels of AST and ALT. A and B represent the levels of AST and ALT in control mice and in mice injected with Ad RS 44 respectively.

IV.5.2 Reduction in total protein and albumin level in Ad RS 44 injected mice

Occurrence of ascites frequently reflects a decrease in the concentration of albumin and total protein in the serum. Albumin is synthesized by hepatocytes, and constitutes 55-65% of the total plasma protein. Serum albumin levels are determined as a part of diagnostic work up of liver diseases, nephritic syndrome, Crohn disease and neoplastic disease. Plasma proteins are synthesized predominantly in the liver, plasma cells, lymph nodes, spleen and bone marrow. Total protein measurements are used in the diagnosis and treatment of liver, kidney and metabolic disorders. Total protein and albumin serum levels were determined at the end of the fifth week after vector injection. As shown in the Figure IV.37 a 50% reduction in albumin levels and a 25%

reduction in total protein were observed in mice injected with Ad RS 44 when compared to control mice. The reduction of total protein and albumin in the serum correlates with the observed ascites.
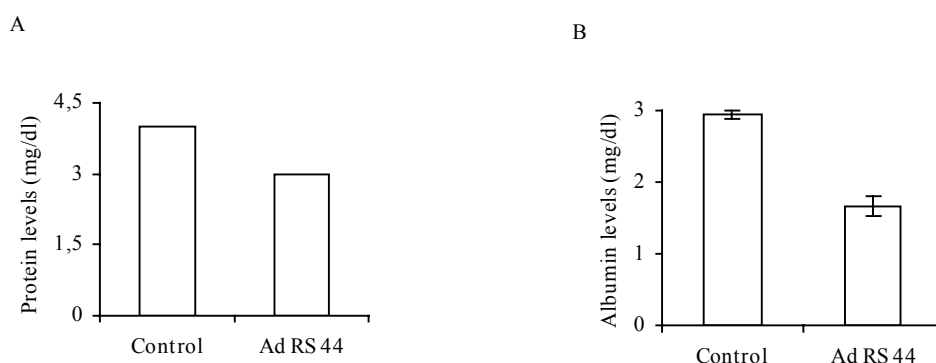
Figure IV.37: Total serum protein (A) and albumin (B) in mice injected with Ad RS 44 having ascites or control mice. Kupffer cell depleted C57BL/6J mice (n=3) were injected with Ad RS 44 at a dose of 1.5×10^9 i.u. Total serum protein and albumin was measured in serum collected at the end of fifth week after vector administration.

IV.5.3 Serum bilirubin and liver histology is unchanged in Ad RS 44 injected mice

Serum bilirubin levels are frequently elevated in certain liver disorders. Serum was collected from mice 5 weeks post injection to determine bilirubin levels. As shown in Figure IV.38, no significant differences in serum bilirubin were observed in vector injected mice when compared to control
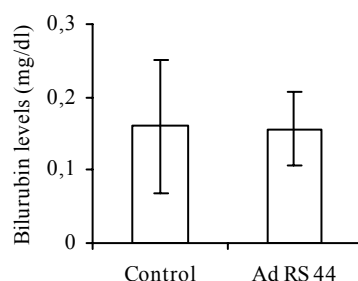
Figure IV.38: Total serum bilirubin in Ad RS 44 injected mice and in controls. Kupffer cell depleted C57BL/6J mice (n=3) were injected with Ad RS 44 at a dose of 1.5×10^9. Total bilirubin was determined in serum collected at the end of the fifth week after vector administration.

mice. To further exclude any gross liver pathology H&E staining of liver sections was performed from Ad RS 44 injected mice and from controls. Interestingly, as can be seen from Figure IV.39 no liver abnormality was detected in either control or Ad RS 44 injected mice. Taken together these data indicated that ascites was not caused by liver dysfunction.
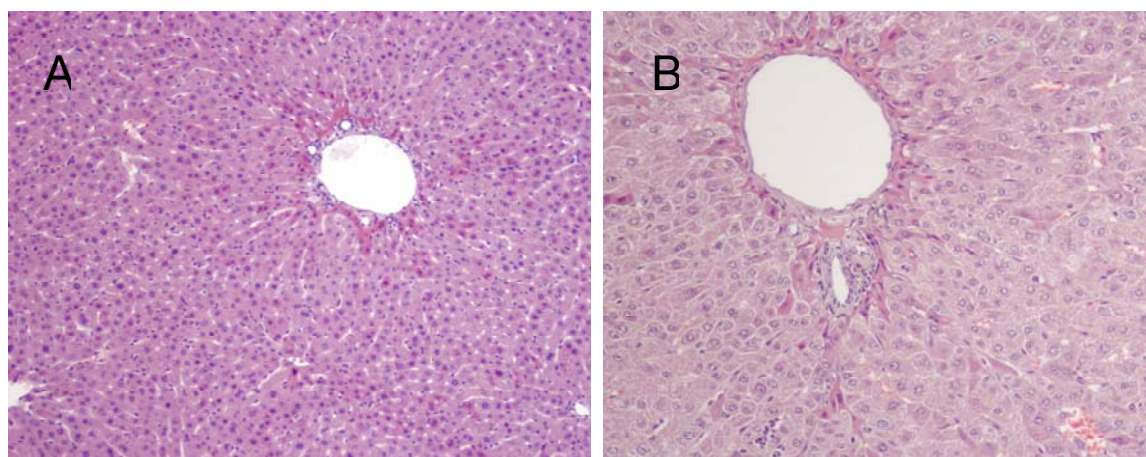
Figure IV.39: H&E staining of liver sections from Ad RS 44 injected mice with ascites (B) and control mice (A). C57BL/6 mice (n=3) were injected with Ad RS 44 at a dose of 1.5×10^9 i.u. H&E stains of liver sections were performed from the mice at the end of the fifth week. H&E staining was performed by Dr. Matilda Bustos.

IV.5.4 Serum urea but not creatinine is increased in Ad RS 44 injected mice

Ascites may also be caused by renal changes. Two parameters frequently measured as a surrogate for renal function are creatinine and urea. Creatinine is excreted by glomerular filtration during normal renal function. Creatinine assays are conducted for diagnostic purposes and for therapeutic monitoring of acute and chronic renal diseases. Urea is a most widely used test for evaluation of renal function. As shown in Figure IV.42 B, the urea levels in Ad RS 44 injected mice were four fold higher than in controls. No significant difference was observed in the levels of creatinine (Figure IV.40 A).
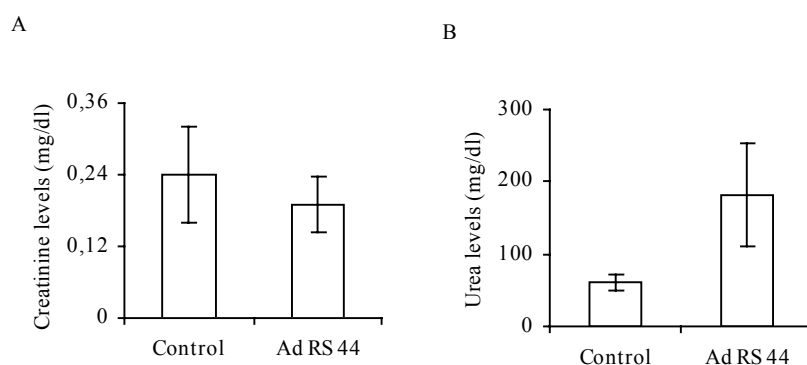
Figure IV.40: Serum levels of creatinine (A) and urea (B) in Ad RS 44 injected mice with ascites and control mice. The levels of urea and creatinine were determined in the serum collected at the end of the fifth week after vector administration.

IV.5.5 Ad RS 44 injected mice exhibit glomerular nephritis

Kidney micrographs were taken from control and from Ad RS 44 administered mice. Glomerular sclerosis was evident in mice injected with Ad RS 44 (Figure IV.41B) but not in control mice (Figure IV.41A). This indicated that the ascites likely was caused by the damage of the kidney.
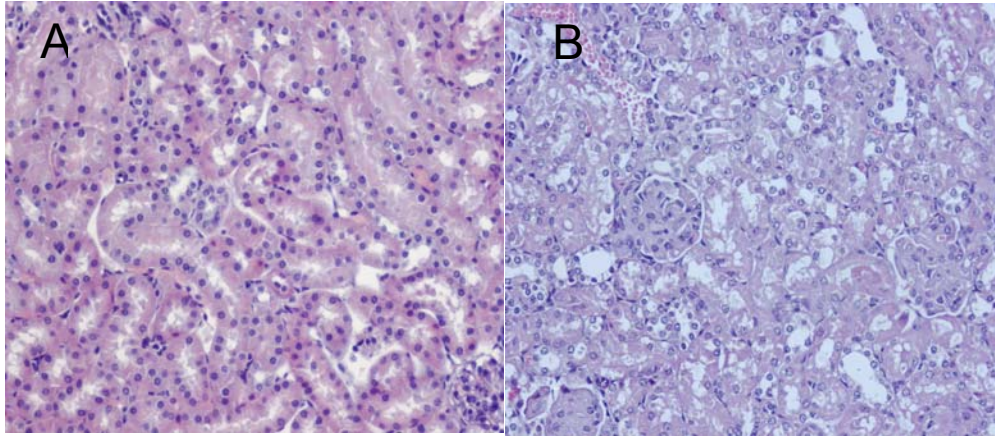
Figure IV.41: H&E stain of kidney section from Ad RS44 injected mice with ascites (B) and control mice (A). Kupffer cell depleted C57BL/6J mice (n=3) were injected with Ad RS 44 at a dose of 1.5×10^9 i.u. H&E stains of kidney section were performed from mice at the end of the fifth week from each group. A shows the kidney micrograph of a control and B shows the kidney micrograph of an Ad RS 44 injected mouse with ascites. H&E staining was performed by Dr. Matilda Bustos.

IV.6 Anti-tumor efficacy of HC-Ad vectors in subcutaneous LLC model

HC-Ad vectors Ad RS 23, Ad RS 44 and Ad RS 45 were tested for anti-tumor efficacy in the subcutaneous Lewis Lung Carcinoma (LLC) model in syngenic C57BL/6J mice. The experiment was performed as described in Chapter III.7.4.

IV.6.1 Constitutive sflt1 expression transiently inhibits LLC tumor progression

Ad RS 44 constitutively expresses sflt1 from the EF1-α promoter. To determine its anti-tumor effect Kupffer cell depleted C57BL/6J mice (n=5) were injected with $1.5x10^9$ i.u of Ad RS 44 (Chapter III.7.3). Kupffer cell depleted control mice were injected with saline (Chapter III.7.3). One week after vector injection (Day=0), the mice were subcutaneously injected with $1x10^6$ LLC cells. The sizes of the tumors were measured at weekly intervals.

Tumor growth in control and Ad RS 44 injected mice is shown in Figure IV.42. Initial sizes of tumors in vector-injected and in control mice were comparable. During the first week the differences in the sizes of the tumors between the controls and Ad RS 44 injected mice, were statistically not significant (two-tailed P value is 0.0556, Mann-Whitney test). At the third week after injection of the LLC cells, there was a decrease in tumor sizes in Ad RS 44 injected mice, when compared to the control mice. This decrease in the tumor sizes was statistically significant (two-tailed P value is 0.0079, Mann-Whitney test). Four weeks after the injection of the cells, 4/5 of the control mice were dead or moribund. At week four (corresponding to week five after administration of the vector) mice injected with Ad RS 44 were moribund and had ascites. All mice with ascites died within two days. Tumor growth in individual mice of control and Ad RS 44 injected groups is depicted in Figure IV.43.

Figure IV.42: Transient suppression of LLC tumor growth in mice injected with Ad RS 44. Kupffer cell depleted C57BL/6J mice were injected with saline or vector Ad RS 44 at a dose of $1.5x10^9$ i.u. One week later, subcutaneous tumors of LLC were established by implantation of $1x10^6$ LLC cells. Tumor sizes were measured at weekly intervals after cell implantation. The figure displays the growth of tumor in Ad RS 44 (n=5) and saline (n=5) injected mice.

Figure IV.43: LLC tumor growth in individual mice injected with saline (A) or Ad RS 44 (B). Kupffer cell depleted mice were injected with Ad RS 44 at a dose of 1.5×10^9 i.u. One week later, subcutaneous tumors of LLC were established by implantation of 1×10^6 LLC cells. Tumor sizes were measured at weekly intervals after implantation of tumors.

The levels of sflt1 protein were measured at weekly intervals after vector injection (Figure IV.44). The levels of sflt1 protein were below 200 ng/ml during the first week and between 200-700 ng/ml during the second and third week. sflt1 levels decreased thereafter in the third and fourth week and were 50-300 ng/ml. The levels of sflt1 in control mice were below the detection limit (not shown). This experiment demonstrated that the tumor growth in Ad RS 44 injected mice was reduced until the third week. Taken together, these experiments indicated that injection of Ad RS 44 resulted in significantly increased sflt1 levels and in an inhibition of the LLC tumor growth rate. Surprisingly, it was also found that all Ad RS 44 injected mice experienced ascites at four weeks after tumor injection (corresponding to week five after administration of the vector) and died within 2 days thereafter.

Figure IV.44: Serum levels of sflt1 in mice injected with 1.5×10^9 i.u of Ad RS 44, during LLC tumor growth. Kupffer cell depleted mice were injected with Ad RS 44. One week later, subcutaneous tumors were established by implantation of 1×10^6 LLC cells. Serum was collected at weekly intervals and levels of sflt1 were determined by ELISA.

IV.6.2 Inducible sflt1 expression transiently inhibits LLC tumor progression

Ad RS 23 expresses sflt1 upon induction by RU 486 in a liver specific manner. To determine its anti-tumor effects, Kupffer cell depleted C57BL/6J mice (n=5) were injected with $2x10^9$ i.u of Ad RS 23. Similarly, Kupffer cell depleted control mice were injected with saline. One week after vector injection the mice were subcutaneously injected with $1x10^6$ LLC cells (Day=0). One-week later RU 486 induction was initiated by daily injections and tumor sizes were determined at weekly intervals (Figure IV.45). The differences in tumor sizes at 1 week between control and Ad RS 23 injected mice were statistically not significant (two-tailed P value is 0.5206, Mann-Whitney test). The sizes of the tumors were measured subsequently for four weeks. At the third week, tumor volume was lower in Ad RS 23 injected mice compared to control mice (difference statistically significant, p= 0.0159, Mann-Whitney test). At the fourth week, 4/5 of the control mice were dead in contrast to RS 23 injected mice in which 2/5 mice had died. At the end of the fifth week, most of the RS 23 injected mice were moribund and were sacrificed. The tumor growth in individual mice in the Ad RS 23 injected and control groups is shown in Fig IV.46.
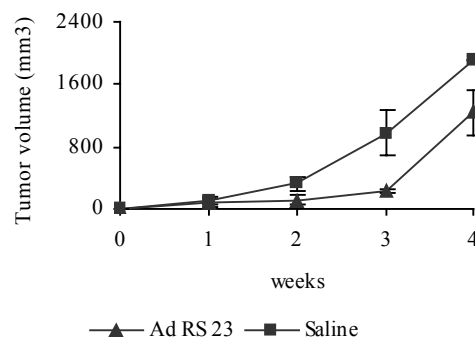
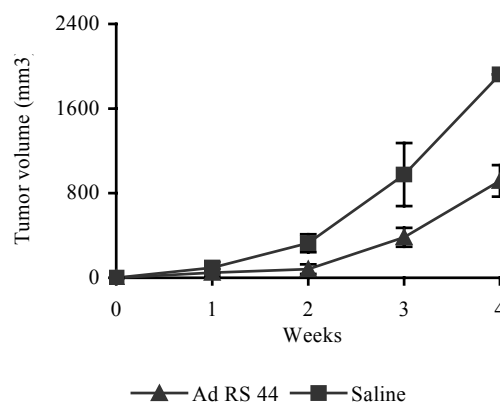**Figure IV.45:** Transient suppression of LLC tumor growth in mice injected with Ad 23. Kupffer cells depleted mice were injected with saline (n=5) or Ad RS 23 (n=4) at a dose of $2x10^9$. One-week later, subcutaneous tumors of LLC were established in syngenic C57BL/6 mice by implantation of LLC cells ($1x10^6$). One week after tumor implantation the vector Ad RS 23 injected mice were induced daily with RU 486 (250 µg/kg of mice) for four weeks to inducibly express sflt1. The figure displays the progress of tumor growth in saline or Ad RS 23 administered mice.
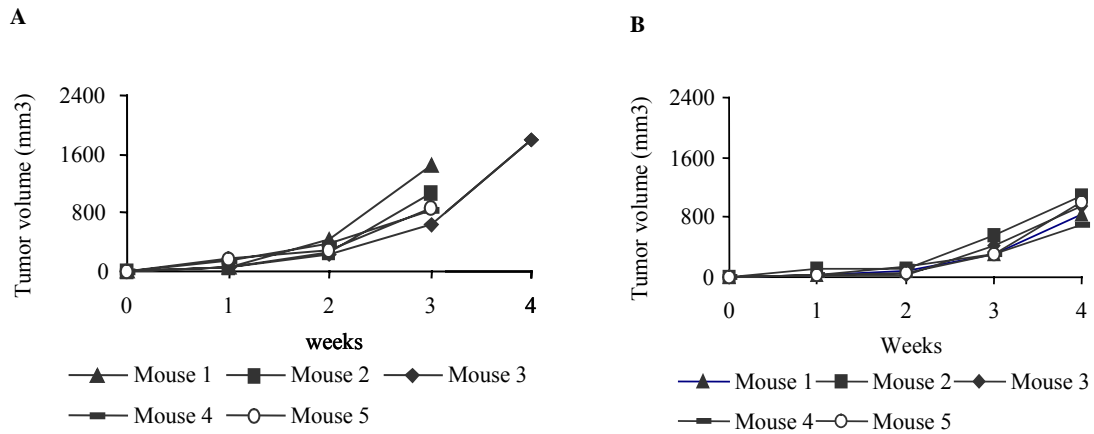
85

Figure IV.46: LLC tumor growth of individual mice injected with saline or with Ad RS 23. Kupffer cell depleted mice were injected with saline or $2x10^9$ i.u. of Ad RS 23. One week later (day=0), subcutaneous tumors of LLC were established in syngenic C57BL/6 mice by implantation of $1x10^6$ LLC cells. One week after tumor implantation, Ad RS 23 injected mice were induced daily with RU 486 (250 µg/kg of mice) for four weeks to induce sflt1 expression. Figures A and B display tumor growth in saline (n=5) or Ad RS 23 (n=4) administered mice respectively. Note that the Figure IV.46 A is also shown in Figure IV.43 A.

The levels of serum sflt1 protein were determined at weekly intervals after Ad RS 23 injection. As shown in Figure IV.47, the levels of sflt1 were between 2000-14000 ng/ml in the first three weeks. In the last week, the levels of sflt1 were below 2000 ng/ml. sflt1 levels in control mice were below the detection limit at all times (not shown).

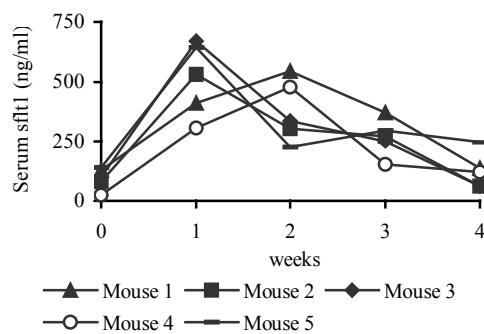**Figure IV.47:** Serum levels of sflt1 in mice injected with Ad RS 23 during LLC tumor growth. Kupffer cell depleted mice were injected with Ad RS 23 at a dose of $2x10^9$.i.u. One-week later, subcutaneous tumors of LLC were established by implantation of $1x10^6$ LLC cells. One week after tumor implantation the Ad RS 23 injected mice received daily injections of RU 486 (250 µg/kg of mice) for four weeks to induce expression of sflt1.
Serum was collected from mice at weekly intervals and the levels of sflt1 were determined using ELISA. The figure displays levels of sflt1 expressed during LLC tumor growth in individual mice injected with Ad RS 23.

IV.6.3 Constitutive stie2 expression does not inhibit LLC tumor growth

Ad RS 45 constitutively expresses stie2 from MCMV promoter (Chapter IV.3). To determine anti-tumor activity of this vector, Kupffer cell depleted C57BL/6J mice (n=5) were injected with $2x10^9$ i.u. of Ad RS 45. Similarly, Kupffer cell depleted control mice were injected with saline. One week after vector injection (Day = 0), the mice were injected with $1x10^6$ LLC cells subcutaneously.
Tumor growth in control and in Ad RS 45 injected mice is shown in Figure IV.48. After one week, there were no differences in tumor sizes between controls and vector treated mice (two tailed P value is 0.9999, Mann-Whitney test). The sizes of the tumors were measured subsequently at weekly intervals. Ad RS 45 mice when compared to the controls did not exhibit any statistically significant difference in tumor volume during the experimental period. During the fourth week, 1/5 of control mice in contrast to 4/5 of Ad RS 45 injected mice were alive. At the end of the fourth week all surviving control and vector-injected mice were moribund and were sacrificed. The results in the individual animals are shown in Figure IV.49. Serum levels of stie2 were determined by ELISA at weekly intervals and were found to be 30-450 ng/ml during the experimental period (Figure IV.50). This experiment demonstrated that constitutive expression of stie2 at significant levels did not result in a statistically significant inhibition of tumor growth in the subcutaneous LLC tumor model.
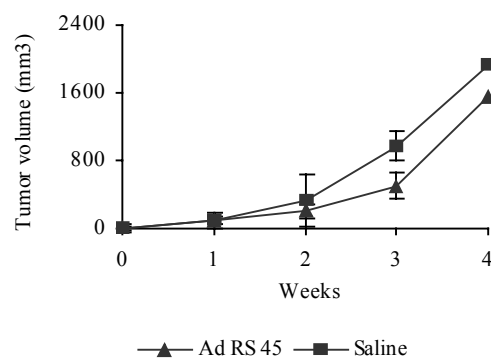
Figure IV.48: Absence of LLC tumor growth inhibition upon injection of Ad RS 45**.** Kupffer cell depleted mice were injected with saline or vector Ad RS 45 at a dose of $2x10^9$ i.u. (n=5 for each group). One week later, subcutaneous tumors of LLC were established by implantation of LLC cells ($1x10^6$). Tumor sizes were measured at weekly intervals after implantation of tumors.
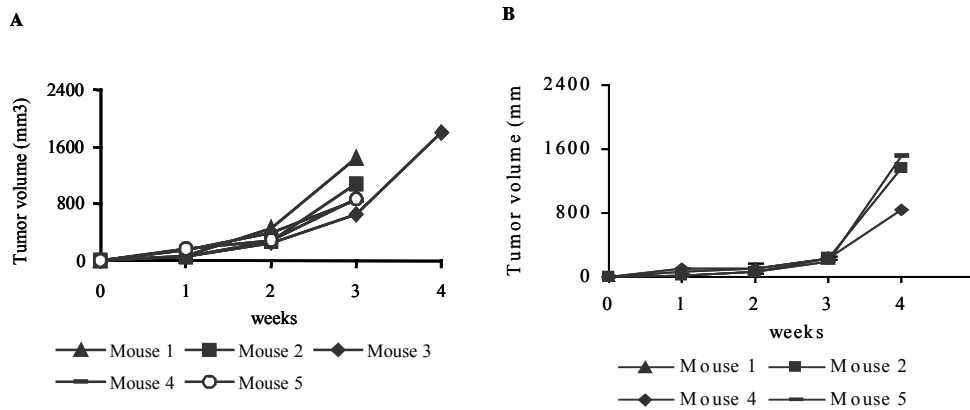
Figure IV.49: LLC tumor growth in individual mice injected with saline (A) or Ad RS 45 (B). Kupffer cell depleted mice were injected with saline or vector Ad RS 45 at a dose of $2x10^9$ i.u. (n=5 for each group). Subcutaneous tumors of LLC were established by implantation of $1x10^6$ LLC cells. Tumor sizes were determined at weekly intervals. Note that the Figure IV.49 A is also shown in Figure IV.43 A.
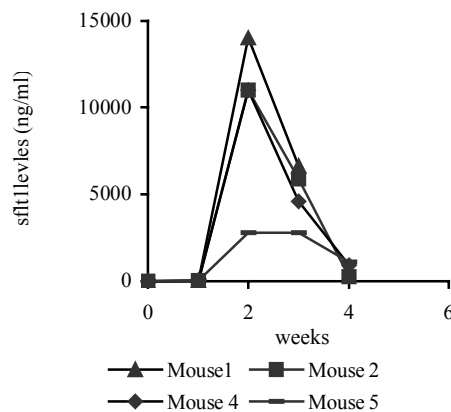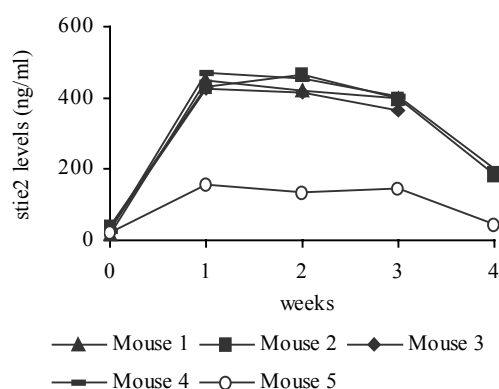

Figure IV.50: Serum levels of stie2 in mice injected with Ad RS 45 during LLC tumor growth. Kupffer cell depleted mice were injected with Ad RS 45 at a dose of $2x10^9$ i.u. One week later, subcutaneous tumors of LLC were established by implantation of $1x10^6$ LLC cells. Serum was collected at weekly intervals and the levels of stie2 were determined using ELISA.

IV.6.4 Inducible expression of mIL-12 transiently suppresses LLC tumor growth

Ad RS 25 expresses mIL-12 upon induction with RU 486 in a liver specific manner (Chapter IV.2). To investigate the anti-tumor effect of mIL-12 in the LLC tumor model, Kupffer cell depleted C57BL/6J mice (n=5) were injected with Ad RS 25 at a dose of 5×10^8 i.u (Chapter III.7.3). Kupffer cell depleted control mice were injected with saline. One week after injection, 1×10^6 LLC cells were injected subcutaneously. One week after injection of the LLC cells, when a palpable tumor had developed, mice were then induced with RU 486 at a dose of 250 µg/kg every 24 hours for a week, during the first and the third week. The injection of RU 486 was discontinued in the second and fourth week to prevent morbidity due to mIL-12 mediated toxicity.

As shown in Figure IV. 51 A, tumor sizes in control and Ad RS 25 injected mice at one week after injection of the cells were similar (two-tailed P value is 0.1508, considered not significant). At the third and fourth week after injection of the cells, the tumors in saline and Ad RS 25 injected mice had grown to different sizes that were statistically significant (two-tailed p value was 0.0079 and 0.0159 for the third and fourth week respectively). At week four, 4/5 of the control mice were dead in contrast to Ad RS 25 injected mice in which all of the mice were still alive. However, Ad RS 25 injected mice were moribund at the end of the fifth week and were sacrificed. LLC tumor growth in individual mice present in the control and the Ad RS 45 group is shown in Figure IV. 52 A.
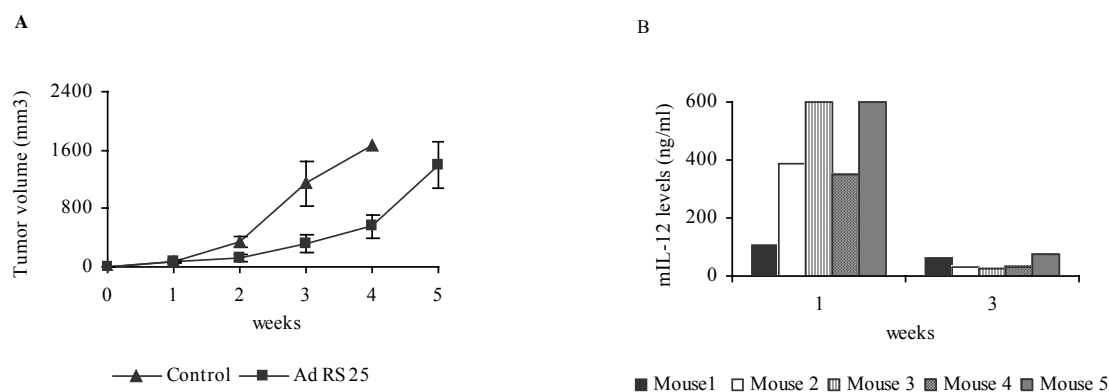
Figure IV.51: Transient LLC tumor suppression upon inducible expression of mIL-12 in vivo. Kupffer cell depleted mice were injected with saline or vector Ad RS 25 at a dose of 5×10^8 i.u. One-week later, subcutaneous tumors of LLC were established by implantation of (1×10^6) LLC cells. Figure A displays LLC tumor progression in mice (n=5 for each group) injected with vector Ad RS 25 or saline (control mice). Figure B displays serum mIL-12 levels in Ad RS 25 injected mice in the first and third week after tumor implantation.

Serum levels of mIL-12, determined during the first and the third week after injection of the tumor cells, were between 100-600 ng/ml in the (first week) of induction and below 60 ng/ml (third week) of induction (Figure IV.51 B). This experiment indicated that reduction in tumor volume was observed in the presence of mIL-12. The levels of mIL-12 dropped during the third week of induction.
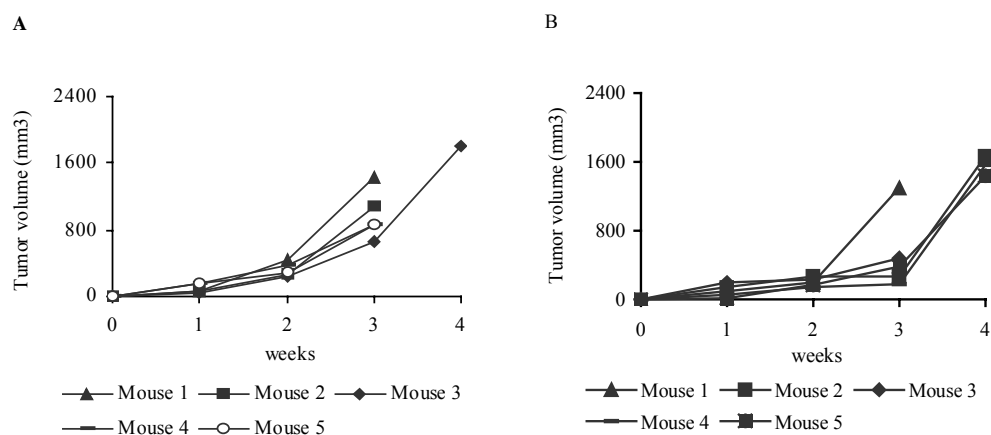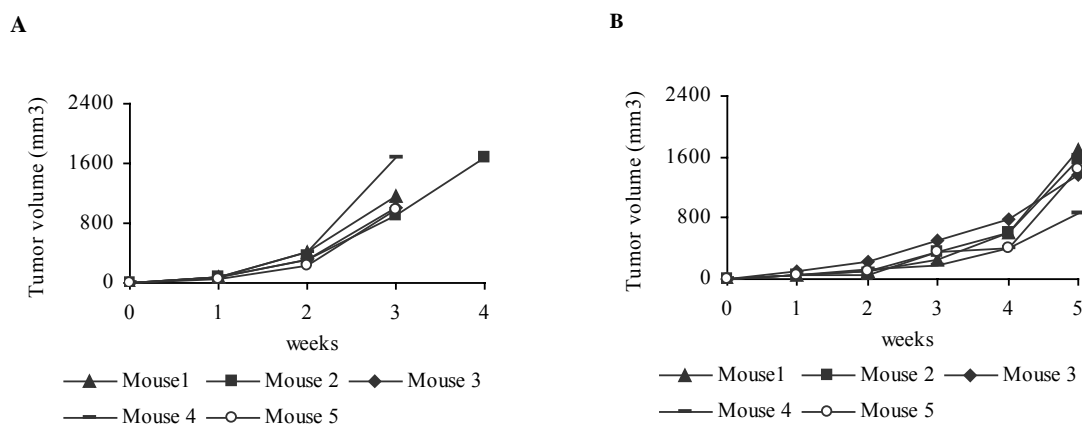
Figure IV.52: LLC tumor growth in individual mice (n=5 for each group) injected with saline (A) or Ad RS 25 (B). Kupffer cell depleted mice were injected with saline or with Ad RS 25 at a dose of 5×10^8 i.u. One week later, subcutaneous tumors of LLC were established by implantation of 1×10^6 LLC cells. The mice were induced with RU 486 during the first and third week to express mIL-12. Note that the figure IV.52 A is also shown in figure IV.54 A.

IV.6.5 Concomitant sflt1 and stie2 expression transiently suppress LLC tumor growth

As shown earlier, expression of sflt1 and stie2 from the different HC-Ad vectors when injected individually had either no (Ad RS 45) or only a transient though statistically significant inhibitory effect on tumor growth and survival in the heterotopic LLC tumor model. Furthermore, ascites and death was observed with the use of Ad RS 44. Since sflt1 and stie2 target different vascular development pathways (endothelial cell proliferation and maturation of blood vessels respectively) we reasoned that combined expression of sflt1 and stie2 might result in a more pronounced effect. Therefore 1.5×10^9 i.u. of Ad RS 23 expressing sflt1 in a liver specific and regulable manner and 2×10^9 i.u. of Ad RS 45 expressing stie2 constitutively were coinjected into Kupffer cell depleted C57BL/6J mice followed by subcutaneous injection of 1×10^6 LLC cells. One week after injection of the LLC cells tumors were palpable. At this time RU 486 induction was initiated.

As shown in Figure IV.53, one week after LLC cell injection, there were no differences in the tumor sizes in control and vector-injected mice (two-tailed P value is 0.0952, Mann-Whitney test). At the third week post LLC cell injection, differences in tumor sizes in control and vector-injected mice were statistically significant (two-tailed P value is 0.0079, Mann-Whitney test). Tumor growth in individual mice of vector and control groups is shown in Figure IV.54.

Serum levels of sflt1 were measured once per week during the experiment (Figure IV.55 B). The levels of sflt1 during the first week of RU 486 administration were between 200 and 1400 ng/ml (Figure IV.55 B). The levels dropped to below 600 ng /ml in the third week of induction. The levels of stie2 were between 30 and 50 ng/ml during the first week (Fig IV.55 A). The levels of stie2 increased to 150-350 ng /ml during the rest of the experimental period. The administration of RU 486 was discontinued after the third week, because the mice developed ascites. Upon withdrawal of RU 486, mice with ascites lost their ascites. However, due to tumor burden mice with both Ad RS 23 and Ad RS 45 became moribund and were sacrificed.

A
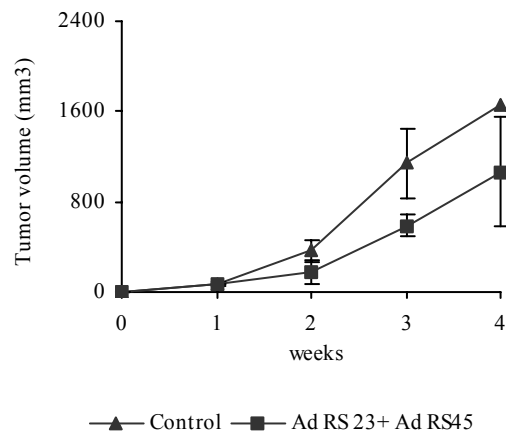
Figure IV.53: Comparison of anti-tumor efficacy in mice (n=5 for each group) injected with saline or with a combination of Ad RS 23 and Ad RS 45. Kupffer cell depleted mice were injected with saline or a combination of Ad RS 23 and Ad RS 45 at a dose of 1.5×10^9 i.u and 2×10^9 i.u. respectively. One week later, subcutaneous tumors were established by implantation of 1×10^6 LLC cells (week=0). At week 1, when tumors were palpable, mice were daily injected with RU 486 (250 µg/kg body weight).
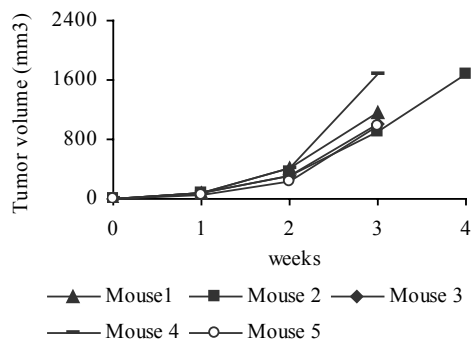
A   **B**

Figure IV.54: Comparison of LLC tumor growth in individual mice (n=5 for each group) injected with saline or with a combination of Ad RS 23 and Ad RS 45. Kupffer cell depleted mice were injected with saline or a combination of vectors Ad RS 23 and Ad RS 45 at doses of 1.5×10^9 i.u. and 2×10^9 i.u. respectively. One week later, subcutaneous tumors were established by implantation of 1×10^6 LLC cells. At week 1, when tumors were palpable, mice were daily injected with RU 486 (250µg/kg body weight). Figure A displays LLC tumor growth in individual mice injected with saline. Figure B displays LLC tumor in mice injected with a combination of Ad RS 23 and Ad RS 45. Note that the figure IV.54 A is also shown in figure IV.52 A.
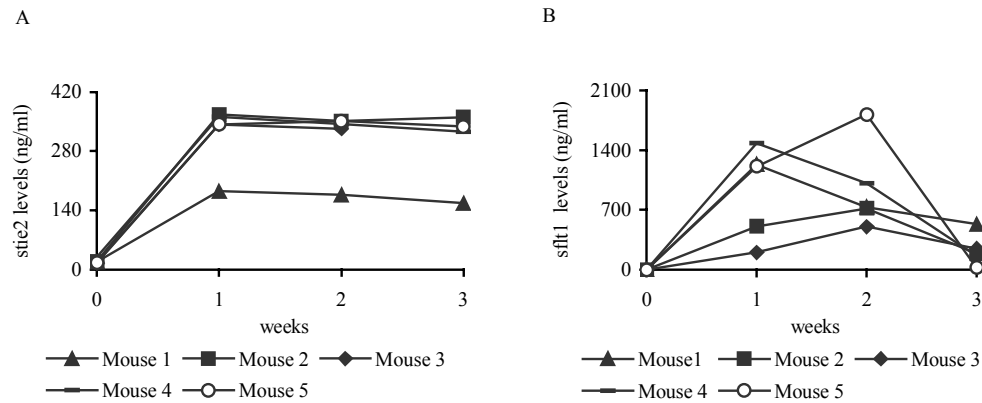
Figure IV.55: Levels of tie2 and sflt1 in mice injected concomitantly with Ad RS 23 and Ad RS 45. Kupffer cell depleted mice were injected with saline (n=5) or a combination of Ad RS 23 and Ad RS 45 (n=5) at doses of $1.5x10^9$ i.u. and $2x10^9$ i.u. respectively. One week later, subcutaneous tumors of LLC were established. Serum was collected at weekly intervals and the levels of sflt1 and stie2 were determined by ELISA.

IV.6.6 Concomitant sflt1 and mIL-12 expression transiently suppress LLC tumor growth

sflt1 and mIL-12 have been shown to have anti-tumor properties in different murine models of cancer. To investigate the combined anticancer effect of sflt1 and mIL-12, Kupffer cell depleted C57BL/6J mice (n=5) were injected with Ad RS 25 and Ad RS 23. Kupffer cell depleted control mice were injected with saline. Ad RS 23 and Ad RS 25 were injected at a dose of $2x10^9$ i.u and $5x10^8$ i.u. respectively. One week after vector injection, the mice received a subcutaneous implantation of $1x10^6$ LLC cells. Initial tumor sizes were measured one week after the injection of the cells. There were no statistically significant differences in the initial sizes of the tumors between the controls and vector-injected mice (the two tailed P value is 0.0556, Man- Whitney test). The tumor growth was followed by weekly measurements. RU 486 induction was initiated at week one and three. Induction was discontinued during the second and the fourth week.

Tumor growth in mice injected both Ad RS 23 and Ad RS 25 is shown in Figure IV.56. At the third week after injection of the LLC cells, the difference in the tumor volume between control and vector injected mice was statistically significant (two-tailed P value is 0.0079, Mann-Whitney test). The mice were further observed for survival time. As shown in Figure IV.57 B, from the vector-injected animals 3/5 survived until six weeks and 1/5 mice survived until eight weeks. In contrast, none of the control mice survived beyond four weeks (Figure IV.57 A). Thus the combined injection of vectors expressing sflt1 and mIL-12 demonstrated an increase in survival time and decreased tumor growth in comparison to mice injected with either of the vector alone. The antitumor effect could have been due either to the combined presence of sflt1 and IL-12 or due to the presence of high levels of mIL-12. The levels of mIL-12 were 2-6 fold higher in this experiment when compared to the mIL-12 levels in which Ad RS 25 was injected alone (Figure IV.51). The levels of mIL-12 and sflt1 expression were assayed during the first and third week of RU 486 induction. As shown in Figure IV.58 A, levels of mIL-12 were between 2500 and 3000 ng/ml, during the first week of induction and between 100 and 1500 in the third week. As shown in Figure IV.58 B, sflt1 levels were in the range of 30 and 120 ng/ml during the first and third week of induction.
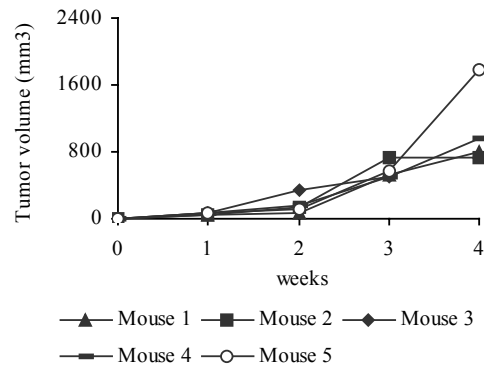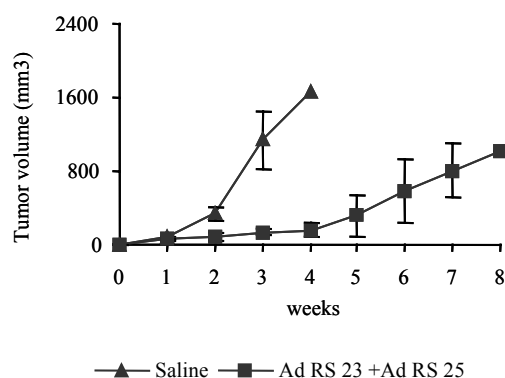
Figure IV.56: Comparison of LLC tumor growth between mice (n=5 for each group) injected with saline or combined with Ad RS 23 and Ad RS 25. Kupffer cell depleted mice were injected with saline or with Ad RS 25 and Ad RS 23 at a dose of $5x10^8$ and $2x10^9$ i.u. respectively. One week later, subcutaneous tumors of LLC were established by implantation of $1x10^6$ LLC cells. RU 486 induction (250 µg/kg) was performed by daily injections during the first and third week.
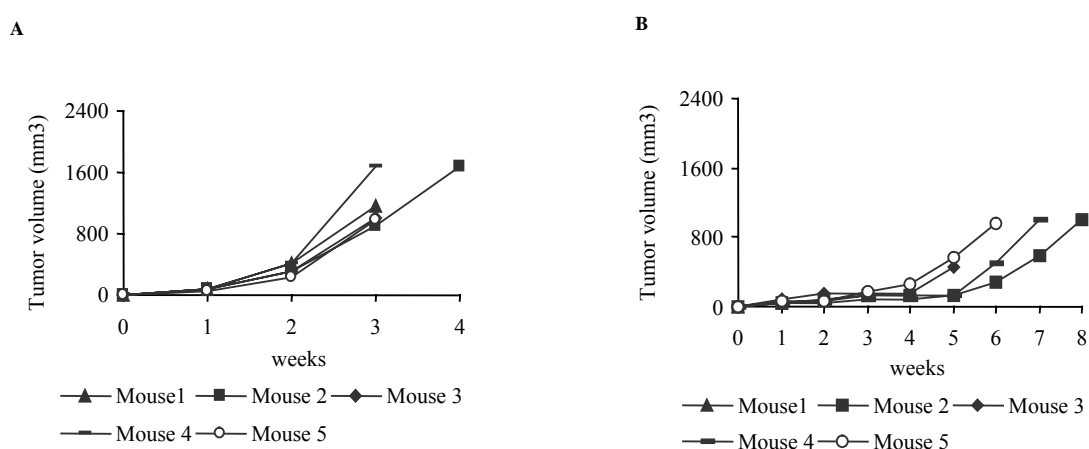
Figure IV.57: Comparison of LLC tumor growth in individual mice injected with saline (A) or combined with Ad RS 23 and Ad RS 25 (B). Kupffer cell depleted mice were injected with saline or with Ad RS 25 and Ad RS 23 at $5x10^8$ i.u. and $2x10^9$ i.u respectively. One week later, subcutaneous tumors were established by implantation of $1x10^6$ LLC cells. Tumor sizes were measured at weekly intervals. RU 486 induction (250 µg/kg) was performed by daily injections during the first and third week. Note that the figure IV.57 A is also shown in figure IV.52 A.
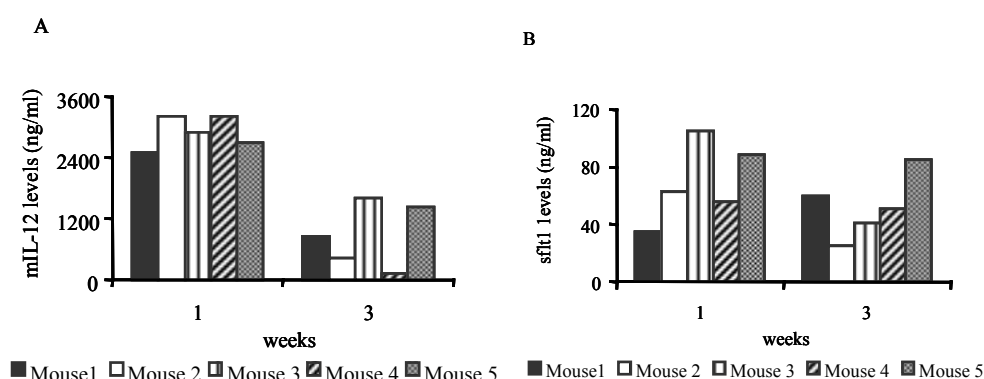

Figure IV.58: Serum levels of mIL-12 (A) and sflt1 (B) in mice injected with Ad RS 23 and Ad RS 25. Kupffer cell depleted mice were injected with saline or combined with Ad RS 25 and Ad RS 23 at a dose of $5x10^8$ and $2x10^9$ i.u. respectively. One week later, subcutaneous tumors were established by implantation of $1x10^6$ LLC cells. RU 486 induction (250 µg/kg) was performed by daily injections during the first and third week.

IV.7 Anti-tumor effects by HC-Ad-mediated expression of sflt1 and mIL-12 in the orthotopic MC-38 tumor model

While in the experiments described above, effects of HC-Ad vectors were tested in a subcutaneous tumor model, a further model was chosen that more closely mimics the clinical situation. The orthotopic MC-38 tumor model is based on the local inoculation of MC-38 colon carcinoma cells into the liver. Tumor growth is very aggressive and recipient mice become moribund within 3-4 weeks from the date of injection. The MC-38 colon carcinoma model was performed as described in chapter III.7.5.

IV.7.1 Inducible or constitutive sflt1 expression does not inhibit MC-38 tumor growth.

Ad RS 23 expresses sflt1 upon induction with RU 486 in a liver specific manner. Ad RS 44 expresses sflt1 under the control of ubiquitously active EF-1α promoter. Liver tumors were established by intrahepatic implantation of MC-38 cells. One week before tumor cell, inoculation, Kupffer cell depleted C57BL/6J mice were injected with Ad RS 23 (n=4) and Ad RS 44 (n=4) at doses of $2x10^9$ i.u. and $1.5x10^9$ i.u. respectively (Chapter III.7.3). Control mice (n=4) were injected with saline. Initial tumor sizes were determined by laparotomy on day 5 post implantation and were found to be about 8 mm^3. Then in the case of Ad RS 23 injected mice, RU 486 induction was initiated by daily injections for 10 days. The tumor size was determined once again on day 20 post implantation. As shown in Figure. IV.59, 2/4 mice injected with vector Ad RS 23 had tumor size less than 500 mm^3. In the case of mice injected with the vector Ad RS 44, 1/4 mice had tumor volumes less than 500 mm^3. All of the control mice had tumor volumes more than 1000 mm^3. In summary, injection of neither Ad RS 23 nor Ad RS 44 resulted in the suppression of MC-38 tumor growth.
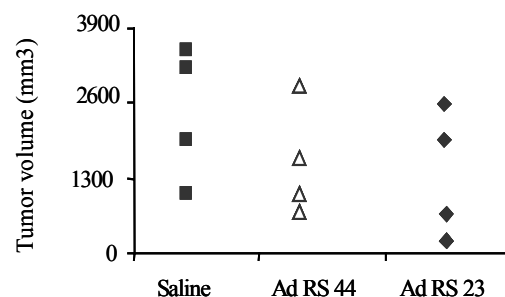
Figure IV.59: MC-38 tumor growth in mice injected with Ad RS 23 or Ad RS 44. Kupffer cell depleted mice were injected with saline, Ad RS 23 or Ad RS 44 at a dose of $2x10^9$ or $1.5x10^9$ i.u. respectively. One week later, liver tumors were established by intrahepatic implantation of 10^6 MC-38 cells. Initial tumor sizes were measured 5 days after tumor implantation. Five days after tumor implantation, in the case of Ad RS 23 injected mice, RU 486 induction was initiated. The mice were analyzed again for tumor growth on day 20 after tumor implantation.

The levels of sflt1 observed in Ad RS 23 and Ad RS 44 injected mice on day 14 after vector injection is shown in Figure IV.60. Ad RS 23 injected mice had levels of 12,000-14,000 ng/ml and Ad RS 44 injected mice had between 900 and 2000 ng/ml. The mice were observed for long-term survival. As shown in Figure IV.61, none of the controls and of mice injected with Ad RS 44 survived beyond 35 days. Although not statistically significant, 1/4 of Ad RS 23 injected mice survived until day 44. In summary there were no significant differences in survival time between the different groups.
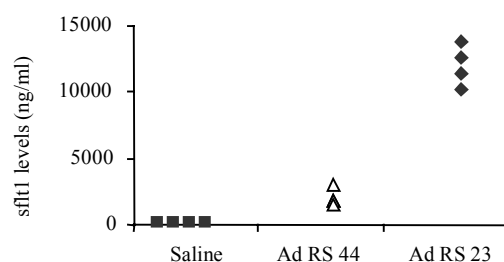
Figure IV.60: Levels of sflt1 during MC-38 tumor growth in mice injected with Ad RS 44 or Ad RS 23 (with RU 486 induction). sflt1 levels were determined on day 14 after vector injection.
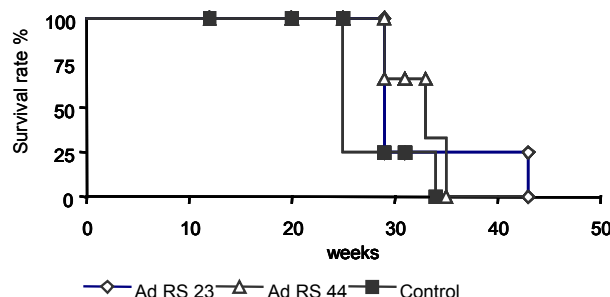
Figure IV.61: Survival rate of mice described in Figures IV.60 and IV.61 injected with Ad RS 23 or Ad RS 44 in the MC-38 orthotopic cancer model.

IV.7.2 Inducible mIL-12 expression inhibits MC-38 tumor growth

Ad RS 25 was designed to express mIL-12 upon induction with RU 486 in a liver specific manner. Ad RS 25 showed anti-tumor activity in the subcutaneous LLC model, which however was not persistent. To investigate the effect of mIL-12 on MC-38 tumor growth, mice were injected with $1x10^8$ i.u. (n=4) or with $5x10^8$ i.u. (n=11) of Ad RS 25. The control mice (n=8) were injected with saline. One week post vector injection, liver tumors were established by intrahepatic injection of MC 38 cells. Five days after implantation of the cells, tumor sizes were determined by laparotomy and were found to be about 8 mm^3. Mice injected with the vector at a dose of $5x 10^8$ i.u (n=7) were induced with RU 486 for 10 days. Control mice (n=3) injected with Ad RS 25 at a dose of $5x 10^8$ i.u. were not induced with RU 486. Five days after termination of induction, tumor sizes were determined again by laparotomy.

As shown in Figure IV.62, control mice injected with saline showed progressive tumor growth, similar to mice that received $5x10^8$ i.u. but without RU 486 induction. In contrast, mice injected with Ad RS 25 at a dose of $5x10^8$, and induced with RU 486 showed complete tumor regression. Animals injected with Ad RS 25 at a lower dose of $1x10^8$ i.u. followed by induction, showed a reduction of the tumor size, but the tumors eventually progressed and the mice finally died due to massive liver tumors. This experiment clearly demonstrated an inhibitory effect of inducible expression of mIL-12 on liver tumor growth.
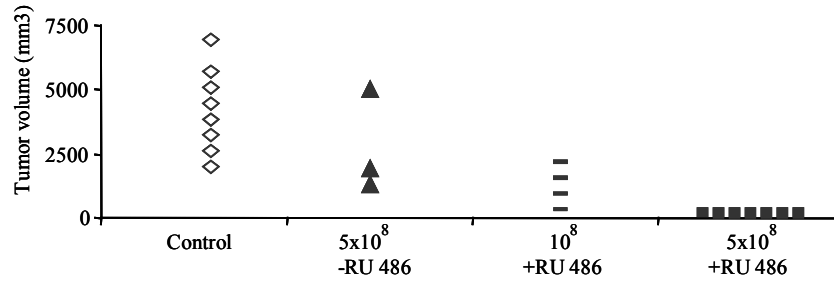
Figure IV.62: MC-38 tumor growth in mice injected with saline or Ad RS 25. Mice were injected with Ad RS 5 at a dose of 10^8 or $5x10^8$ i.u. Control mice were injected with saline. One week post vector injection, liver tumors were established by intrahepatic injection of 10^6 MC-38 cells. The initial tumor sizes were determined at day 5 after implantation. Then, the mice were induced with RU 486 for 10 days. Tumor size was determined again 20 days after implantation.

The figure displays tumor size of control mice (rhombus, n = 8), mice injected with $5x10^8$ i.u. of the vector without RU486 induction (triangles, n = 3), mice injected with 10^8 i.u. of the vector plus RU 486 induction (lines, n = 4), and mice treated with the vector at $5x10^8$ i.u. plus RU 486 induction (squares, n = 7). + or – refers to presence or absence of induction with RU 486.

Representative photographs of liver tumors before and after therapy in two mice that had been injected with Ad RS 25 at a dose of $5x10^8$ i.u. are shown in Figure IV.63. Both the mice represented by Figure IV.63 A and Figure IV.63 B respectively, had MC-38 tumors five days after implantation of MC-38 cells. The animal shown in Figure IV.63 A was not induced with RU 486. This animal showed tumor progression and died 20 days after the end of the induction period. As shown in Figure IV.63 C, the uninduced mice had a tumor mass exceeding 20 mm in diameter, peritoneal dissemination (white asterisk) and lung metastases (black asterisk).

In contrast, the animal shown in Figure IV.63 B had been induced with RU 486 for 10 days. The mouse was tumor free on day 35 and the tumor was completely eradicated as shown in Figure IV.63 D.

This experiment demonstrated that inducible expression of mIL-12 resulted in complete tumor regression.
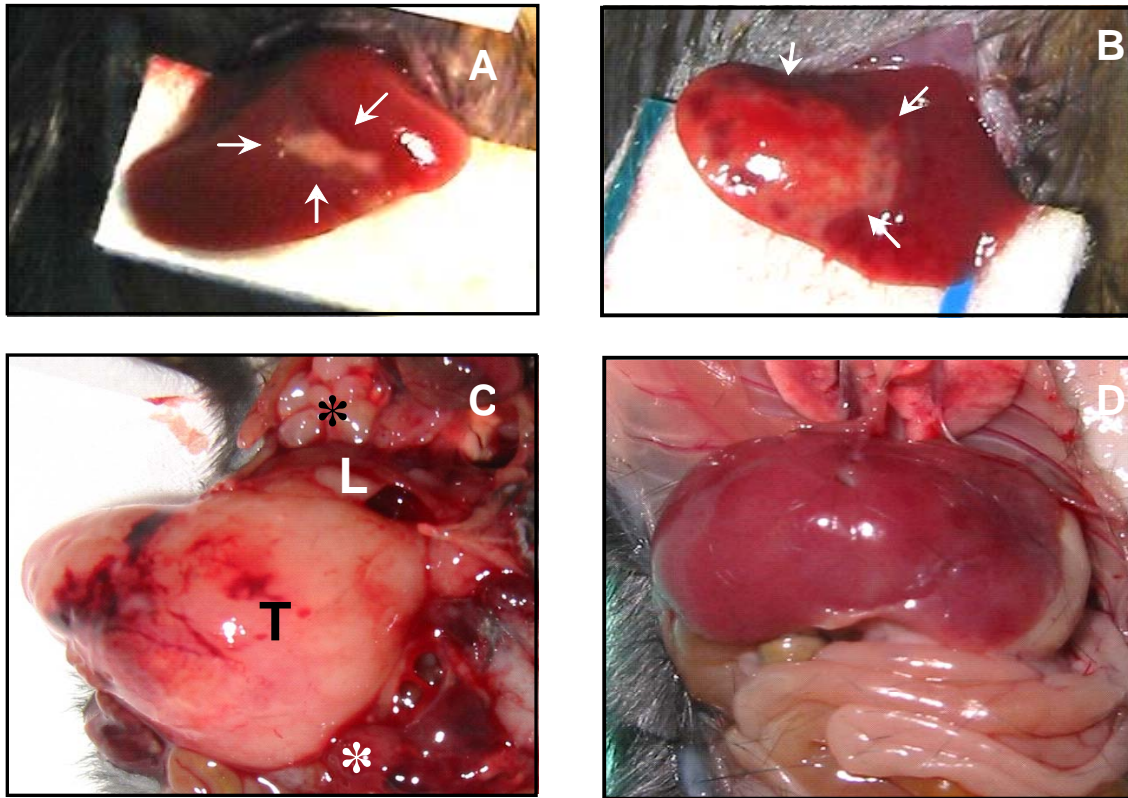
Figure IV.63: Photographs of representative tumors in mice treated with Ad RS 25. Ad RS 25 (5×10^8 i.u. per mice) was injected intravenously. One week later, liver tumors were established by intrahepatic injection of 10^6 MC-38 cells. A and B corresponds to livers of 2 mice 5 days after cell implantation. The margins of the tumor mass are indicated with white arrows. From this moment, the mouse shown in A was left untreated, and the one in B received daily intraperitoneal injections of RU 486 (250 µg/kg) for a total of 10 days. C shows tumor progression in the untreated animal that died 20 days after end of induction period showing a massive tumor (indicated as T) that occupied most of the liver (indicated as L), peritoneal dissemination (white asterisk), and lung metastases (black asterisk). D shows tumor eradication in the mouse treated with the vector plus RU 486.

Long-term disease free survival is a clear indicator of the effectiveness of a therapy. The survival rate of animals used in the above experiment is shown in Figure IV.64. Both the control and the uninduced mice did not survive beyond the 35th day. Mice injected with of 1×10^8 i.u. and induced with RU 486 survived longer when compared to control mice, but eventually succumbed. Mice injected with Ad RS 25 at a dose of 5×10^8 i.u. and induced with RU 486 survived longer than the control or uninduced mice. 90% of the mice that had received 5×10^8 i.u. of RS 25 and RU 486 survived beyond day 53 and were disease free when the experiment was terminated.

97
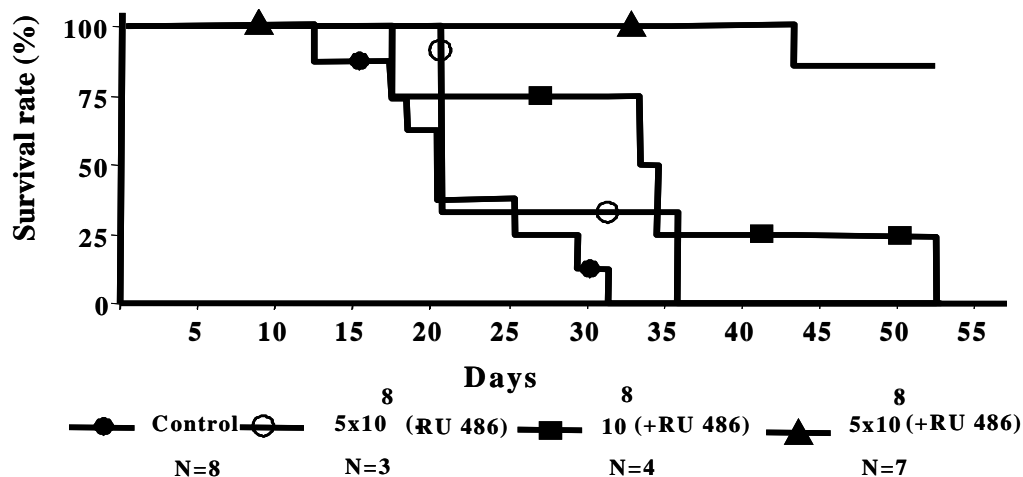
Figure IV.64: Survival rate in the MC-38 tumor model of mice injected with Ad RS 25 with or without RU 486 induction as indicated.

The vector Ad RS 25 expresses mIL-12 upon induction with or without RU 486 induction, as indicated in a liver specific manner. To determine the levels of mIL-12 observed during MC-38 tumor growth, serum was collected 10 hours post induction. As shown in Figure IV.65, control mice and uninduced vector injected mice did not express mIL-12. In contrast, high levels of mIL-12 of up to 8000 ng/ml were found in sera from mouse receiving the high vector dose (5×10^8 i.u.) following induction with RU486. The lowest mIL-12 value obtained with this viral dose, that still showed anti-tumor efficacy, was 170 ng/ml. However, mice injected with the lower vector dose (10^8 i.u.) had serum levels of mIL-12 of around 1–2.5 ng/ml after induction. These data indicated that the efficacy of treatment was related to the level of mIL-12 obtained following induction with RU 486. This experiment showed that the levels of mIL-12 correlate with the tumor free survival of the mouse. The minimal amount of mIL-12 that was therapeutic was above 160 ng/ml. mIL-12 levels in the range of 2.5 ng/ml or less were subtherapeutic.
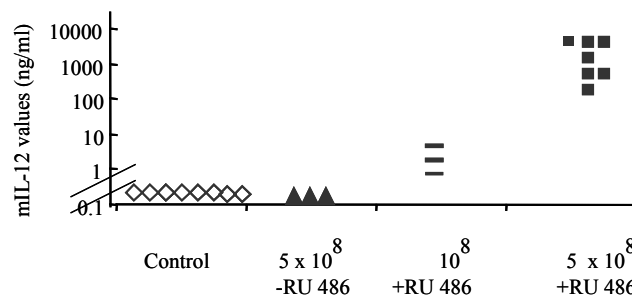
Figure IV.65: Levels of mIL-12 in Ad RS 25 injected mice during tumor growth. Serum mIL-12 levels were determined on day 5 of induction that were subjected to vector injection in the MC-38 tumor model (Figure IV.64).

IV.7.3 Inducible mIL-12 expression causes transient toxicity in the MC-38 tumor model

To test for a potential toxicity due to high local expression of mIL-12, serum ALT levels, an accepted marker for hepatocyte damage, were determined in MC-38 tumor bearing mice. These animals had received 5×10^8 i.u. of Ad RS 25. Part of the animals (n=5) was induced with RU 486 (250µg/kg body weight). Control mice were left uninduced. A further group neither received vector nor RU 486. ALT levels were determined on days 1, 7 and 35.
As shown in Figure IV.66 on days 1 and 7 elevated serum ALT level was only observed in Ad RS 25 animals that had been induced with RU 486 not in the control groups. On day 45 (35 days following cessation of RU 486 induction) ALT levels had normalized in Ad RS 25/RU 486 (+) mice. The control groups did not survive long enough to be tested at the 45-day time point.

Histological examination of liver tissue was performed to determine whether elevated ALT levels were reflected by alterations in liver morphology. As seen in Figure IV.67, neither RU 486 injection alone (A) nor vector injection alone (B) were accompanied by histological abnormalities. However, modest infiltration of inflammatory cells was observed in Ad RS 25 injected animals that had received RU 486 for 4 days (C). Liver pathology had normalized in Ad RS 25/RU 486(+) animals 35 days after termination of RU 486 induction (D).

Together, this data indicates that vector-mediated mIL-12 expression in hepatocytes resulted in a modest/mild inflammation response as evidenced by infiltration of mononuclear cells and increased serum ALT levels. This response was transient upon cessation of mIL-12 expression.
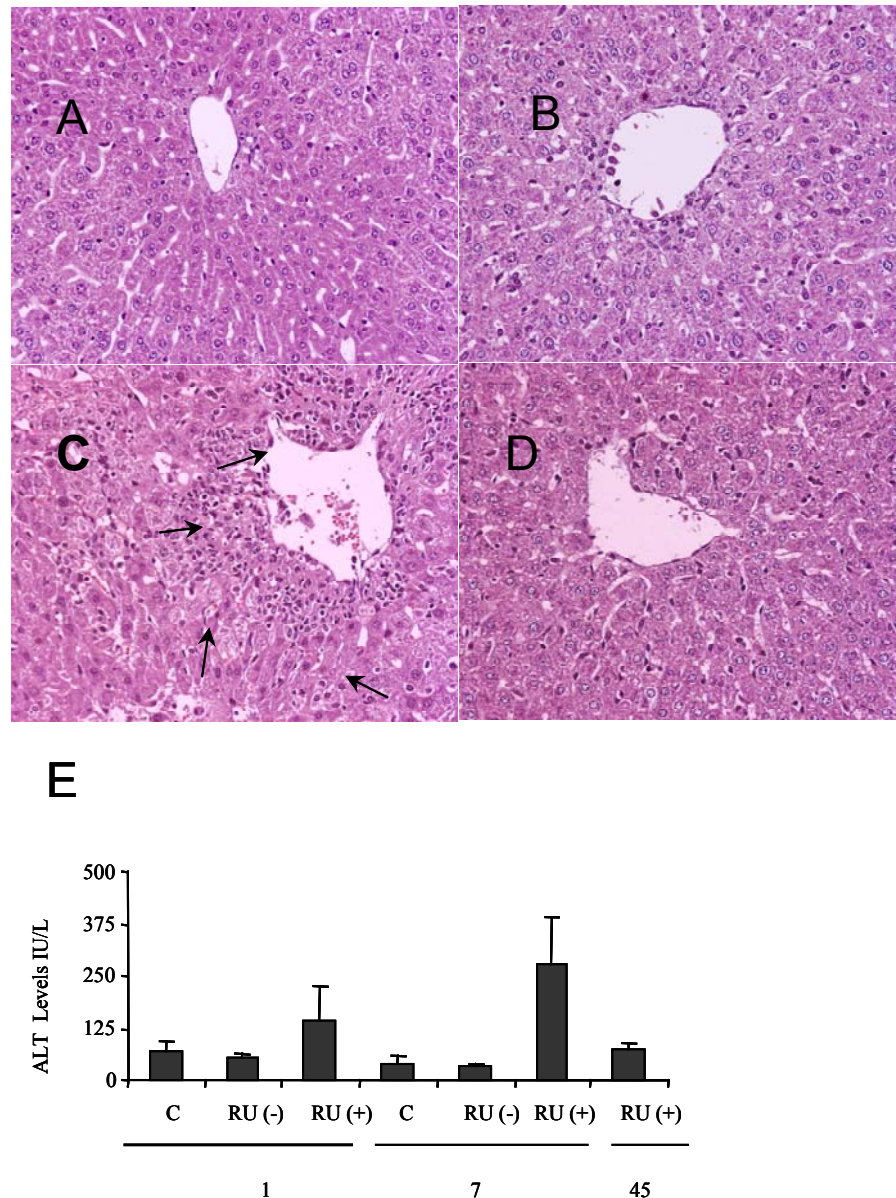
Figure IV.66: Indicators of mIL-12 mediated toxicity in the MC-38 model. Figure A shows a liver micrograph from an animal injected with RU 486 alone for 10 days. Figure B shows a micrograph from a mouse injected with Ad RS 25. Figure C shows a micrograph from an animal injected with Ad RS 25 and induced with RU 486. The arrows show the infiltration of inflammatory cells. Figure D shows a liver a micrograph from an animal 35 days after cessation of induction. Figure E shows the ALT levels on day 1 and 7of mice injected with saline or with Ad RS 25 that either had received (+) or had not received (-) RU 486. The right column in each group corresponds to the animals treated with vector plus RU 486 35 days after the end of induction. H&E staining was performed by Dr. Matilda Bustos.

V Discussion

Conventional tumor therapy like chemotherapy, surgery, and radiation has limitations. New strategies are therefore required for tumor treatment. Gene transfer is a new means to locally express therapeutic proteins for the treatment of tumor. In this thesis, we tested the hypothesis whether vector mediated expression of transgenes was able to arrest tumor growth. As transgenes we tested the therapeutic potential of three different molecules. As vector we chose HC-Ad vectors because they do not integrate into the host genome, can carry multiple transgenes up to a maximum capacity of 27 kb and are capable of expressing transgenes for a long period.

V.1 Selection of transgenes

Tumor growth is dependent on angiogenesis. We hypothesized that blocking of growth factors which promote angiogenesis would arrest tumor growth. Therefore, soluble receptors of VEGF and angiopoietins namely sflt1 and stie2 were chosen as transgenes. In addition IL-12 was chosen as an immunostimulatory transgene to arrest tumor growth. IL-12, despite having impressive antitumor activity is extremely toxic when injected as a recombinant protein or expressed using a first generation Ad vector. As discussed in the following chapter a new strategy was devised to overcome IL-12 mediated toxicity by regulating its expression.

V.2 Requirement of regulation of transgene expression

Cancer gene therapy in contrast to gene therapy for inherited disorders may require the expression of cytokines, growth factors or suicide genes, molecules, which may have severe side effects when expressed constitutively and at high levels for a long time. In addition, many cytokines need to be present only for a short interval to improve haematopoiesis following cancer chemotherapy. Therefore, it becomes necessary to develop systems, which would allow the regulation of transgene expression both at quantitative and qualitative levels. Optimally, the expression of a transgene would occur only upon addition of an external drug, become induced in a particular tissue and the expression could be turned off in its absence. Thereby adverse events related to the transgene could be avoided and the levels of transgenes could be fine-tuned to achieve expression wthin a therapeutic window. In some situations and depending upon the tumor type it would be necessary to constitutively express the transgenes for a required period. In the case of relapsing or recurring tumors it would be desirable to turn on gene expression at different time schedules. In principle, several systems offer the possibility to regulate transgene expression, although few have been tested in gene transfer experiments in vivo. Some systems are based on induction by heat, UV irradiation and metal, which cannot be applied in vivo. In contrast, four systems with in vivo potential have been developed, including regulation by the antibiotic tetracycline, the insect steroid ecdysone or its analogs, the antiprogestin mifepristone (RU 486), and chemical dimerizers such as the immunosuppressant rapamycin and its analogs. They all involve the drug-dependent recruitment of a transcriptional activation factor to a basal promoter that controls the expression of the gene of interest, but differ in the mechanism of recruitment. In the mifepristone system drug related control of transcription is achieved by fusing the heterologous DNA-binding domain of the yeast GAL4 protein and the p65 activation domain of NF-kB to a mutant human progesterone receptor that is unaffected by endogenous hormones but is activated by synthetic antiprogestins at doses sufficiently low to avoid side effects in human. The properties of the mifepristone-regulated system have been investigated in transgenic animals and using injection of plasmid DNA in muscle. Additionally an HC-Ad vector incorporating the mifepristone system was shown to express the human growth hormone gene in an inducible manner. Interestingly, it was demonstrated that background transcription was undetectable in vitro and in vivo and human growth hormone production could be cycled on and off 3 times for over 50 days or alternatively

maintained at steady state levels by delivery of the RU 486. Therefore, we used the RU 486 system for inducible expression of transgenes.

V.3 Expression kinetics of HC-Ad vectors

HC-Ad vectors expressing transgenes constitutively demonstrate linear relationship between vector dose and transgene expression. However, such information is unavailable for HC-Ad vectors expressing transgenes upon induction. Therefore, in this study a reporter vector that expresses hIL-12 upon RU 486 induction was used to characterize the tissue distribution of the vector, the transgene expression, as well as the kinetics of the induction with respect to the dose of the vector, the dose of the inducer, and the periodicity of the induction. The vector expressing hIL-12 was chosen as a reporter vector because hIL-12 has minimal biological activity and no toxicity in mice [83].

hIL-12 expression was first detectable at 4 hours post RU 486 induction, followed by a peak at 10 hours. hIL-12 expression was low again at 24 hours and was undetectable at 48 hours. Similar results were observed with the vectors expressing sflt1 and mIL-12, upon single induction with the inducer RU 486. Similar kinetics of transgene expression has been earlier reported using a HC-Ad vector expressing hGH [10]. Interestingly, two other systems based on either tetracycline or rapamycin induction have been investigated for inducible transgene expression. An HC-Ad vector based on the tet expression system demonstrated a comparable kinetics of inducible mIFNα expression. Inducible gene expression based on rapamycin has been earlier studied using Ad or AAV vectors [129]. In this study based on the rapamycin system, it was observed that the level of reporter gene was high for 12 days post single rapamycin induction [130].

The reporter vector was further analyzed for levels of hIL-12 obtained upon increasing both the dosage of the vector and the inducer RU 486. It was observed that the levels of transgene expression increased with the increase in both the dose of the vector and the drug RU 486. A similar result has been earlier demonstrated in another study using transgenic mice based on the RU 486 system. In this study, a RU 486 dose dependent increase in inhibin A levels and a supra-physiological concentration of inhibin A was achieved when the mice were induced at a dose of 500 μg/kg [104]. The possibility to modulate the levels of hIL-12 expression by varying the vector and the inducer dosage is especially important in limiting the toxicity and provides a vital opportunity to finetune hIL-12 expression to attain therapeutic levels during treatment.

In some situations and depending on the nature of the disease successful application of inducible gene expression system for the treatment of diseases would require the maintenance of therapeutic levels of the transgenic protein for a longer period of time until it can be turned off. In order to investigate the minimum time interval required for the maintenance of stable hIL-12 levels mice were induced with RU 486 at different time intervals (every 12 hours, 24 hours and 48 hours for a week). Stable levels of IL-12 expression were observed when the mice were injected every 12 hours or 24 hours. Mice induced with RU 486 every 48 hours with RU 486 a saw like pattern of hIL-12 expression was detected. Based on these data, we selected induction every 24 hours to analyze whether prolonged administration of the inducer could maintain its efficacy at stimulating hIL-12 expression. So, a different group of mice was injected with RU 486 for a period of 21 days. Interestingly the mice showed levels of hIL-12, which were stable during the 21-day induction period. In this group of mice, the serum level of hIL-12 remained constant until the ninth day of sustained induction and decreased moderately after this time point but still was above 50% of its initial value on day 21. These findings provide insight about the functioning of the mifepristone-based regulatory system and are relevant for appropriate regulation of transgene expression in clinical trials. The mice which were induced every 12 hours, 24 hours or 48 hours were further induced again at weeks 19, 28, 33, and 48 week to determine the duration of the activity of Ad RS 24. In all cases, hIL-12 was undetectable in serum before the injection of RU486 and was detectable at 10 hours after induction, indicating that the system remained operative for at least 48 weeks. This information is of interest because of the fact that anti-adenovirus antibodies generated after the first dose of the vector may prevent its re-administration. However, in contrast to the

similar levels of hIL-12 at week 2 and 28, a 45% reduction in cytokine serum value was observed at week 45. This drop in the expression of hIL-12 could be explained by the normal turnover of hepatocytes. Thus, the long-term inducible expression of hIL-12 using RU 486 system is attributed to several factors. The superiority of HC-Ad vectors for long-term transgene expression has been demonstrated by different groups [110]. HC-Ad vectors have been shown to express transgenes like α-antitrypsin for more than one year demonstrating its persistence and safety [12]. In this study, long-term expression of transgenes using an HC-Ad vector has been demonstrated. The use of tissue specific promoters such as the TTRB promoter in this study has been shown to prolong the expression of transgenes by limiting the activation of the immune system [131]. Also the pSwitch molecule, which specifically transcribes the transgenes, is 85% humanized thereby limiting the generation of CTLs against the protein [102].

Interestingly, sflt1 and mIL-12 expressing vectors based on the RU 486 system demonstrated vector kinetics similar to the reporter vector, reconfirming that the activity of the RU 486 system was independent of the expressed transgenes. In addition, inducible mIL-12 expression was able to completely eradicate the orthotopic MC-38 tumors. In the case of the LLC tumor model, withdrawal of RU 486 during the second and fourth week resulted in the complete recovery of mice demonstrating prevention of IL-12 medaited toxicity by intermittent expression.

Interestingly, constitutive sflt1 expression caused ascites and subsequent death of mice. Ascites was observed upon administration of a vector expressing sflt1 constitutively or by constitutive induction with RU 486 pellets of a vector expressing inducible sflt1. Interestingly, ascites was not observed when sflt1 was inducibly expressed upon daily injection of RU 486 thereby validating the inducible gene expression system. In summary, these data clearly indicated that the expression of toxic genes could be optimized using the RU 486 system to derive a possible therapeutic benefit. The reason behind the occurrence of ascites in mice expressing sflt1 constitutively is discussed in the following chapter.

V.4 Toxicity of sflt1

Endothelial cells are quiescent in the adult vasculature unless they are stimulated in conditions like inflammation, wound healing and during menstruation [26]. The proliferation of endothelial cells has been shown to be mediated by specific growth factors like VEGF, whose absence can be lethal during embryonic growth [66]. In the present study, vectors expressing sflt1 were generated to study a potential anticancer effect of VEGF blockade. It was unexpectedly observed that all mice injected with vector expressing sflt1 constitutively developed ascites at the end of fifth week after injection followed by death. To investigate the reasons pertaining to the death of mice, biochemical analysis and histological analysis of different tissues were performed.

Histological analysis of Ad RS 44 (constitutive expression of sflt1) injected mice revealed that liver histology was normal. Serological analyses demonstrated that there was no significant change in liver parameters such as serum bilurubin, ALT etc. These data excluded liver damage to be responsible for the occurrence of ascites. Histological analysis of kidneys from animals with ascites demonstrated renal damage. Serological analyses revealed marked changes in the concentration of serum albumin, total protein, and urea. Together these data suggested kidney damage as the important pathogenic factor for the observed alterations and the death of the mice.

The importance of VEGF in the maintenance of glomerular function during development and adulthood has been demonstrated in earlier studies [132-134]. Glomeruli in the kidneys consist of a barrel of glomerular basement membrane (GBM) surrounded by glomerular endothelial cells on the inside and glomerular epithelial cells, also called podocytes, on the outside. Capillary endothelial cells, the basement membrane, and podocytes constitute the filtration membrane of the kidney. The blood initially is filtered as it passes through the fenestrae present in the endothelial cells. The resulting fluid then passes through the GBM and then through the filtration slit present between the podocytes. The fluid is finally collected in the capsular space before it is reabsorbed into the blood. It has been suggested that there exists a reciprocal relationship between podocytes and endothelial cells, which is responsible for the mutual survival of these cell types [135].

Interestingly it has been demonstrated using knock out technology, that mice completely deficient for VEGFA expression in the podocytes die perinataly and that mice heterozygous for VEGFA developed end stage kidney failure by 9 weeks after birth [134]. This experiment confirmed the importance of VEGF signalling and the fact that appropriate amounts of VEGF are required for maintenance of kidney function. The significance of VEGF blocking in the development of kidney disease has also been demonstrated by other elegant experiments. It was shown that in mice neutralization of circulating VEGF by mouse anti-VEGF antibodies or murine sflt1 induced proteinuria and injection of VEGF was sufficient to prevent the disease [132]. It was further shown that injection of sflt1 resulted in endothelial cell detachment from the GBM and occasional loss of filtration slits indicating kidney damage and resulting in proteinuria. In another study, it was observed that during the use of anti VEGF antibody in phase I and phase II cancer clinical trial, subjects developed proteinuria indicating that VEGF is essential for normal kidney function not only in mice but also in men [136]. Also, it is of great interest to note that sflt1 serum levels were significantly increased in patients with preeclampsia [137]. Preeclampsia is a syndrome affecting 5% of pregnancies that causes substantial maternal and fetal morbidity and mortality. The pathophysiology of preeclampsia had remained largely unknown and it has been hypothesized that placental ischemia is an early event, leading to placental production of a soluble factor or factors that cause maternal endothelial dysfunction, resulting in the clinical findings of hypertension, proteinuria, and edema. It has now been demonstrated that the elusive factor could be sflt1, which is found in large excess in the serum of patients and is responsible for decreased circulating levels of free VEGF and PIGF, resulting in endothelial dysfunction [138]. In a related study, administration of sflt1 to pregnant rats induced hypertension, proteinuria, and glomerular endotheliosis [139]. Collectively these studies suggest that high levels of sflt1 cause endothelial dysfunction owing to its sequestration effect on VEGF. Ascites followed by death has also been reported in 14 % mice injected with a first generation Ad vector expressing sflt1 [140]. In contrast, during the current study all mice constitutively expressing sflt1 developed ascites, which was followed by the death of all the animals five weeks post vector injection. Based on the observations of this study together with the published observations discussed above it is evident that the systemic use of sflt1 is accompanied by significant toxicity. It is therefore questionable whether systemic blockade of VEGF will become a viable option for cancer therapy.

V.5 Anticancer activity of sflt1, stie2 and mIL-12 expressing vectors in the LLC tumor model

The LLC model is a simple and rapid cancer model for screening molecules with potential anticancer activity. In this study, constitutive sflt1 and stie2 expression or inducible expression of sflt1 and mIL-12 were tested. Additionally, the combination of constitutive sflt1 and stie2 expression or combinations of inducible sflt1 and mIL-12 expression were tested.

Inducible or constitutive sflt1 expression resulted in LLC tumor reduction until three weeks post tumor injection. Thus, despite the difference in the kinetics and levels of serum sflt1 the tumor growth rate was similar in both groups of mice. A similar study using a first generation Ad vector expressing murine sflt1 under the control of hCMV promoter demonstrated a delay in LLC tumor growth for two weeks post LLC cell injection [140]. In this study the vector had been injected after a tumor had become palpable. sflt1 expression was observed for two weeks post infection and it was suggested that the levels of sflt1 to be therapeutic should be above 2 μg/ml. It was also speculated that tumor re-growth after a two-week delay was due to the loss of transgene expression or alternatively to a change of endothelial cells in their dependance upon growth factors. In our study levels as high as 14 μg/ml were observed after the injection of vector Ad RS 23. In the case of mice injected with vector expressing sflt1 constitutively, sflt1 levels were between 200 and 700 ng/ml. Unlike in the published study with ascites observed in only 14% of mice, all of the Ad RS 44 injected animals developed ascites demonstrating the fact that toxic levels of sflt1 had been achieved. Therefore, the probable reason responsible for the absence of anti-tumor effects of sflt1 beyond two weeks could have been the presence of alternative proangiogenic molecules such as aFGF, bFGF, FGF-3, FGF-4, HGF and IL-8, molecules, which have been shown to non-specifically stimulate endothelial cells [141, 142]. It is also possible that the LLC tumor cells could have induced the expression of any or a combination of these growth factors, which could contribute to the growth of endothelial cells and tumor re-growth. In the case of breast cancer tumors it has been observed that 50% of newly diagnosed breast cancers produce VEGF only. However, during subsequent tumor progression, recurrences and metastases, other angiogenic factors including FGF-2, PIGF, PD-ECGF and pleiotrophin are produced [16]. Taken together it is evident that inhibition of tumor angiogenesis by targeting VEGF alone may not be therapeutic for aggressive tumors like LLC.

Unlike sflt1, expression of stie2 did not result in LLC tumor inhibition or in an increase in survival time. It has been earlier reported that in BALB/c mice constitutive expression of stie2 using a first generation Ad viral vector resulted in a delay in tumor growth in the 4T1 and B16F10.9 tumor model [128]. The absence of anticancer activity upon stie2 expression may be attributed to lower levels of stie2 expression achieved during our study. It is also possible, similar to VEGF, that the role of Ang2 has been replaced by other growth factors during tumor progression.

Since VEGF and Ang2 act by inducing endothelial proliferation and vessel remodeling, we hypothesized that simultaneous blocking of both growth factors might have an additive effect in LLC tumor treatment. Coinjection of sflt1 and stie2 expressing vectors resulted in a statistically significant decrease in tumor volume at three weeks post tumor cell injection. Nevertheless, an increase in survival time was not observed. Surprisingly, the mice were moribund at three weeks post tumor cell injection and had ascites, which could have been likely due to simultaneous inhibition of VEGF and Ang2. Interestingly, inducible expression of sflt1 or stie2 alone did not result in ascites. However, further experiments need to be performed to confirm this observation. In summary, the simultaneous blocking of both VEGF and Ang2 did not result in a significant therapeutic effect. As discussed earlier, the reason could be the presence of multiple angiogenic factors, which might replace VEGF and Ang2.

Despite its anticancer activity a therapeutic use of IL-12 is limited by its systemic toxicity. Therefore, anticancer effects of IL-12 were investigated expressing IL-12 in an inducible manner. Similar to earlier observations, IL-12 mediated toxicity was observed after one week of mIL-12

expression. Consequently, IL-12 expression was induced only during the first and the third week post vector injection. Interestingly, the animals, showing toxicity after one week of inducion, recovered completely during the second week and during the fourth week when daily RU 486 injection was discontinued. Induction beyond three weeks was averted to prevent death of mice and to study if the current induction schedule resulted in tumor rejection and immunological memory. However, the current schedule resulted only in a one-week increase in survival of the mice bearing LLC tumors.

IFN γ has been shown to mediate the anticancer activity of mIL-12. It has also been shown that a local expression of mIL-12, which might activate the host immune system locally, is required for tumor growth inhibition. However, it remains to be tested, if inducible expression of mIL-12 every 48 hours or other schedules might be able to inhibit LLC tumor growth. Nevertheless, this result is significant with respect to toxicity, because mIL-12 mediated toxicity was absent when RU 486 induction was discontinued. Thus, a rapid reversal of mIL-12 induced toxicity could be demonstrated, an objective of this study.

Inducible expression of mIL-12 alone showed a delay in LLC tumor growth for four weeks and a modest increase in survival by one week. Conversely, inducible expression of sflt1 showed a delay in tumor growth for three weeks post injection. The two strategies represent alternative principles to inhibit tumor growth. IL-12 acts predominantly by the activation of cell types like NK cells, T cells, macrophages, B cells and by inducing the production of IFN γ [81]. sflt1 acts by sequestering VEGF, an endothelial specific growth factor. Therefore sflt1 and mIL-12 were injected together in the LLC model to investigate if they had synergistic anticancer effects. Importantly, injection of RU 486 was performed only during the first and third week to prevent mIL-12 mediated toxicity observed earlier when mIL-12 expressing vector was injected alone. Interestingly, a delay in tumor growth was observed until the fifth week post LLC tumor cell injection and at least one mouse survived until eight weeks. In contrast, only one mouse survived until the fourth week in the control group. The delay in tumor growth and increased survival rate compared to control mice or injection of single vector may be explained in two ways. The levels of mIL-12 observed in this study were 2 to 5 fold higher compared to the study when the vector expressing mIL-12 was injected alone. The differences in the expression of mIL-12 in spite of administration of similar amounts of vector expressing mIL-12 can be explained by an increased transduction efficiency due to the presence of vector expressing sflt1, lowering the threshold for transducion. Thus, the results may be explained solely by the high levels of serum mIL-12. As alternative explanation, the presence of sflt1 could have contributed to the increase in survival. However, the levels of sflt1 were low when compared to levels attained by injection of the vector expressing sflt1 alone. Nevertheless, the levels of sflt1 are still significantly high because negligible sflt1 levels are observed in normal mice. Thus, it is possible that sflt1 could have had an additive effect in the inhibition of tumor growth. Evidence exists for the presence of sflt1 receptors in numerous cells types apart from endothelial cells such as HSCs, monocytes, smooth muscle cells and dendritic cells [143-145]. It has been demonstrated that VEGF inhibits the maturation of dendritic cells and it was suggested that this could help the tumor cells to evade immune surveillance [65, 143, 146]. As described earlier DCs are the most important APCs and their loss of function is attributed to the development of tumors. It has been demonstrated that an antibody against VEGF was effective in inhibition of tumor growth by improving the function of dendritic cells [146]. Therefore, it is possible that the presence of both sflt1 and mIL-12 was responsible for the delayed LLC tumor growth and the decreased mortality rate. However, this can be confirmed only by assaying the function of dendritic cells, which was not performed. Nevertheless, the delay in tumor growth was encouraging and it is tempting to propose that combinations of both anti-angiogenic and immunotherapy might effectively supplement conventional cancer therapy strategies. Recently, it was shown in a syngenic tumor model that combinations of antibodies against VEGFR2 and IL-12 resulted in tumor regression [147]. This strengthens the concept that the combination of anti-angiogenic and immunotherapy could be synergistic in the treatment of cancer.

V.6 Anticancer activity of sflt1 and mIL-12 in the MC-38 model

The MC-38 colon carcinoma model, compared to the LLC model, mimics more closely the human condition. Since the use of sflt1 and mIL-12 expressing vectors had resulted in modest anticancer activities in the LLC tumor model they were further evaluated in the MC-38 model.

Inducible or constitutive sflt1 expression did not reduce tumor growth or prolong survival in this model. The lack of inhibition of tumor growth or increase in survival rate can be explained in several ways. It is possible that MC-38 tumors express or induce other proangiogenic growth factors, which overcome the VEGF requirement for angiogenesis. Incidentally it has been demonstrated using immunohistochemisty of human tumor specimens that aggressive hepatic tumors are often associated with high levels of IL-8, FGFs and PDGF [39]. It is also possible that there are unidentified growth factors which specifically act on hepatic endothelial cells similar to EG VEGF, which has been shown to specifically stimulate endothelial cells in endocrine glands [148]. In this regard it has been suggested that endothelial cells undergo tissue specific modification and therefore may respond to therapies in different ways [149]. Liver is composed of different cell types such as hepatocytes, fibroblasts, endothelial cells and Kupffer cells, all of which provide a favorable milieu for tumor cell implantation and initiation of angiogenesis. In addition, the analysis is further complicated by the unique anatomic nature of liver, which is richly supplied with vessels and has been shown to receive 30% of cardiac output. To conclude, it is evident that the blockade of VEGF did not result in a significant suppression of MC-38 tumor growth or in an increase in survival time. It would be very interesting to test in the future a combined action of vectors simultaneously expressing different transgenes in the MC-38 colon carcinoma model.

In contrast to sflt1 expression, inducible mIL-12 expression resulted in a significant MC-38 tumor inhibition and in a tumor free survival in the post treatment period. Tumor inhibition correlated directly with serum mIL-12 levels. Additionally, it was observed that mice injected with the mIL-12 expressing vector but were left uninduced also succumbed to the tumor reflecting the tightness of the system. The significant anti-tumor activity in the MC-38 model in contrast to that observed in the LLC model may have been due to the local expression of mIL-12, which has been shown to result in a concentration gradient with high levels peritumorally and lower amounts systemically. The importance of mIL-12 expression in the tumor vicinity has been demonstrated by using cell lines expressing increasing concentrations of mIL-12 [150]. It has been shown that the C26 colon carcinoma cell line expressing increasing amounts of mIL-12 exhibited decreased tumor formation and was associated with increased CD8+ cells and NK cells recruitment in the tumor microenvironment [150].

The regression of hepatic metastases using adenovirus vectors expressing IL-12 has been demonstrated before. First generation Ad vectors expressing mIL-12 constitutively, when injected directly into the syngenic CT26 tumor implanted in the liver, resulted in tumor regression in about 76% of mice. In addition, the tumor disappeared within 7-10 days post injection and was resistant to rechallenge [151]. In a similar study, hepatic metastases of MCA-26 colon carcinoma were treated with a tumor injection of Ad vector expressing mIL-12. Treated animals survived longer than untreated controls. This treatment was superior to a combined treatment with Ad vectors expressing herpes simplex virus type 1 thymidine kinase (HSV-tk) and mIL-2 (357). Incidentally in our study, mice injected with mIL-12 expressing vector succumbed to tumors in the absence of induction reflecting the tightness of the system. Another significant feature of our study relates to the reversal of mIL-12 associated toxicity upon withdrawal of RU 486 induction. This was confirmed by monitoring serum ALT levels and by histological analysis of liver sections.

Although the mechanisms by which IL-12 exerts anti-tumor activity have been difficult to dissect, it has been shown to involve cell types such as NK cells, NKT cells, macrophages, and CD8+ cells, cytokines like IFNγ and chemokines like interferon-gamma-inducible protein-10 (IP-10) and Mig [151-153]. Among all the factors it has been clearly demonstrated that toxicity of IL-12 is mediated by IFNγ and the levels need to be continuously monitored in a clinical setting to avoid adverse events. During a phase II clinical trial with recombinant hIL-12 two deaths were reported due to

mIL-12 mediated toxicity [126]. Therefore it is important that despite the confirmation of impressive anti-tumor of activity of hIL-12, serious emphasis must be laid on controlling the levels of mIL-12.

The importance of regulation and safe administration of mIL-12 for anticancer activity has been one of the major focuses of this work. It has been demonstrated in this study that varying the dose of vector and the drug RU 486 can modulate the levels of IL-12. Complete remission of hepatic tumors was observed only by inducible and locally expressed mIL-12. Thus, vector-mediated expression of IL-12 and incorporating an inducible system for expression control may have significant potential for the treatment of hepatic tumors and metastases.

VI Summary

This work was based on the hypothesis that vector-mediated long-term expression of antiangiogenic or immunomodulatory proteins may represent an attractive strategy to control the growth of malignant neoplasms. The experiments focused on two antiangiogenic molecules, sflt1 and stie2, and on one molecule with well-known immunomodulatory function, IL-12.

HC-Ad vectors were chosen for gene delivery since long-term expression in hepatocytes is generally achieved following intravenous vector injection. The vectors were designed to express the molecules either in a constitutive manner (sflt1 and stie2) or in the context of a RU 486-inducible expression system thereby allowing for drug control of expression (sflt1, mIL-12 and hIL-12).

Following in vitro characterisation of the different vectors their biological activity was analysed in murine cancer models, the subcutaneous LLC model and the orthotopic (liver) MC-38 model. The analysis of each vector started with an analysis of expression levels and kinetics following intravenous injection. Very significant and stable serum levels of all molecules were achieved in vivo. It was also found that the RU 486 system allowed for exquisite liver-specific and long-term expression control with practically negligible expression of the transgenes in the absence of RU 486. Thus, the RU 486 inducible expression system is very well suited to control expression of potentially toxic proteins, as also demonstrated in this study for sflt1 and IL-12.

A significant result of this study was the observation that RU 486-induced expression of mIL-12 in the orthotopic MC-38 model resulted in complete tumor eradication. This was surprising since the MC-38 model is a very aggressive model of liver cancer. It is likely that the local expression of high mIL-12 levels in the tumor environment was essential for this positive result.

In contrast, constitutive or RU 486-induced expression of sflt1 in the same model had no tumor-inhibitory effect.

Less promising results were observed with any of the vectors when tested in the subcutaneous LLC cancer model. None of the vectors, when injected alone, resulted in tumor eradication, although there was a tendency for tumor growth inhibition following injection of the sflt1 expressing vector. A similar tumor growth inhibitory effect was observed upon combined injection of the sflt1 and stie2 expressing vectors. When sflt1 and mIL-12 were expressed in combination, a moderate increase in survival time was found. However, complete tumor regression was not observed in the LLC tumor model with any of the vectors alone or in combination.

Unexpected was the observation that VEGF blockade by expressing sflt1 over a longer period of time resulted in toxicity and death of the animals, likely due to dysfunction of renal endothelial cells and kidney failure. This result suggested that upon therapeutic VEGF-inhibition close attention has to be paid to possible side effects in particular with respect to renal function.

VII Zusammenfassung

Diese Arbeit beruhte auf der Hypothese, dass langzeitige Vektor-vermittelte Expression von anti-angiogenetischen oder immunmodulatorischen Proteinen eine vielversprechende Strategie zur Kontrolle des Wachstums maligner Neoplasmen sein könnte. Die experimentelle Arbeit konzentrierte sich auf zwei anti-angiogenetische Moleküle, sflt1 und stie2, sowie das immunmodulatorische IL-12.

Adenovirale Vektoren mit hoher DNA-Kapazität wurden als Vektorsystem gewählt, da sie in vivo nach intravenöser Injektion Langzeitexpression in Hepatozyten ermöglichen. Die Vektoren exprimierten die Transgene entweder konstitutiv (sflt1 und stie2) oder RU 486-induzierbar (mIL-12 und hIL-12), so dass eine medikamentöse Steuerung der Genexpression möglich war.

Nach der in-vitro-Charakterisierung der einzelnen Vektoren wurde ihre biologische Aktivität in dem subkutanen LLC-Tumormodell und dem orthotopen MC-38 Modell in der Labormaus untersucht. Die Analyse beinhaltete zunächst die Untersuchung von Expressionsstärke und Expressionskinetik nach intravenöser Injektion. Hierbei wurden stabile Serumkonzentrationen aller Moleküle auf hohem Niveau beobachtet. Des weiteren konnte gezeigt werden, dass die auf dem RU 486-System beruhenden Vektoren eine leber-spezifische und langzeitige Expressionskontrolle ermöglichten, und insbesondere ohne nennenswerte Expression der Transgene in Abwesenheit von RU 486. Diese Daten zeigen, dass das induzierbare RU 486-System gut zur Kontrolle der Expression potentiell toxischer Transgene geeignet ist, wie am Beispiel von sflt1 und IL-12 hier verdeutlicht.

Ein wesentliches Ergebnis dieser Arbeit war die Beobachtung, dass die Expression von mIL-12 mittels des RU 486-Systems in dem orthotopen MC-38 Tumormodell zur kompletten Tumor Remission führte. Die war umso überraschender, als das MC-38 Modell ein sehr aggressives Lebertumormodell ist. Es ist wahrscheinlich, dass die starke Expression von mIL-12 in der Tumorumgebung wesentlich für dieses positive Ergebnis verantwortlich war. Im Gegensatz hierzu hatte die Expression von sflt1 im selben Modell weder bei konstitutiver noch bei induzierbarer Expression einen tumor-inhibitorischen Effekt.
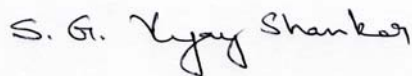
Weniger vielversprechende Ergebnisse wurden mit den verwendeten Vektoren in dem subkutanen LLC-Tumormodell erzielt. Bei alleiniger Injektion führte keiner der Vektoren zur kompletten Tumor Remission, wenngleich eine Tendenz zur Inhibition des Tumorwachstums nach Injektion des sflt1 Expressionsvektors zu beachten war. Ein ähnlicher inhibitorischer Effekt konnte bei gemeinsamer Injektion der Expressionsvektoren für sflt1 und stie2 nachgewiesen werden und ein moderater Anstieg der Überlebenszeit wurde bei gleichzeitiger Expression der beiden Vektoren beobachtet. Allerdings konnte eine vollständige Tumor Remission mit keiner der Vektorkombinationen im LLC-Modell erzielt werden.

Unerwartet war die Beobachtung, dass VEGF Blockade durch langzeitige Expression von sflt1 von starker Toxizität begleitet war und den Tod der Tiere zur Folge hatte, vermutlich verursacht durch eine Störung der renalen Endothelzellfunktion gefolgt von Nierenversagen. Dieses Ergebnis deutete darauf hin, dass bei therapeutischer VEGF-Inhibition auf Nebenwirkungen und insbesondere auf Störung der Nierenfunktion zu achten ist.

Erklärung

Ich versichere, dass ich die von mir vorgelegte Dissertation selbständig angefertigt, die benutzten Quellen und Hilfsmittel vollständig angegeben und die Stellen der Arbeit - einschließlich Tabellen und Abbildungen -, die anderen Werke in Wortlaut oder dem Sinn nach entnommen sind, in jedem Einzelfall als Entlehnung kenntlich gemacht habe; dass diese Dissertation noch keiner anderen Fakultät oder Universität zur Prüfüng vorgelegen hat; dass sie - abgesehen von unten angegebenen Teilpublikationen - noch nicht veröffenlicht worden ist sowie, dass ich eine solche Veröffentlichung vor Abschluss des Promotionsverfahrens nicht vornehmen werde.
Die Bestimmungen dieser Promotionsordnung sind mir bekannt. Die von mir vorgelegte Dissertation wurde von Herrn PD Dr. Stefan Kochanek betreut worden.

S.G.Vijayshankar
Köln
23.4.06

Teilpublikationen:

1) Wang L, Hernandez-Alcoceba R, Shankar V, Zabala M, Kochanek S, Sangro B, Kramer MG, Prieto J, Qian C. Prolonged and inducible transgene expression in the liver using gutless adenovirus: a potential therapy for liver cancer. Gastroenterology. 2004 Jan; 126 (1): 78-89.

Curriculum Vitae

S.G. Vijayshankar
AG Dr. Kochanek
Center for Molecular Medicine
University of Cologne
50931 Cologne

Nationality: Indian

13.03.1975	Born in Erode, India
1980-1990	10th class examination, Kanpur, India
1990-1992	12th class examination, Madras, India
1992-1995	Bachelors of Science degree in biochemistry awarded by University of Madras, India
1995-1997	Masters of Science degree in biochemistry awarded by University of Madras, India
1997-1998	Junior Research Fellow at Department of Biochemistry, Cancer Research Institute (WIA) Adayar, Madras, India
1998-2004	Graduate student under the supervision of PD Dr. Stefan Kochanek, at the Faculty of Mathematics and Natural Sciences, at the Center for Molecular Medicine, Cologne.

Lebenslauf

S.G.Vijayshankar
AG Dr. Kochanek
Zentrum für Molekulare Medizin
Universitat zu Köln
50931 Köln

Staatsangehörigkeit: Indisch

13.03.1975	geboren in Erode, Indien
1980-1990	Abschlußprüfung 10.Klasse, Kanpur Indien
1990-1992	Abschlußprüfung 12.Klasse, Madras, Indien
1992-1995	Bachelors of Science degree. Hauptfach: Biochemie Universität zu Madras, Indien
1995-1997	Masters of Science degree. Hauptfach: Biochemie Universität zu Madras, Indien
1997-1998	Junior Research Fellow at Department of Biochemistry, Cancer Research Institute (WIA) Adayar, Madras Indien
1998-2004	Doktorand unter der Betreuung von PD. Dr. Stefan Kochanek Fakultät für Mathematik und Naturwissenschaften, Universität zu Köln

References:

1.   Evan, G.I. and K.H. Vousden, *Proliferation, cell cycle and apoptosis in cancer.* Nature, 2001. **411**(6835): p. 342-8.
2.   Sporn, M.B., *The war on cancer.* Lancet, 1996. **347**(9012): p. 1377-81.
3.   Jacks, T. and R.A. Weinberg, *Taking the study of cancer cell survival to a new dimension.* Cell, 2002. **111**(7): p. 923-5.
4.   Harris, C.C., *p53 tumor suppressor gene: from the basic research laboratory to the clinic--an abridged historical perspective.* Carcinogenesis, 1996. **17**(6): p. 1187-98.
5.   Weinberg, R.A., *The retinoblastoma protein and cell cycle control.* Cell, 1995. **81**(3): p. 323-30.
6.   Lengauer, C., K.W. Kinzler, and B. Vogelstein, *Genetic instabilities in human cancers.* Nature, 1998. **396**(6712): p. 643-9.
7.   Rosenberg, S.A., *Progress in human tumour immunology and immunotherapy.* Nature, 2001. **411**(6835): p. 380-4.
8.   Folkman, J., *Angiogenesis and angiogenesis inhibition: an overview.* Exs, 1997. **79**: p. 1-8.
9.   Rosenberg, S.A., et al., *Prospective randomized trial of the treatment of patients with metastatic melanoma using chemotherapy with cisplatin, dacarbazine, and tamoxifen alone or in combination with interleukin-2 and interferon alfa-2b.* J Clin Oncol, 1999. **17**(3): p. 968-75.
10.   Burcin, M.M., et al., *Adenovirus-mediated regulable target gene expression in vivo.* Proc Natl Acad Sci U S A, 1999. **96**(2): p. 355-60.
11.   Morsy, M.A., et al., *An adenoviral vector deleted for all viral coding sequences results in enhanced safety and extended expression of a leptin transgene.* Proc Natl Acad Sci U S A, 1998. **95**(14): p. 7866-71.
12.   Morral, N., et al., *High doses of a helper-dependent adenoviral vector yield supraphysiological levels of alpha1-antitrypsin with negligible toxicity.* Hum Gene Ther, 1998. **9**(18): p. 2709-16.
13.   Coussens, L.M. and Z. Werb, *Inflammation and cancer.* Nature, 2002. **420**(6917): p. 860-7.
14.   Hanahan, D. and R.A. Weinberg, *The hallmarks of cancer.* Cell, 2000. **100**(1): p. 57-70.
15.   Khong, H.T. and N.P. Restifo, *Natural selection of tumor variants in the generation of "tumor escape" phenotypes.* Nat Immunol, 2002. **3**(11): p. 999-1005.
16.   Relf, M., et al., *Expression of the angiogenic factors vascular endothelial cell growth factor, acidic and basic fibroblast growth factor, tumor growth factor beta-1, platelet-derived endothelial cell growth factor, placenta growth factor, and pleiotrophin in human primary breast cancer and its relation to angiogenesis.* Cancer Res, 1997. **57**(5): p. 963-9.
17.   Sinkovics, J.G., *Kaposi's sarcoma: its 'oncogenes' and growth factors.* Crit Rev Oncol Hematol, 1991. **11**(2): p. 87-107.
18.   Jensen, R.L., *Growth factor-mediated angiogenesis in the malignant progression of glial tumors: a review.* Surg Neurol, 1998. **49**(2): p. 189-95; discussion 196.
19.   Eliceiri, B.P., *Integrin and growth factor receptor crosstalk.* Circ Res, 2001. **89**(12): p. 1104-10.
20.   Hood, J.D. and D.A. Cheresh, *Role of integrins in cell invasion and migration.* Nat Rev Cancer, 2002. **2**(2): p. 91-100.
21.   Hodivala-Dilke, K.M., A.R. Reynolds, and L.E. Reynolds, *Integrins in angiogenesis: multitalented molecules in a balancing act.* Cell Tissue Res, 2003. **314**(1): p. 131-44.
22.   Evan, G. and T. Littlewood, *A matter of life and cell death.* Science, 1998. **281**(5381): p. 1317-22.
23.   Loeb, L.A., *Mutator phenotype may be required for multistage carcinogenesis.* Cancer Res, 1991. **51**(12): p. 3075-9.
24.   Green, D.R. and J.C. Reed, *Mitochondria and apoptosis.* Science, 1998. **281**(5381): p. 1309-12.

25.　Hahn, W.C., et al., *Creation of human tumour cells with defined genetic elements.* Nature, 1999. **400**(6743): p. 464-8.

26.　Folkman, J. and M. Klagsbrun, *Angiogenic factors.* Science, 1987. **235**(4787): p. 442-7.

27.　Sieczkiewicz, G.J., M. Hussain, and E.C. Kohn, *Angiogenesis and metastasis.* Cancer Treat Res, 2002. **107**: p. 353-81.

28.　Reynolds, L.P., S.D. Killilea, and D.A. Redmer, *Angiogenesis in the female reproductive system.* Faseb J, 1992. **6**(3): p. 886-92.

29.　Bogenrieder, T. and M. Herlyn, *Cell-surface proteolysis, growth factor activation and intercellular communication in the progression of melanoma.* Crit Rev Oncol Hematol, 2002. **44**(1): p. 1-15.

30.　Vicari, A.P. and C. Caux, *Chemokines in cancer.* Cytokine Growth Factor Rev, 2002. **13**(2): p. 143-54.

31.　Sledge, G.W., Jr. and K.D. Miller, *Angiogenesis and antiangiogenic therapy.* Curr Probl Cancer, 2002. **26**(1): p. 1-60.

32.　Pepper, M.S., *Extracellular proteolysis and angiogenesis.* Thromb Haemost, 2001. **86**(1): p. 346-55.

33.　Ruegg, C. and A. Mariotti, *Vascular integrins: pleiotropic adhesion and signaling molecules in vascular homeostasis and angiogenesis.* Cell Mol Life Sci, 2003. **60**(6): p. 1135-57.

34.　Nehls, V., K. Denzer, and D. Drenckhahn, *Pericyte involvement in capillary sprouting during angiogenesis in situ.* Cell Tissue Res, 1992. **270**(3): p. 469-74.

35.　Folkman, J., *Angiogenesis in cancer, vascular, rheumatoid and other disease.* Nat Med, 1995. **1**(1): p. 27-31.

36.　Folkman, J., *The role of angiogenesis in tumor growth.* Semin Cancer Biol, 1992. **3**(2): p. 65-71.

37.　Bogenrieder, T. and M. Herlyn, *Axis of evil: molecular mechanisms of cancer metastasis.* Oncogene, 2003. **22**(42): p. 6524-36.

38.　Ruoslahti, E., *Fibronectin and its integrin receptors in cancer.* Adv Cancer Res, 1999. **76**: p. 1-20.

39.　Radinsky, R. and L.M. Ellis, *Molecular determinants in the biology of liver metastasis.* Surg Oncol Clin N Am, 1996. **5**(2): p. 215-29.

40.　Jakobisiak, M., W. Lasek, and J. Golab, *Natural mechanisms protecting against cancer.* Immunol Lett, 2003. **90**(2-3): p. 103-22.

41.　Dranoff, G., *Cytokines in cancer pathogenesis and cancer therapy.* Nat Rev Cancer, 2004. **4**(1): p. 11-22.

42.　Bingle, L., N.J. Brown, and C.E. Lewis, *The role of tumour-associated macrophages in tumour progression: implications for new anticancer therapies.* J Pathol, 2002. **196**(3): p. 254-65.

43.　Ardavin, C., S. Amigorena, and C. Reis e Sousa, *Dendritic cells: immunobiology and cancer immunotherapy.* Immunity, 2004. **20**(1): p. 17-23.

44.　Whiteside, T.L. and C. Odoux, *Dendritic cell biology and cancer therapy.* Cancer Immunol Immunother, 2004. **53**(3): p. 240-8.

45.　Whiteside, T.L., N.L. Vujanovic, and R.B. Herberman, *Natural killer cells and tumor therapy.* Curr Top Microbiol Immunol, 1998. **230**: p. 221-44.

46.　Igney, F.H. and P.H. Krammer, *Immune escape of tumors: apoptosis resistance and tumor counterattack.* J Leukoc Biol, 2002. **71**(6): p. 907-20.

47.　Fehervari, Z. and S. Sakaguchi, *CD4+ Tregs and immune control.* J Clin Invest, 2004. **114**(9): p. 1209-17.

48.　Cavallo, F., et al., *Immune events associated with the cure of established tumors and spontaneous metastases by local and systemic interleukin 12.* Cancer Res, 1999. **59**(2): p. 414-21.

49.　Fehniger, T.A. and M.A. Caligiuri, *Interleukin 15: biology and relevance to human disease.* Blood, 2001. **97**(1): p. 14-32.

50. Kaplan, D.H., et al., *Demonstration of an interferon gamma-dependent tumor surveillance system in immunocompetent mice.* Proc Natl Acad Sci U S A, 1998. **95**(13): p. 7556-61.

51. Chopra, V., T.V. Dinh, and E.V. Hannigan, *Circulating serum levels of cytokines and angiogenic factors in patients with cervical cancer.* Cancer Invest, 1998. **16**(3): p. 152-9.

52. Chada, S., R. Ramesh, and A.M. Mhashilkar, *Cytokine- and chemokine-based gene therapy for cancer.* Curr Opin Mol Ther, 2003. **5**(5): p. 463-74.

53. Bussolino, F., A. Mantovani, and G. Persico, *Molecular mechanisms of blood vessel formation.* Trends Biochem Sci, 1997. **22**(7): p. 251-6.

54. Thurston, G., *Role of Angiopoietins and Tie receptor tyrosine kinases in angiogenesis and lymphangiogenesis.* Cell Tissue Res, 2003. **314**(1): p. 61-8.

55. Jones, N., et al., *Tie receptors: new modulators of angiogenic and lymphangiogenic responses.* Nat Rev Mol Cell Biol, 2001. **2**(4): p. 257-67.

56. Suri, C., et al., *Requisite role of angiopoietin-1, a ligand for the TIE2 receptor, during embryonic angiogenesis.* Cell, 1996. **87**(7): p. 1171-80.

57. Thurston, G., et al., *Leakage-resistant blood vessels in mice transgenically overexpressing angiopoietin-1.* Science, 1999. **286**(5449): p. 2511-4.

58. Maisonpierre, P.C., et al., *Angiopoietin-2, a natural antagonist for Tie2 that disrupts in vivo angiogenesis.* Science, 1997. **277**(5322): p. 55-60.

59. Sato, T.N., et al., *Distinct roles of the receptor tyrosine kinases Tie-1 and Tie-2 in blood vessel formation.* Nature, 1995. **376**(6535): p. 70-4.

60. Sato, T.N., et al., *Tie-1 and tie-2 define another class of putative receptor tyrosine kinase genes expressed in early embryonic vascular system.* Proc Natl Acad Sci U S A, 1993. **90**(20): p. 9355-8.

61. Lee, H.J., et al., *Biological characterization of angiopoietin-3 and angiopoietin-4.* Faseb J, 2004. **18**(11): p. 1200-8.

62. Berse, B., et al., *Vascular permeability factor (vascular endothelial growth factor) gene is expressed differentially in normal tissues, macrophages, and tumors.* Mol Biol Cell, 1992. **3**(2): p. 211-20.

63. Neufeld, G., et al., *Vascular endothelial growth factor (VEGF) and its receptors.* Faseb J, 1999. **13**(1): p. 9-22.

64. Thurston, G. and N.W. Gale, *Vascular endothelial growth factor and other signaling pathways in developmental and pathologic angiogenesis.* Int J Hematol, 2004. **80**(1): p. 7-20.

65. Gabrilovich, D., et al., *Vascular endothelial growth factor inhibits the development of dendritic cells and dramatically affects the differentiation of multiple hematopoietic lineages in vivo.* Blood, 1998. **92**(11): p. 4150-66.

66. Carmeliet, P., et al., *Abnormal blood vessel development and lethality in embryos lacking a single VEGF allele.* Nature, 1996. **380**(6573): p. 435-9.

67. Carmeliet, P., et al., *Impaired myocardial angiogenesis and ischemic cardiomyopathy in mice lacking the vascular endothelial growth factor isoforms VEGF164 and VEGF188.* Nat Med, 1999. **5**(5): p. 495-502.

68. Tischer, E., et al., *The human gene for vascular endothelial growth factor. Multiple protein forms are encoded through alternative exon splicing.* J Biol Chem, 1991. **266**(18): p. 11947-54.

69. Ruhrberg, C., *Growing and shaping the vascular tree: multiple roles for VEGF.* Bioessays, 2003. **25**(11): p. 1052-60.

70. Dor, Y., R. Porat, and E. Keshet, *Vascular endothelial growth factor and vascular adjustments to perturbations in oxygen homeostasis.* Am J Physiol Cell Physiol, 2001. **280**(6): p. C1367-74.

71. Tsuzuki, Y., et al., *Vascular endothelial growth factor (VEGF) modulation by targeting hypoxia-inducible factor-1alpha--> hypoxia response element--> VEGF cascade differentially regulates vascular response and growth rate in tumors.* Cancer Res, 2000. **60**(22): p. 6248-52.

72. Joukov, V., et al., *A novel vascular endothelial growth factor, VEGF-C, is a ligand for the Flt4 (VEGFR-3) and KDR (VEGFR-2) receptor tyrosine kinases.* Embo J, 1996. **15**(7): p. 1751.

73. Achen, M.G., et al., *Vascular endothelial growth factor D (VEGF-D) is a ligand for the tyrosine kinases VEGF receptor 2 (Flk1) and VEGF receptor 3 (Flt4).* Proc Natl Acad Sci U S A, 1998. **95**(2): p. 548-53.

74. Shibuya, M., *Vascular endothelial growth factor receptor-2: its unique signaling and specific ligand, VEGF-E.* Cancer Sci, 2003. **94**(9): p. 751-6.

75. Ferrara, N., H.P. Gerber, and J. LeCouter, *The biology of VEGF and its receptors.* Nat Med, 2003. **9**(6): p. 669-76.

76. Fong, G.H., et al., *Increased hemangioblast commitment, not vascular disorganization, is the primary defect in flt-1 knock-out mice.* Development, 1999. **126**(13): p. 3015-25.

77. Hiratsuka, S., et al., *Flt-1 lacking the tyrosine kinase domain is sufficient for normal development and angiogenesis in mice.* Proc Natl Acad Sci U S A, 1998. **95**(16): p. 9349-54.

78. Kendall, R.L. and K.A. Thomas, *Inhibition of vascular endothelial cell growth factor activity by an endogenously encoded soluble receptor.* Proc Natl Acad Sci U S A, 1993. **90**(22): p. 10705-9.

79. Shalaby, F., et al., *Failure of blood-island formation and vasculogenesis in Flk-1-deficient mice.* Nature, 1995. **376**(6535): p. 62-6.

80. Kaipainen, A., et al., *Expression of the fms-like tyrosine kinase 4 gene becomes restricted to lymphatic endothelium during development.* Proc Natl Acad Sci U S A, 1995. **92**(8): p. 3566-70.

81. Colombo, M.P. and G. Trinchieri, *Interleukin-12 in anti-tumor immunity and immunotherapy.* Cytokine Growth Factor Rev, 2002. **13**(2): p. 155-68.

82. Kobayashi, M., et al., *Identification and purification of natural killer cell stimulatory factor (NKSF), a cytokine with multiple biologic effects on human lymphocytes.* J Exp Med, 1989. **170**(3): p. 827-45.

83. Trinchieri, G., *Interleukin-12 and the regulation of innate resistance and adaptive immunity.* Nat Rev Immunol, 2003. **3**(2): p. 133-46.

84. Presky, D.H., et al., *A functional interleukin 12 receptor complex is composed of two beta-type cytokine receptor subunits.* Proc Natl Acad Sci U S A, 1996. **93**(24): p. 14002-7.

85. Brunda, M.J., et al., *Antitumor and antimetastatic activity of interleukin 12 against murine tumors.* J Exp Med, 1993. **178**(4): p. 1223-30.

86. Dornburg, R., *The history and principles of retroviral vectors.* Front Biosci, 2003. **8**: p. d818-35.

87. Somia, N. and I.M. Verma, *Gene therapy: trials and tribulations.* Nat Rev Genet, 2000. **1**(2): p. 91-9.

88. Hildinger, M. and A. Auricchio, *Advances in AAV-mediated gene transfer for the treatment of inherited disorders.* Eur J Hum Genet, 2004. **12**(4): p. 263-71.

89. Buning, H., et al., *AAV-based gene transfer.* Curr Opin Mol Ther, 2003. **5**(4): p. 367-75.

90. Russell, W.C., *Update on adenovirus and its vectors.* J Gen Virol, 2000. **81**(Pt 11): p. 2573-604.

91. Biederer, C., et al., *Replication-selective viruses for cancer therapy.* J Mol Med, 2002. **80**(3): p. 163-75.

92. McCormick, F., *Cancer gene therapy: fringe or cutting edge?* Nat Rev Cancer, 2001. **1**(2): p. 130-41.

93. Fang, B. and J.A. Roth, *Tumor-suppressing gene therapy.* Cancer Biol Ther, 2003. **2**(4 Suppl 1): p. S115-21.

94. Vassaux, G. and P. Martin-Duque, *Use of suicide genes for cancer gene therapy: study of the different approaches.* Expert Opin Biol Ther, 2004. **4**(4): p. 519-30.

95. Parney, I.F. and L.J. Chang, *Cancer immunogene therapy: a review.* J Biomed Sci, 2003. **10**(1): p. 37-43.

96. Wildner, O., *Comparison of replication-selective, oncolytic viruses for the treatment of human cancers.* Curr Opin Mol Ther, 2003. **5**(4): p. 351-61.

97. Bischoff, J.R., et al., *An adenovirus mutant that replicates selectively in p53-deficient human tumor cells.* Science, 1996. **274**(5286): p. 373-6.

98. Robson, T. and D.G. Hirst, *Transcriptional Targeting in Cancer Gene Therapy.* J Biomed Biotechnol, 2003. **2003**(2): p. 110-137.

99. Hart, I.R., *Tissue specific promoters in targeting systemically delivered gene therapy.* Semin Oncol, 1996. **23**(1): p. 154-8.

100. Ngan, E.S., et al., *The mifepristone-inducible gene regulatory system in mouse models of disease and gene therapy.* Semin Cell Dev Biol, 2002. **13**(2): p. 143-9.

101. Ulmann, A. and C. Dubois, *Clinical trials with RU 486 (mifepristone): an update.* Acta Obstet Gynecol Scand Suppl, 1989. **149**: p. 9-11.

102. Nordstrom, J.L., *The antiprogestin-dependent GeneSwitch system for regulated gene therapy.* Steroids, 2003. **68**(10-13): p. 1085-94.

103. Sirin, O. and F. Park, *Regulating gene expression using self-inactivating lentiviral vectors containing the mifepristone-inducible system.* Gene, 2003. **323**: p. 67-77.

104. Pierson, T.M., et al., *Regulable expression of inhibin A in wild-type and inhibin alpha null mice.* Mol Endocrinol, 2000. **14**(7): p. 1075-85.

105. Davison, A.J., M. Benko, and B. Harrach, *Genetic content and evolution of adenoviruses.* J Gen Virol, 2003. **84**(Pt 11): p. 2895-908.

106. Bewley, M.C., et al., *Structural analysis of the mechanism of adenovirus binding to its human cellular receptor, CAR.* Science, 1999. **286**(5444): p. 1579-83.

107. Graham, F.L., et al., *Characteristics of a human cell line transformed by DNA from human adenovirus type 5.* J Gen Virol, 1977. **36**(1): p. 59-74.

108. Graham, F.L. and L. Prevec, *Methods for construction of adenovirus vectors.* Mol Biotechnol, 1995. **3**(3): p. 207-20.

109. Mitani, K., et al., *Rescue, propagation, and partial purification of a helper virus-dependent adenovirus vector.* Proc Natl Acad Sci U S A, 1995. **92**(9): p. 3854-8.

110. Kochanek, S., *High-capacity adenoviral vectors for gene transfer and somatic gene therapy.* Hum Gene Ther, 1999. **10**(15): p. 2451-9.

111. Parks, R.J. and F.L. Graham, *A helper-dependent system for adenovirus vector production helps define a lower limit for efficient DNA packaging.* J Virol, 1997. **71**(4): p. 3293-8.

112. Schiedner, G., et al., *Variables affecting in vivo performance of high-capacity adenovirus vectors.* J Virol, 2002. **76**(4): p. 1600-9.

113. Vorburger, S.A. and K.K. Hunt, *Adenoviral gene therapy.* Oncologist, 2002. **7**(1): p. 46-59.

114. Brown, B.D., et al., *Helper-dependent adenoviral vectors mediate therapeutic factor VIII expression for several months with minimal accompanying toxicity in a canine model of severe hemophilia A.* Blood, 2004. **103**(3): p. 804-10.

115. Blagosklonny, M.V., et al., *Effects of p53-expressing adenovirus on the chemosensitivity and differentiation of anaplastic thyroid cancer cells.* J Clin Endocrinol Metab, 1998. **83**(7): p. 2516-22.

116. Cirielli, C., et al., *Adenovirus-mediated wild-type p53 expression induces apoptosis and suppresses tumorigenesis of experimental intracranial human malignant glioma.* J Neurooncol, 1999. **43**(2): p. 99-108.

117. Cirielli, C., et al., *Adenovirus-mediated gene transfer of wild-type p53 results in melanoma cell apoptosis in vitro and in vivo.* Int J Cancer, 1995. **63**(5): p. 673-9.

118. Putzer, B.M., et al., *Combination therapy with interleukin-2 and wild-type p53 expressed by adenoviral vectors potentiates tumor regression in a murine model of breast cancer.* Hum Gene Ther, 1998. **9**(5): p. 707-18.

119. Goebel, E.A., et al., *Tumor reduction in vivo after adenoviral mediated gene transfer of the herpes simplex virus thymidine kinase gene and ganciclovir treatment in human head and neck squamous cell carcinoma.* Otolaryngol Head Neck Surg, 1998. **119**(4): p. 331-6.

120. Sterman, D.H., et al., *Adenovirus-mediated herpes simplex virus thymidine kinase/ganciclovir gene therapy in patients with localized malignancy: results of a phase I clinical trial in malignant mesothelioma.* Hum Gene Ther, 1998. **9**(7): p. 1083-92.

121. Rogulski, K.R., et al., *Double suicide gene therapy augments the antitumor activity of a replication-competent lytic adenovirus through enhanced cytotoxicity and radiosensitization.* Hum Gene Ther, 2000. **11**(1): p. 67-76.

122. Schiedner, G., S. Hertel, and S. Kochanek, *Efficient transformation of primary human amniocytes by E1 functions of Ad5: generation of new cell lines for adenoviral vector production.* Hum Gene Ther, 2000. **11**(15): p. 2105-16.

123. Kuzmin, A.I., M.J. Finegold, and R.C. Eisensmith, *Macrophage depletion increases the safety, efficacy and persistence of adenovirus-mediated gene transfer in vivo.* Gene Ther, 1997. **4**(4): p. 309-16.

124. Chuah, M.K., et al., *Therapeutic factor VIII levels and negligible toxicity in mouse and dog models of hemophilia A following gene therapy with high-capacity adenoviral vectors.* Blood, 2003. **101**(5): p. 1734-43.

125. Schiedner, G., et al., *Selective depletion or blockade of Kupffer cells leads to enhanced and prolonged hepatic transgene expression using high-capacity adenoviral vectors.* Mol Ther, 2003. **7**(1): p. 35-43.

126. Leonard, J.P., et al., *Effects of single-dose interleukin-12 exposure on interleukin-12-associated toxicity and interferon-gamma production.* Blood, 1997. **90**(7): p. 2541-8.

127. Peters, K.G., et al., *Functional significance of Tie2 signaling in the adult vasculature.* Recent Prog Horm Res, 2004. **59**: p. 51-71.

128. Lin, P., et al., *Antiangiogenic gene therapy targeting the endothelium-specific receptor tyrosine kinase Tie2.* Proc Natl Acad Sci U S A, 1998. **95**(15): p. 8829-34.

129. Aurisicchio, L., et al., *Regulated and prolonged expression of mIFN(alpha) in immunocompetent mice mediated by a helper-dependent adenovirus vector.* Gene Ther, 2001. **8**(24): p. 1817-25.

130. Pollock, R. and T. Clackson, *Dimerizer-regulated gene expression.* Curr Opin Biotechnol, 2002. **13**(5): p. 459-67.

131. Ye, X., et al., *Ligand-inducible transgene regulation for gene therapy.* Methods Enzymol, 2002. **346**: p. 551-61.

132. Sugimoto, H., et al., *Neutralization of circulating vascular endothelial growth factor (VEGF) by anti-VEGF antibodies and soluble VEGF receptor 1 (sFlt-1) induces proteinuria.* J Biol Chem, 2003. **278**(15): p. 12605-8.

133. Foster, R.R., et al., *Functional evidence that vascular endothelial growth factor may act as an autocrine factor on human podocytes.* Am J Physiol Renal Physiol, 2003. **284**(6): p. F1263-73.

134. Eremina, V., et al., *Glomerular-specific alterations of VEGF-A expression lead to distinct congenital and acquired renal diseases.* J Clin Invest, 2003. **111**(5): p. 707-16.

135. Pavenstadt, H., W. Kriz, and M. Kretzler, *Cell biology of the glomerular podocyte.* Physiol Rev, 2003. **83**(1): p. 253-307.

136. Yang, J.C., et al., *A randomized trial of bevacizumab, an anti-vascular endothelial growth factor antibody, for metastatic renal cancer.* N Engl J Med, 2003. **349**(5): p. 427-34.

137. Roes, E.M., et al., *High levels of urinary vascular endothelial growth factor in women with severe preeclampsia.* Int J Biol Markers, 2004. **19**(1): p. 72-5.

138. Maynard, S.E., et al., *Excess placental soluble fms-like tyrosine kinase 1 (sFlt1) may contribute to endothelial dysfunction, hypertension, and proteinuria in preeclampsia.* J Clin Invest, 2003. **111**(5): p. 649-58.

139. Luttun, A. and P. Carmeliet, *Soluble VEGF receptor Flt1: the elusive preeclampsia factor discovered?* J Clin Invest, 2003. **111**(5): p. 600-2.

140. Kuo, C.J., et al., *Comparative evaluation of the antitumor activity of antiangiogenic proteins delivered by gene transfer.* Proc Natl Acad Sci U S A, 2001. **98**(8): p. 4605-10.

141. Klagsbrun, M., *Regulators of angiogenesis: stimulators, inhibitors, and extracellular matrix.* J Cell Biochem, 1991. **47**(3): p. 199-200.

142. Carmeliet, P., *Angiogenesis in health and disease.* Nat Med, 2003. **9**(6): p. 653-60.

143. Gabrilovich, D.I., et al., *Production of vascular endothelial growth factor by human tumors inhibits the functional maturation of dendritic cells.* Nat Med, 1996. **2**(10): p. 1096-103.

144. Asahara, T., et al., *Isolation of putative progenitor endothelial cells for angiogenesis.* Science, 1997. **275**(5302): p. 964-7.

145. Grosskreutz, C.L., et al., *Vascular endothelial growth factor-induced migration of vascular smooth muscle cells in vitro.* Microvasc Res, 1999. **58**(2): p. 128-36.

146. Gabrilovich, D.I., et al., *Antibodies to vascular endothelial growth factor enhance the efficacy of cancer immunotherapy by improving endogenous dendritic cell function.* Clin Cancer Res, 1999. **5**(10): p. 2963-70.

147. Rakhmilevich, A.L., et al., *Treatment of experimental breast cancer using interleukin-12 gene therapy combined with anti-vascular endothelial growth factor receptor-2 antibody.* Mol Cancer Ther, 2004. **3**(8): p. 969-76.

148. LeCouter, J. and N. Ferrara, *EG-VEGF and Bv8. a novel family of tissue-selective mediators of angiogenesis, endothelial phenotype, and function.* Trends Cardiovasc Med, 2003. **13**(7): p. 276-82.

149. Conway, E.M. and P. Carmeliet, *The diversity of endothelial cells: a challenge for therapeutic angiogenesis.* Genome Biol, 2004. **5**(2): p. 207.

150. Colombo, M.P., et al., *Amount of interleukin 12 available at the tumor site is critical for tumor regression.* Cancer Res, 1996. **56**(11): p. 2531-4.

151. Weber, S.M., et al., *Interleukin-12 gene transfer results in CD8-dependent regression of murine CT26 liver tumors.* Ann Surg Oncol, 1999. **6**(2): p. 186-94.

152. Hirschowitz, E.A., et al., *Regional treatment of hepatic micrometastasis by adenovirus vector-mediated delivery of interleukin-2 and interleukin-12 cDNAs to the hepatic parenchyma.* Cancer Gene Ther, 1999. **6**(6): p. 491-8.

153. Xu, S., et al., *Rapid high efficiency sensitization of CD8+ T cells to tumor antigens by dendritic cells leads to enhanced functional avidity and direct tumor recognition through an IL-12-dependent mechanism.* J Immunol, 2003. **171**(5): p. 2251-61.